SRF

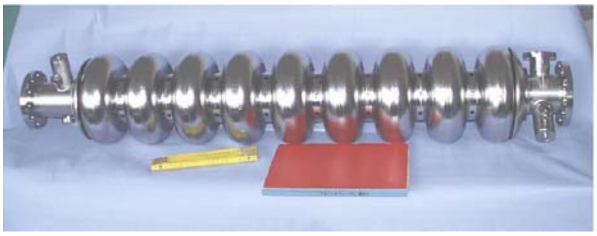

CARE/JRA1 Annual report 2005

Research and Development on Superconducting Radio-Frequency Technology for Accelerator Application

Acronym: SRF

Co-Coordinators: D. Proch, DESY, T.Garvey, CNRS-Orsay

Participating Laboratories and Institutes:

Institute (Participating number)	**Acronym**	**Country**	**Coordinator**	**SRF Scientific Contact**	**Associated to**
DESY (6)	DESY	D	D. Proch	D. Proch	
CEA/DSM/DAPNIA (1)	CEA	F	R. Aleksan	O. Napoly	
CNRS-IN2P3-Orsay (3)	CNRS-Orsay	F	T. Garvey	T. Garvey	CNRS
INFN Legnaro (10)	INFN-LNL	I	S. Guiducci	E. Palmieri	INFN
INFN Milano (10)	INFN-Mi	I	S. Guiducci	C. Pagani	INFN
INFN Roma2 (10)	INFN-Ro2	I	S. Guiducci	S. Tazzari	INFN
INFN Frascati (10)	INFN-LNF	I	S. Guiducci	M. Castellano	INFN
Paul Scherrer Institute (19)	PSI	CH	V. Schlott	V. Schlott	
Technical University of Lodz (12)	TUL	PL	A. Napieralski	M. Grecki	
Warsaw University of Technology (14)	WUT-ISE	PL	R. Romaniuk	R. Romaniuk	
IPJ Swierk (13)	IPJ	PL	M. Sadowski	M. Sadowski	

Industrial Involvement:

Company Name	**Country**	**Contact Person**
ACCEL Instruments GmbH	D	M. Peiniger
WSK Mess- und Datentechnik GmbH	D	F. Schölz
E. ZANON SPA	I	G. Corniani
Henkel Lohnpoliertechnik GmbH	D	B. Henkel

Work supported by the European Community-Research Infrastructure Activity under the FP6 “Structuring the European Research Area” programme (CARE, contract number RII3-CT-2003-506395).

CARE/JRA1 Annual report 2005

Research and Development on Superconducting Radio-Frequency Technology for Accelerator Applications

Acronym: SRF

Co-Coordinators: D. Proch, DESY, T.Garvey, CNRS-Orsay

Participating Laboratories and Institutes:

Institute (Participating number)	**Acronym**	**Country**	**Coordinator**	**SRF Scientific Contact**	**Associated to**
DESY (6)	DESY	D	D. Proch	D. Proch	
CEA/DSM/DAPNIA (1)	CEA	F	O. Napoly	O. Napoly	
CNRS-IN2P3-Orsay (3)	CNRS-Orsay	F	T.Garvey	T.Garvey	CNRS
INFN Legnaro (10)	INFN-LNL	I	S. Guiducci	E. Palmieri	INFN
INFN Milano (10)	INFN-Mi	I	S. Guiducci	P. Michelato	INFN
INFN Roma2 (10)	INFN-Ro2	I	S. Guiducci	S. Tazzari	INFN
INFN Frascati (10)	INFN-LNF	I	S. Guiducci	M. Castellano	INFN
Paul Scherrer Institute (19)	PSI	CH	V. Schlott	V. Schlott	
Technical University of Lodz (12)	TUL	PL	A.Napieralski	M. Grecki	
Warsaw University of Technology (14)	WUT-ISE	PL	R.Romaniuk	R. Romaniuk	
IPJ Swierk (13)	IPJ	PL	M. Sadowski	M. Sadowski	

Industrial Involvement:

Company Name	**Country**	**Contact Person**
ACCEL Instruments GmbH	D	M. Peiniger
WSK Mess- und Datentechnik GmbH	D	F. Schölz
E. ZANON SPA	I	G. Corniani
Henkel Lohnpoliertechnik GmbH	D	B. Henkel

Table of contents

Executive Summary

The aim of the JRA on Superconducting RF Technology is to improve the quality and performance of the superconducting test accelerator TTF (Tesla Test Facility), a unique test facility to explore the operating conditions of a high gradient superconducting accelerator, at DESY.
The ultimate objectives of this research activity are

- to increase the accelerating gradient from 25 to 35 MV/m and
- to increase the quality factor from 5×10^9 to 2×10^{10},
- to improve the reliability, operating performance and availability of the superconducting accelerating system,
- to achieve a cost reduction of the SRF cavities and their associated components. .

Use and Dissemination of knowledge.

Communication is an important aspect of the JRA-SRF, both between participating institutes as well as with external institutes who share our interest in high gradient, low loss superconducting cavities. Contributions from JRA-SRF members were given to several conferences and meetings, the major ones being as follows:

-The 12th International Workshop on RF Superconductivity (Ithaca, NY)
-The SPIE International Conference on Optics and Opto-electronics (Warsaw).
-The 2005 United States Particle Accelerator Conference (Tennessee).
-The 2nd ILC (International Linear Collider) meeting (Snowmass),
Papers and talks were also presented at TESLA Technology Collaboration meetings in this reporting year as well as at the annual CARE meeting held at CERN in November. The impressive progress made in Work-Packages 8 (Tuners) and 9 (Low-level RF) earned the WP leaders the opportunity to give *highlight* talks at this meeting. The presentations can be found on the meeting WEB site.

The SPIE meeting, held in Warsaw, is particularly worth noting as an entire session was devoted by the organizers to CARE issues and several CARE-SRF participants were asked to make invited presentations within this session.

Annual SRF Meeting

In addition to the above conferences and meetings, the SRF JRA held their dedicated annual meeting at the INFN Legnaro laboratory. This meeting included an entire review of all work-packages and tasks therein. It was the opportunity for the external scientific advisory committee to review the program of work. Their findings can be found later within this report. What was clear from the Legnaro meeting is that, despite some delay in certain milestones / deliverables, the project has made enormous progress in the last twelve months. The technical summaries to be found in later sections bears witness to this.

There continues to be a strong connection between the R&D activities in JRA-SRF and the European X-FEL and International Linear Collider projects. It seems likely that many of the results of the work from SRF will have a major impact on both these projects.

List of Work packages, tasks and responsibilities

2 Improved Standard Cavity Fabrication (ISCF)	***P.Michelato***	INFN Mi
2.1 Reliability analysis	L. Lilje	DESY
2.2 Improved component design	P.Michelato	INFN Mi
2.3 EB welding	J. Tiessen	DESY
3 Seamless Cavity Production (SCP)	***W.-D. Moeller***	DESY
3.1 Seamless cavity production by spinning	E. Palmieri	INFN LNL
3.2 Seamless cavity production by hydroforming	W. Singer	DESY
4 Thin Film Cavity Production (TFCP)	***M. Sadowski***	IPJ
4.1 Linear arc cathode	J. Langner	IPJ
4.2 Planar arc cathode	S. Tazzari	INFN Ro2
5 Surface Preparation (SP)	***L. Lilje***	DESY
5.1 EP on single cells	C. Antoine	CEA
5.2 EP on multicells	A Matheisen	DESY
5.3 Automated EP	E. Palmieri	INFN LNL
5.4 Dry ice cleaning	D. Reschke	DESY
6 Material Analysis (MA)	***E. Palmieri***	INFN LNL
6.1 Squid scanning	W. Singer	DESY
6.2 Flux gate magnetometry	M. Valentino	INFN LNL
6.3 DC field emission studies of Nb samples	X. Singer	DESY
7 Couplers (COUP)	***A. Variola***	CNRS-Orsay
7.1 New proto-types	L. Grandsire	CNRS-Orsay
7.2 Titanium-nitride coating system	L. Grandsire	CNRS-Orsay
7.3 Conditioning studies	P. Lepercq	CNRS-Orsay
8 Tuners (TUN)	***P. Sekalski***	TUL
8.1 UMI Tuner	A. Bosotti	INFN-Milano
8.2 Magnetostrictive Tuner	A. Grecki	TUL
8.3 CEA Tuner	P. Bosland	CEA
8.4 IN2P3 activities	M. Fouaidy	CNRS-Orsay
9 Low Level RF (LLRF)	***S. Simrock***	DESY
9.1 Operability and Technical performance	S. Simrock	DESY
9.2 Cost and reliabilty	M. Grecki	TUL
9.3 Hardware technolgy	R. Romaniuk	WUT-ISE
9.4 Software technology	Jezynski	WUT-ISE
10 Cryostat Integration Tests	***B. Visentin***	CEA
11 Beam Diagnostics (BD)	***M. Castellano***	INFN-LNF
11.1 Beam position monitor	C. Magne	CEA
11.2 Emittance monitor	M. Castellano	INFN-LNF

Overview of status of JRA1 SRF

N°	Task Name	MS, Deliverable	Contractor	% Compl.
2	WP2 IMPROVED STANDARD CAVITY FABRICATION			36%
2.1	Reliability Analysis		DESY	62%
2.1.1	Review of data bank: cavity fabrication		DESY	100%
2.1.2	Review of data bank: cavity treatment		DESY	100%
2.1.3	Review of data bank: cavity VT performance		DESY	100%
2.1.4	Review of data bank: string assembly		DESY	100%
2.1.5	Review of data bank: string performance		DESY	27%
2.1.6	Establish correlations		DESY	10%
2.1.7	Final report on reliability issue	Final Report	DESY	0%
2.2	Improved component design			32%
2.2.1	Documentation retrieving		INFN-MI	61%
2.2.1.1	Start up meetings		INFN-MI	100%
2.2.1.2	Access and study of Jlab, DESY, LLAN, KEK experience		INFN-MI	100%
2.2.1.3	Summary report on the status of the art on ancillaries	Summary Repo	INFN-MI	100%
2.2.1.4	Sealing material and shape design		INFN-MI	100%
2.2.1.5	Flange preliminary design		INFN-MI	100%
2.2.1.6	Material and geometric compatibility		INFN-MI	100%
2.2.1.7	Final assembly design		INFN-MI	50%
2.2.1.8	End plate preliminary design		INFN-MI	50%
2.2.1.9	Report about new design for components	Design Repor	INFN-MI	100%
2.2.1.10	Stiffness optimization		INFN-MI	40%
2.2.1.11	Manufacturing procedure analysis		INFN-MI	30%
2.2.1.12	Final assembly design		INFN-MI	20%
2.2.1.13	Other ancillaries design		INFN-MI	6%
2.2.1.14	Final Report for new components	Report	INFN-MI	40%
2.2.2	Review of criticality in welding procedures		INFN-MI	8%
2.2.2.1	Review of available parameters on vendor welding machine		INFN-MI	13%
2.2.2.2	Definition of prototype requirements for tests		INFN-MI	10%
2.2.2.3	Welding test on specimens		INFN-MI	0%
2.2.2.4	Analysis of the results		INFN-MI	0%
2.2.2.5	Report about welding parameters	Report	INFN-MI	0%
2.2.3	Finalize new component design		INFN-MI	0%
2.2.3.1	Do drawings		INFN-MI	0%
2.2.3.2	New components design finished	Design repor	INFN-MI	0%
2.2.4	Finalize new cavity design		INFN-MI	0%
2.2.4.1	Make drawings		INFN-MI	0%
2.2.4.2	New cavity design finished	Design repor	INFN-MI	0%
2.2.5	Fabrication of new cavity		INFN-MI	0%
2.2.5.1	Fabrication		INFN-MI	0%
2.2.5.2	New cavity finished	Cavity Prototyp	INFN-MI	0%
2.3	EB welding		DESY	38%
2.3.1	Design tooling		DESY	100%
2.3.1.1	Tools for flange welding		DESY	100%
2.3.1.2	Tools for pipe welding		DESY	100%
2.3.1.3	Tools for stiffening rings		DESY	100%
2.3.1.4	Tools for single cell welding		DESY	100%
2.3.1.5	Tools for 9-cells		DESY	100%
2.3.1.6	Tools design finished	Design repor	DESY	100%
2.3.2	Tools production		DESY	74%
2.3.2.1	Tools for flange welding		DESY	100%
2.3.2.2	Tools for pipe welding		DESY	100%
2.3.2.3	Tools for stiffening rings		DESY	100%
2.3.2.4	Tools for single cell welding		DESY	100%
2.3.2.5	Tools for 9-cells		DESY	20%
2.3.2.6	Tools fabrication finished	Tools Read	DESY	15%
2.3.3	Welding		DESY	19%
2.3.3.1	Commissioning welding machine		DESY	100%
2.3.3.2	Test welding		DESY	85%
2.3.3.3	Start production welding of components	Commissionin	DESY	10%
2.3.3.4	Single cell welding		DESY	10%
2.3.3.5	Multicell welding		DESY	3%
2.3.3.6	Welding of prototypes of components finished	Prototype	DESY	5%

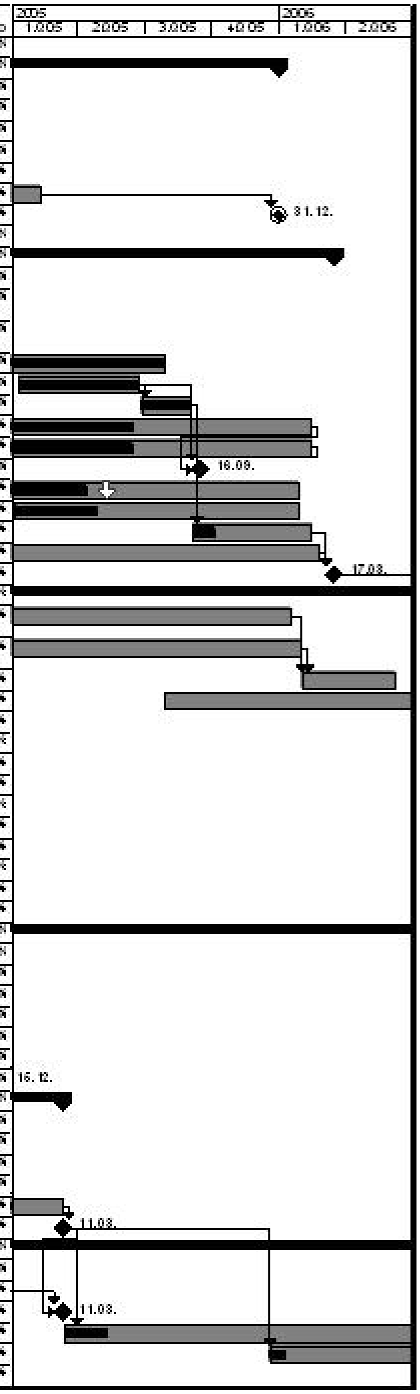

N°	Task Name	MS, Deliverable	Contractor	% schlo
3	WP3 SEAMLESS CAVITY PRODUCTION			64%
3.1	Seamless by spinning		INFN-LNL	41%
3.1.1	Design spinning machine		INFN-LNL	100%
3.1.1.1	Drawings of the matrices		INFN-LNL	100%
3.1.1.2	Drawings of the support system		INFN-LNL	100%
3.1.1.3	Drawings of spinning machine finished	Design repor	INFN-LNL	100%
3.1.2	Fabrication of spinning machine		INFN-LNL	76%
3.1.2.1	Fabrication of machine parts		INFN-LNL	100%
3.1.2.2	Software for the machine		INFN-LNL	100%
3.1.2.3	Assembly of machine		INFN-LNL	50%
3.1.2.4	Commissioning of the machine		INFN-LNL	10%
3.1.2.5	Spinning machine ready	Commissionin	INFN-LNL	10%
3.1.3	Evaluation of spinning parameters		INFN-LNL	31%
3.1.3.1	Drawings of the support system and turning mechanism		INFN-LNL	10%
3.1.3.2	Drawings of the necking mechanism		INFN-LNL	40%
3.1.3.3	Fabrication of the tube necking machine		INFN-LNL	40%
3.1.3.4	Commissioning of the machine		INFN-LNL	10%
3.1.3.5	Spinning parameters defined	Design Repor	INFN-LNL	20%
3.1.4	Spinning of 1-cell cavities		INFN-LNL	0%
3.1.4.1	Material and fabrication of bulk Nb test tubes		INFN-LNL	0%
3.1.4.2	Material and fabrication of bimetallic NbCu test tubes		INFN-LNL	0%
3.1.4.3	1-cell spinning parameters defined		INFN-LNL	0%
3.1.5	Extension of spinning apparatus to multicells		INFN-LNL	0%
3.1.5.1	Computer simulation of the necking		INFN-LNL	0%
3.1.5.2	Start of Multi-cell spinning	Start spinning	INFN-LNL	10%
3.1.6	Spinning of multi-cell cavities cavities		INFN-LNL	0%
3.1.6.1	Computer simulation of the spinning		INFN-LNL	0%
3.1.6.2	Spinning of bulk Nb 9-cell cavities		INFN-LNL	0%
3.1.6.3	Parameters of multi-cell spinning defined	Design repor	INFN-LNL	0%
3.1.7	Series production of multi-cell cavities		INFN-LNL	0%
3.1.7.1	Spinning		INFN-LNL	0%
3.1.7.2	Multi-cell cavities finished	Final Report, Cavity	INFN-LNL	0%
3.2	Seamless by hydroforming		DESY	76%
3.2.1	Design hydro forming machine		DESY	100%
3.2.1.1	Drawings of the matrices		DESY	100%
3.2.1.2	Drawings of the support system		DESY	100%
3.2.1.3	Drawings matrix & support finished	Design repor	DESY	100%
3.2.2	Construction of hydro forming machine		DESY	100%
3.2.2.1	Hydraulic for machine		DESY	100%
3.2.2.2	Software for the machine		DESY	100%
3.2.2.3	Machine fabrication		DESY	100%
3.2.2.4	Commissioning of the machine		DESY	100%
3.2.2.5	Hydro forming machine ready	Commissionin	DESY	100%
3.2.3	Construction of tube necking machine		DESY	100%
3.2.3.1	Drawings of the support system and turning mechanism		DESY	100%
3.2.3.2	Drawings of the necking mechanism		DESY	100%
3.2.3.3	Fabrication of the tube necking machine		DESY	100%
3.2.3.4	Software for the tube necking machine		DESY	100%
3.2.3.5	Construction tube necking machine finished	Design repor	DESY	100%
3.2.4	Development of seamless tubes for 9-cell cavities		DESY	100%
3.2.4.1	Material and fabrication of bulk Nb test tubes		DESY	100%
3.2.4.2	Material and fabrication of bimetallic NbCu test tubes		DESY	100%
3.2.4.3	Seamless tubes ready	Design repor	DESY	100%
3.2.5	Development of tube necking		DESY	32%
3.2.5.1	Computer simulation of the necking		DESY	60%
3.2.5.2	Experiments on tube necking at ire		DESY	0%
3.2.5.3	Tube necking machine operational	Commissionin	DESY	0%
3.2.6	Hydro forming of seamless cavities		DESY	24%
3.2.6.1	Computer simulation of the hydro forming		DESY	40%
3.2.6.2	Hydro forming of bulk Nb 9-cell cavities		DESY	0%
3.2.6.3	Hydro formed 9-cell cavities ready	Cavity Prototype	DESY	0%

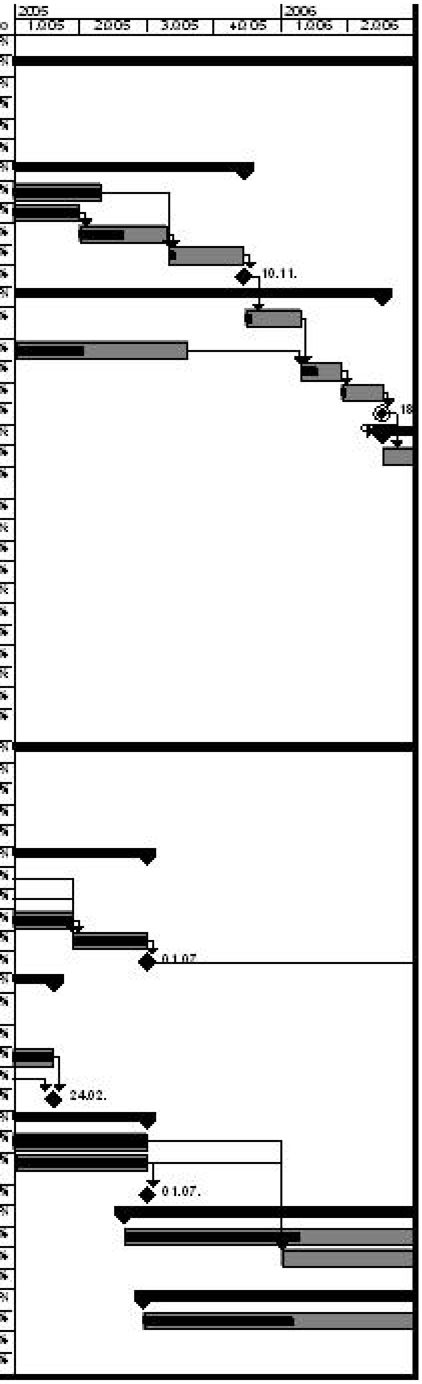

N°	Task Name	MS, Deliverable	Contactor	% schdo
4	WP4 THIN FILM CAVITY PRODUCTION			66%
4.1	Linear-arc cathode coating		IPJ	66%
4.1.1	Installation & commissioning of coating apparatus		IPJ	78%
4.1.1.1	Modification of a prototype facility for single cells		IPJ	100%
4.1.12	Optimization of a triggering system		IPJ	100%
4.1.13	Prototype facility ready	Commissionin	IPJ	100%
4.1.14	Study of arc current reduction and stabilization		IPJ	100%
4.1.15	Optimization of powering system		IPJ	100%
4.1.16	Coating apparatus operational	Apparatus read	IPJ	100%
4.1.17	Coating single cells		IPJ	69%
4.1.17.1	Coating of single cells without micro droplet filtering		IPJ	70%
4.1.17.2	Design and construction of a micro droplet filter sys		IPJ	70%
4.1.17.3	Droplet filter ready	Hardware read	IPJ	25%
4.1.17.4	Coating of single cell with micro droplet filtering		IPJ	0%
4.1.2	Coating multi-cell		IPJ	0%
4.1.2.1	Design and commissioning		IPJ	0%
4.1.22	First multicell coating		IPJ	0%
4.2	Planar-arc cathode coating		INFN-Ro2	63%
4.2.1	Modification of a planar-arc & trigger system		INFN-Ro2	100%
4.2.1.1	Modification		INFN-Ro2	100%
4.2.12	Optimization of the laser triggering system		INFN-Ro2	100%
4.2.13	Planar arc system fully tested	Status Repor	INFN-Ro2	100%
4.2.2	Routine Operation of planar arc system		INFN-Ro2	92%
4.2.2.1	Characterization of samples coated at different conditions		INFN-Ro2	95%
4.2.22	Characterization of Nb-coated sapphire samples		INFN-Ro2	90%
4.2.23	Characterization of Nb-coated copper samples		INFN-Ro2	90%
4.2.24	Summary report on quality of planar arc coating	Status Repor	INFN-Ro2	100%
4.2.3	Studies of other HTC superconducting coating		INFN-Ro2	26%
4.2.3.1	Study of superconducting properties		INFN-Ro2	25%
4.2.32	Report on quality of superconducting properties	Final Report	INFN-Ro2	0%

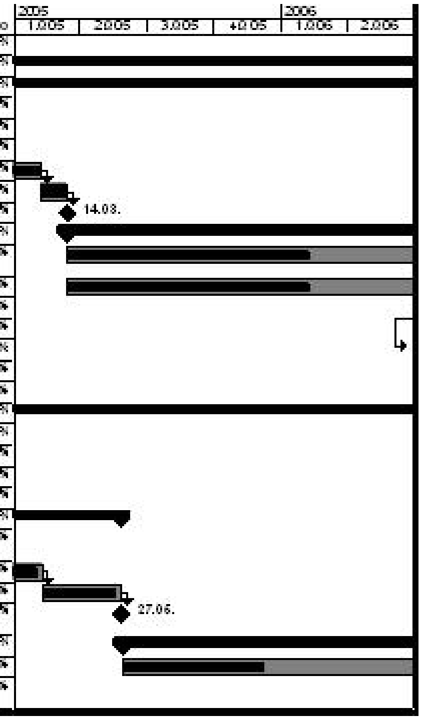

N°	Task Name	MS, Deliverable	Contractor	% sched
6	WP5 SURFACE PREPARATION			32%
6.1	EP on single cells		CEA	40%
6.1.1	EP on samples		CEA	68%
5.1.1.1	Establishing method of surface characterization		CEA	100%
5.1.1.2	Surface characterization fixed	Design Repor	CEA	100%
5.1.1.3	Series of EP with samples for surface investigations		CEA	50%
5.1.1.4	Best EP parameters	Final Report	CEA	0%
6.1.2	Single cell cavities		CEA	100%
5.1.2.1	Order Nb and fabricate 3 cavities		CEA	100%
5.1.2.2	3 cavities fabricated	Cavities read	CEA	100%
6.1.3	Build EP chemistry for single cells		CEA	43%
5.1.3.1	Design of EP set-up		CEA	90%
5.1.3.2	Fabrication of EP set-up		CEA	95%
5.1.3.3	Commissioning of EP set-up		CEA	0%
5.1.3.4	First operation of EP set-up	Commissionin	CEA	0%
6.1.4	Operation of single cell EP		CEA	0%
5.1.4.1	Continuous single cell operation		CEA	0%
5.1.4.2	Define working parameters for single cells	Design Repor	CEA	0%
6.1.5	Continuous operation, search for best parameters		CEA	0%
5.1.5.1	Parametrising EP procedure		CEA	0%
5.1.5.2	EP parameters fixed	Final Report	CEA	0%
6.2	EP on multi-cells		DESY	36%
6.2.1	Transfer of parameters from 1 cell to multi cell equipment		DESY	66%
6.2.1.1	Finish EP setup nine-cells at DESY		DESY	82%
5.2.1.1.1	Improved gas cleaning system		DESY	100%
5.2.1.1.2	Design for hot water rinsing		DESY	90%
5.2.1.1.3	Proof-of-Principle experiment hot water rinsi	Status Repor	DESY	0%
6.2.1.2	Optimize electrode shape		DESY	46%
5.2.1.2.1	Develop computer model / Evaluate software		DESY	100%
5.2.1.2.2	Design improved electrode		DESY	0%
5.2.1.2.3	Electrode design fixed	Design repor	DESY	0%
6.2.1.3	Fix process parameters / Quality control		DESY	49%
5.2.1.3.1	Setup chemical lab		DESY	100%
5.2.1.3.2	Bath aging		DESY	70%
5.2.1.3.3	Bath mixture		DESY	50%
5.2.1.3.4	Alternative (salt) mixtures		DESY	0%
5.2.1.3.5	Process parameters fixed	Final Report	DESY	1%
6.2.2	Laser roughness		DESY	6%
5.2.2.1	Evaluate existing systems		DESY	20%
5.2.2.2	Specify laser system		DESY	0%
5.2.2.3	Built laser system		DESY	0%
5.2.2.4	Roughness measurement finished	Equipment read	DESY	0%
6.2.3	Oxipolishing as final chemical cleaning		DESY	38%
5.2.3.1	Laboratory studies		DESY	30%
5.2.3.2	Design of OP system		DESY	70%
5.2.3.3	Setup one-cell system		DESY	77%
5.2.3.4	Proof-of-Principle experiment Oxipolishing	Status Repor	DESY	0%
5.2.3.5	Design OP for nine-cells		DESY	30%
5.2.3.6	Build OP for 9-cells		DESY	0%
5.2.3.7	OP for 9-cells ready	Commissionin	DESY	0%
5.2.3.8	Study op with 9-cell cavities		DESY	0%
5.2.3.9	Evaluate experiments	Status Repor	DESY	0%
6.2.4	Transfer Electropolishing technology to industry		DESY	4%
5.2.4.1	Qualify industry with one-cells		DESY	10%
5.2.4.2	Industrial design study on setup for multi-cells		DESY	10%
5.2.4.3	Report on industrial design	Report	DESY	0%
5.2.4.4	Fabricate EP multi-cell industrial prototype		DESY	0%
5.2.4.5	Commission EP multi-cell industrial prototype		DESY	0%
5.2.4.6	EP multi-cell industrial prototype ready	Commissionin	DESY	0%
5.2.4.7	Operate EP multi-cell industrial prototype		DESY	0%
5.2.4.8	Final report on industrial EP	Final Report	DESY	0%

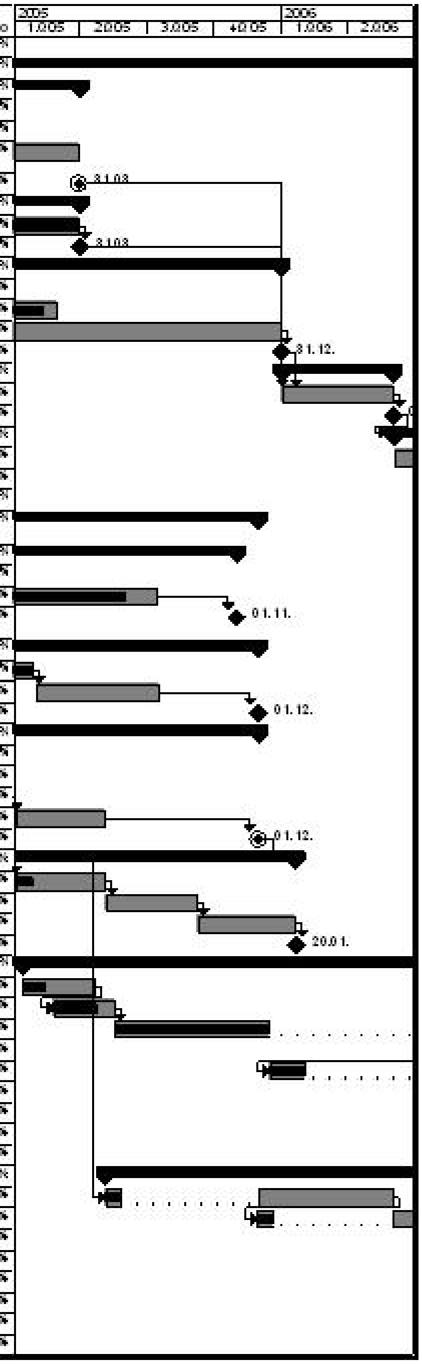

N°	Task Name	MS, Deliverable	Contractor	% Schlo
6.3	Automated EP (AEP)		INFN-LNL	38%
6.3.1	Prototype EP installation		INFN-LNL	99%
5.3.1.1	Design installation		INFN-LNL	100%
5.3.12	Fabricate/ order components		INFN-LNL	100%
5.3.13	Assemble EP installation		INFN-LNL	100%
5.3.14	First operation of automated EP	Commissionin	INFN-LNL	0%
6.3.2	EP computer control		INFN-LNL	96%
5.3.2.1	Design control architecture		INFN-LNL	100%
5.3.22	Developed software		INFN-LNL	100%
5.3.23	Test of software		INFN-LNL	80%
5.3.24	Software ready	Status Repor	INFN-LNL	80%
6.3.3	Operation of AEP prototype		INFN-LNL	30%
5.3.3.1	Correlate surface finish/ conductance		INFN-LNL	30%
5.3.32	Determine optimum conductance		INFN-LNL	80%
5.3.33	Optimize automated operation		INFN-LNL	0%
5.3.34	Design report on AEP		INFN-LNL	0%
5.3.35	Automated EP is defined	Final Report	INFN-LNL	0%
6.3.4	Alternative electrolytes		INFN-LNL	13%
5.3.4.1	Review of EP chemistry		INFN-LNL	50%
5.3.42	Proposal for alternative electrolytes	Report	INFN-LNL	50%
5.3.43	Experiments with alternative electrolytes		INFN-LNL	0%
5.3.44	Conclude experimental results	Status Repor	INFN-LNL	0%
6.3.5	Define best AEP		INFN-LNL	0%
5.3.5.1	Compare standard/new electrolyte method		INFN-LNL	0%
5.3.52	Modify AEP installation for best electrolyte		INFN-LNL	0%
5.3.53	Operate modified AEP		INFN-LNL	0%
5.3.54	Design report on best AEP		INFN-LNL	0%
5.3.55	Conclude on best electrolyte	Final Report	INFN-LNL	0%
6.4	Dry ice cleaning		DESY	12%
6.4.1	Installation of full system for 1-3 cell cavities		DESY	88%
5.4.1.1	Installation of CO2 piping		DESY	100%
5.4.12	Installation of motion system		DESY	100%
5.4.13	Installation of control system		DESY	80%
5.4.14	Commissioning		DESY	40%
5.4.15	Installation finished	Commissionin	DESY	40%
6.4.2	Optimization of cleaning parameters		DESY	0%
5.4.2.1	Sample cleaning		DESY	0%
5.4.22	1-cell cavity cleaning		DESY	0%
5.4.23	Fix best cleaning parameters		DESY	0%
5.4.24	Cleaning parameters fixed	Final Report	DESY	0%
6.4.3	VT 9-cell cleaning apparatus		DESY	0%
5.4.3.1	Design 9-cell apparatus VT		DESY	0%
5.4.32	Fabricated 9-cell apparatus		DESY	0%
5.4.33	Installation of 9-cell apparatus		DESY	0%
5.4.34	Commissioning of 9-cell apparatus		DESY	0%
5.4.35	VT Cleaning installation finished	Commissionin	DESY	0%
6.4.4	VT Cleaning of 9-cell cavities		DESY	0%
5.4.4.1	Continuous cleaning		DESY	0%
5.4.42	Evaluation of experimental results	Final repor	DESY	0%
6.4.5	Design & construction of H 9-cell cleaning apparatus		DESY	0%
5.4.5.1	Design 9-cell apparatus VT		DESY	0%
5.4.52	Fabricated 9-cell apparatus		DESY	0%
5.4.53	Installation of 9-cell apparatus		DESY	0%
5.4.54	Commissioning of 9-cell apparatus		DESY	0%
5.4.55	Start H 9-cell cleaning	Commissionin	DESY	0%
6.4.6	Cleaning of horizontal nine-cell cavity		DESY	0%
5.4.6.1	Continuous cleaning		DESY	0%
5.4.62	Evaluation of experimental results	Final repor	DESY	0%

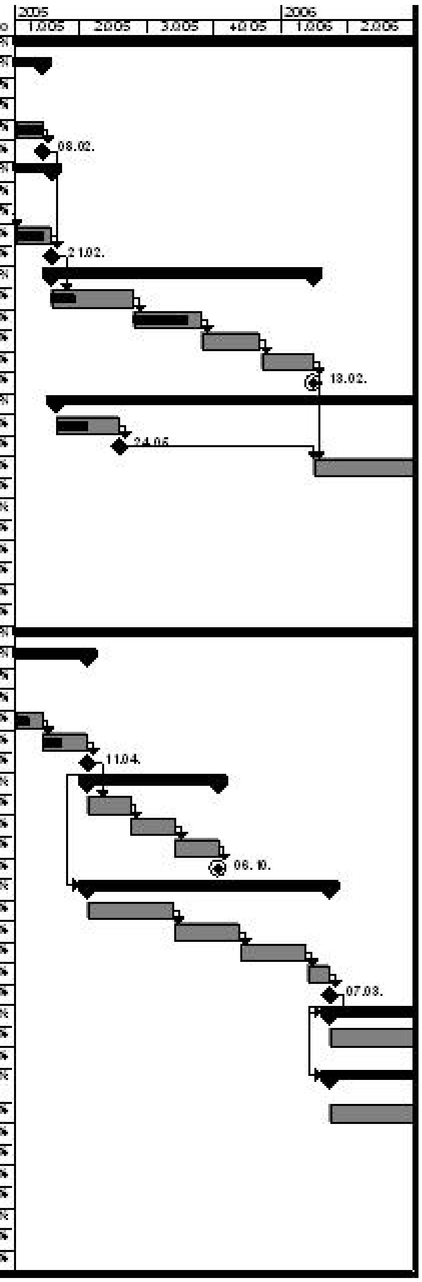

N°	Task Name	MS, Deliverable	Contactor	% schlo
6	WP6 MATERIAL ANALYSIS			31%
6.1	SQUID scanning		DESY	64%
6.1.1	Produce calibration defects		DESY	100%
6.1.1.1	Production of surface defects		DESY	100%
6.1.1.2	Production of bulk defects		DESY	100%
6.1.1.3	Calibration defects finished	Status Repor	DESY	100%
6.1.2	Design components of Squid scanner		DESY	100%
6.1.2.1	Design of the scanning table and support		DESY	100%
6.1.2.2	Design of the SQUID cooling system		DESY	100%
6.1.2.3	Design Scanner finished	Design repor	DESY	100%
6.1.3	Construction of scanning apparatus		DESY	100%
6.1.3.1	Fabrication of the SQUID		DESY	100%
6.1.3.2	Fabrication and purchase of components for SQUID apparatus		DESY	100%
6.1.3.3	Software for the SQUID scanner		DESY	100%
6.1.3.4	Commissioning and calibration of scanning apparatus		DESY	100%
6.1.3.5	Scanning apparatus operational	Commissionin	DESY	100%
6.1.4	Scanning of sheets with artificial defects		DESY	8%
6.1.4.1	Scanning of sheets with artificial surface defects		DESY	10%
6.1.4.2	Scanning of sheets with artificial bulk defects		DESY	10%
6.1.4.3	Development of algorithm for material defects classification		DESY	0%
6.1.4.4	Classification of defects finished	Status Repor	DESY	0%
6.1.5	Scanning of production sheets		DESY	0%
6.1.5.1	Scanning of sheets of different producers		DESY	0%
6.1.5.2	Identification of defects by (EDX, SURFA etc.)		DESY	0%
6.1.5.3	Conclusive comparison with eddy current data		DESY	0%
6.1.5.4	Final report on SQUID scanning	Final Report	DESY	0%
6.2	Flux gate magnetometry		INFN-LNL	40%
6.2.1	Produce calibration defects		INFN-LNL	41%
6.2.1.1	Production of surface defects		INFN-LNL	100%
6.2.1.2	Production of bulk defects		INFN-LNL	0%
6.2.1.3	Calibration defects finished	Status Repor	INFN-LNL	63%
6.2.2	Design components of flux gate head		INFN-LNL	100%
6.2.2.1	Design electronics		INFN-LNL	100%
6.2.2.2	Design of flux gate head		INFN-LNL	100%
6.2.2.3	Design of operations software		INFN-LNL	100%
6.2.2.4	Design flux gate head finished	Design repor	INFN-LNL	100%
6.2.3	Fabrication of flux gate detector		INFN-LNL	63%
6.2.3.1	Fabrication of flux gate head		INFN-LNL	90%
6.2.3.2	Fabrication of mechanics		INFN-LNL	60%
6.2.3.3	Implementation of software		INFN-LNL	60%
6.2.3.4	Commissioning of flux gate detector		INFN-LNL	30%
6.2.3.5	Calibration of flux gate detector		INFN-LNL	60%
6.2.3.6	Flux gate detector operational	Design report, sta operation	INFN-LNL	58%
6.2.4	Commissioning of flux gate detector		INFN-LNL	0%
6.2.4.1	Operational tuts tests		INFN-LNL	0%
6.2.4.2	Evaluation of test results		INFN-LNL	0%
6.2.4.3	Flux gate scanner commissioned	Status Repor	INFN-LNL	0%
6.2.5	Operation of flux gate detector		INFN-LNL	0%
6.2.5.1	Regular operation		INFN-LNL	0%
6.2.5.2	Report of operation		INFN-LNL	0%
6.2.5.3	Conclusion of flux gate scanning operation	Status Repor	INFN-LNL	0%
6.2.6	Comparison with SQUID scanner		INFN-LNL	0%
6.2.6.1	Compare measurements		INFN-LNL	0%
6.2.6.2	Conclude SQUID scanner vs. flux gate detector	Final Report	INFN-LNL	0%
6.3	DC field emission studies of Nb samples		DESY	6%
6.3.1	Quality control scans		DESY	14%
6.3.1.1	Modification of Scanning apparatus		DESY	100%
6.3.1.2	Calibration of Scanning apparatus		DESY	100%
6.3.1.3	Start scanning activity	Start Operatio	DESY	100%
6.3.1.4	BCP and HPR samples		DESY	30%
6.3.1.5	EP and HPR samples		DESY	10%
6.3.1.6	BCP/EP and DIC samples		DESY	0%
6.3.1.7	First report on BCP/EP and DIC surface	Interim Repor	DESY	0%
6.3.1.8	Continue QA scanning		DESY	0%
6.3.1.9	Evaluation of scanning results	Final Report	DESY	0%
6.3.2	Detailed measurements on strong emitters		DESY	0%
6.3.2.1	Calibrate apparatus for high current		DESY	0%
6.3.2.2	Start strong emitter evaluation	Start Measuremen	DESY	0%
6.3.2.3	I/V curves and current limits		DESY	0%
6.3.2.4	SEM and AES		DESY	0%
6.3.2.5	Influence of heat treatment and ion impact		DESY	0%
6.3.2.6	Evaluate strong emitter investigations	Final Report	DESY	0%

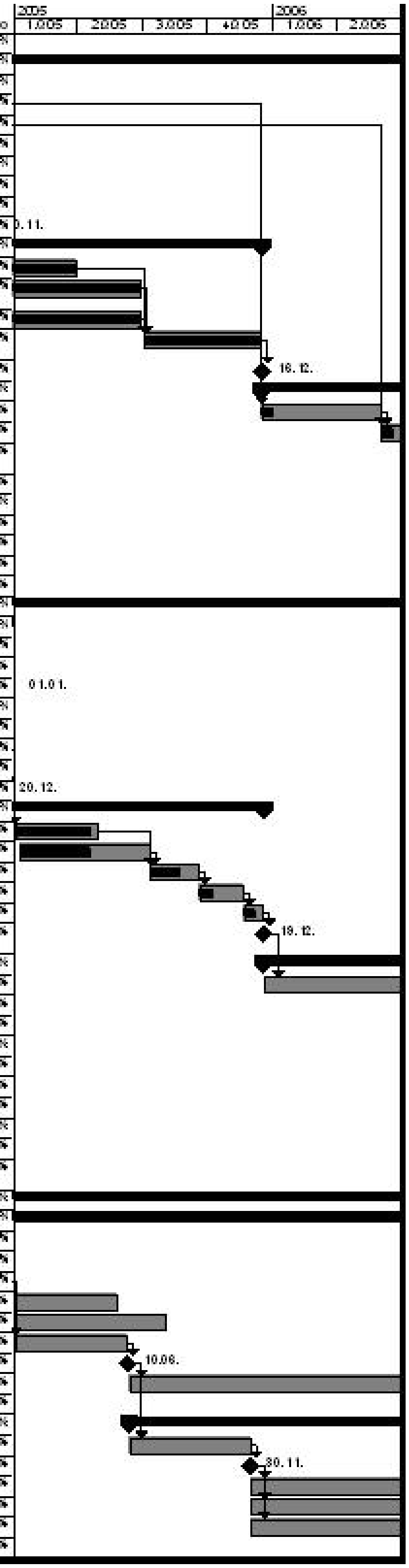

N°	Task Name	MS, Deliverable	Contactor	% schlo
7	WP7 COUPLERS			18%
7.1	New Prototype Coupler		CNRS-Orsay	60%
7.1.1	RF Simulations of Coupler		CNRS-Orsay	100%
7.1.2	Report on Simulation		CNRS-Orsay	100%
7.1.3	Detailed Engineering Drawings		CNRS-Orsay	100%
7.1.4	Engineering complete		CNRS-Orsay	100%
7.1.5	Call for tenders		CNRS-Orsay	100%
7.1.6	Prototype Fabrication in Industry		CNRS-Orsay	0%
7.1.7	Low Power tests		CNRS-Orsay	0%
7.1.8	Ready for High Power Tests	Coupler Prototyp	CNRS-Orsay	0%
7.2	Fabrication of TiN Coating System		CNRS-Orsay	0%
7.2.1	Mechanical design of vacuum chamber		CNRS-Orsay	0%
7.2.2	Fabrication drawings		CNRS-Orsay	0%
7.2.3	Construction of vacuum chamber		CNRS-Orsay	0%
7.2.4	Define vacuum needs		CNRS-Orsay	0%
7.2.5	Appropriation of vacuum equipment		CNRS-Orsay	0%
7.2.6	Design of electronic circuitry		CNRS-Orsay	0%
7.2.7	Fabrication of electronics in industry		CNRS-Orsay	0%
7.2.8	Installation and Test at Orsay		CNRS-Orsay	0%
7.2.9	First Window Coating	Commissionin	CNRS-Orsay	0%
7.3	Conditioning Studies of Proto-type Couplers		CNRS-Orsay	0%
7.3.1	Conditioning of couplers		CNRS-Orsay	0%
7.3.2	Evaluate conditioning results		CNRS-Orsay	0%
7.3.3	Final report on conditioning	Final Report	CNRS-Orsay	0%

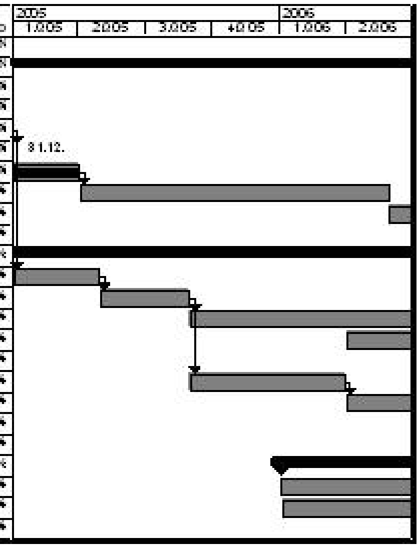

N°	Task Name	MS, Deliverable	Contactor	% schlo
8	WP8 TUNERS			68%
8.1	UMI TUNER		INFN-MI	41%
8.1.1	Control electronics		INFN-MI	100%
8.1.2	Mechanical tuner design, leverage system/motor		INFN-MI	100%
8.1.3	Integration piezo design		INFN-MI	100%
8.1.4	Choice of transducer/actuator		INFN-MI	100%
8.1.5	Report UMI tuner	Design repor	INFN-MI	100%
8.1.6	Tuner fabrication		INFN-MI	70%
8.1.7	Piezo fabrication and bench tests		INFN-MI	0%
8.1.8	Cavity-tuner-coupler integration		INFN-MI	0%
8.1.9	Pulsed RF tests		INFN-MI	0%
8.1.10	Evaluation of tuner operation	Final Report	INFN-MI	0%
8.2	Magneto-strictive Tuner		TUL	61%
8.2.1	Complete specification		TUL	100%
8.2.2	Conceptual design		TUL	100%
8.2.3	Prototype and performance evaluation		TUL	95%
8.2.4	Finalize tuner and drive electronics design		TUL	100%
8.2.5	Test of tuner		TUL	25%
8.2.6	Report on magneto-strictive Tuner	Status repor	TUL	0%
8.3	CEA Tuner		CEA	88%
8.3.1	Design Piezo + Tuning System		CEA	100%
8.3.2	Fabrication		CEA	100%
8.3.3	Installation RF		CEA	100%
8.3.4	Start of Integrated Experiments	Tuner Prototyp	CEA	70%
8.4	IN2P3 Activity		CNRS-Orsay	68%
8.4.1	Characterize actuators/piezo-sensors at low temperature		CNRS-Orsay	100%
8.4.2	Report on actuator/piezo sensor		CNRS-Orsay	80%
8.4.3	Test radiation hardness of piezo tuners		CNRS-Orsay	100%
8.4.4	Report on radiation hardness test		CNRS-Orsay	80%
8.4.5	Integration of piezo and cold tuner		CNRS-Orsay	100%
8.4.6	Cryostat tests		CNRS-Orsay	20%
8.4.7	Tests with pulsed RF		CNRS-Orsay	0%
8.4.8	Report on IN2P3 tuner activities	Final Report	CNRS-Orsay	30%

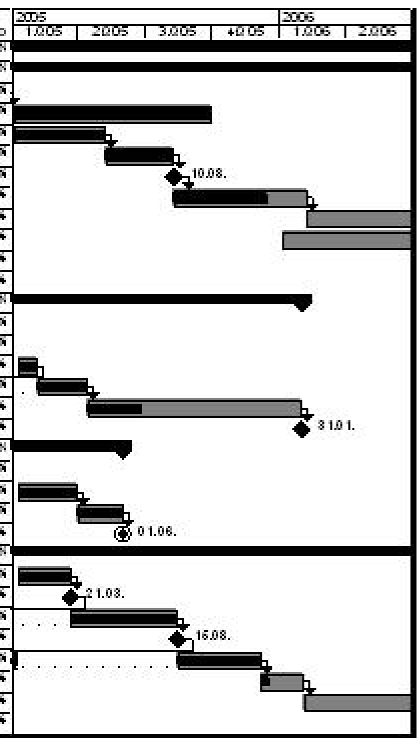

N°	Task Name	MS, Deliverable	Contractor	% Abschlo
9	WP9 LOW LEVEL RF (LLRF)			61%
9.1	Operability and technical performance		DESY	46%
9.1.1	Transient detector		DESY	86%
9.1.1.1	Define requirements		DESY	100%
9.1.12	Electronics design		DESY	100%
9.1.13	Build prototype and evaluate		DESY	100%
9.1.14	Final design of detector		DESY	100%
9.1.15	Installation and commissioning		DESY	100%
9.1.16	Test with beam		DESY	0%
9.1.17	Report on transient detector test	Status Repor	DESY	0%
9.1.2	LLRF Automation		TUL/DESY	60%
9.1.2.1	Dialogue with industrial experts		TUL/DESY	100%
9.1.22	Develop full specification		TUL/DESY	100%
9.1.23	Implement FMS for subsystems		TUL/DESY	100%
9.1.24	Test and evaluation		TUL/DESY	100%
9.1.25	Implement improvements		TUL/DESY	70%
9.1.26	Evaluation and acceptance by operators		TUL/DESY	0%
9.1.27	Report on LLRF atomization design	Status Repor	TUL/DESY	0%
9.1.3	Control optimization		WUT-ISE/DESY	86%
9.1.3.1	Specification of system		WUT-ISE/DESY	100%
9.1.32	Conceptual design of controller		WUT-ISE/DESY	100%
9.1.33	Performance simulation		WUT-ISE/DESY	100%
9.1.34	Implementation in DSP hardware		WUT-ISE/DESY	80%
9.1.35	Implementation and tests on TTF		WUT-ISE/DESY	0%
9.1.36	Evaluation of test results	Status repor	WUT-ISE/DESY	0%
9.1.4	Exceptional handling routines		DESY	67%
9.1.4.1	Specification		DESY	100%
9.1.42	Design of exceptional handler		DESY	100%
9.1.43	Implementation and test on TTF		DESY	60%
9.1.44	Report on exceptional handler operation	Status Repor	DESY	0%
9.2	LLRF cost and reliability study		TUL	44%
9.2.1	Cost and reliability study		TUL	47%
9.2.1.1	Identify cost drivers of present LLRF		TUL	100%
9.2.12	Develop cost reduction ideas		TUL	100%
9.2.13	Build prototypes and evaluate		TUL	100%
9.2.14	Final design of LLRF system		TUL	15%
9.2.15	Complete design of LLRF system for reduced co	Status Repor	TUL	0%
9.2.2	Radiation damage study		TUL	42%
9.2.2.1	Identify critical electronics issues		TUL	100%
9.2.22	Evaluate TESLA radiation		TUL	100%
9.2.23	Develop tests for components		TUL	100%
9.2.24	Procure and assemble test setup		TUL	100%
9.2.25	Data acquisition from radiation tests		TUL	100%
9.2.26	Analyze results and develop countermeasures		TUL	80%
9.2.27	Implement countermeasures and verify		TUL	10%
9.2.28	Report on radiation damage studies	Status Repor	TUL	0%
9.3	Hardware		WUT-ISE	70%
9.3.1	Multichannel downconverter		WUT-ISE	100%
9.3.1.1	Study and compare technologies		WUT-ISE	100%
9.3.12	Select optimum PCB design		WUT-ISE	100%
9.3.13	Build prototype and evaluate		WUT-ISE	100%
9.3.14	Finalize multichannel downconverter		WUT-ISE	100%
9.3.15	Determine characteristics		WUT-ISE	100%
9.3.2	Third generation RF control		WUT-ISE	80%
9.3.2.1	Integrate system generator with VHDL		WUT-ISE	100%
9.3.22	Complete specification		WUT-ISE	100%
9.3.23	Demonstrate simulator		WUT-ISE	100%
9.3.24	Final design of RF electronic board		WUT-ISE	90%
9.3.25	Evaluate performance		WUT-ISE	20%
9.3.3	Stable frequency distribution		WUT-ISE	60%
9.3.3.1	Complete specification		WUT-ISE	100%
9.3.32	Conceptional design of frequency		WUT-ISE	100%
9.3.33	Build prototype and evaluate		WUT-ISE	100%
9.3.34	Final design		WUT-ISE	100%
9.3.35	Procurement and assembly of subsystems		WUT-ISE	100%
9.3.36	Installation and commissioning		WUT-ISE	30%
9.3.37	Performance test with beam		WUT-ISE	0%
9.3.38	Report on new LLRF hardware components	Final Report	WUT-ISE	0%

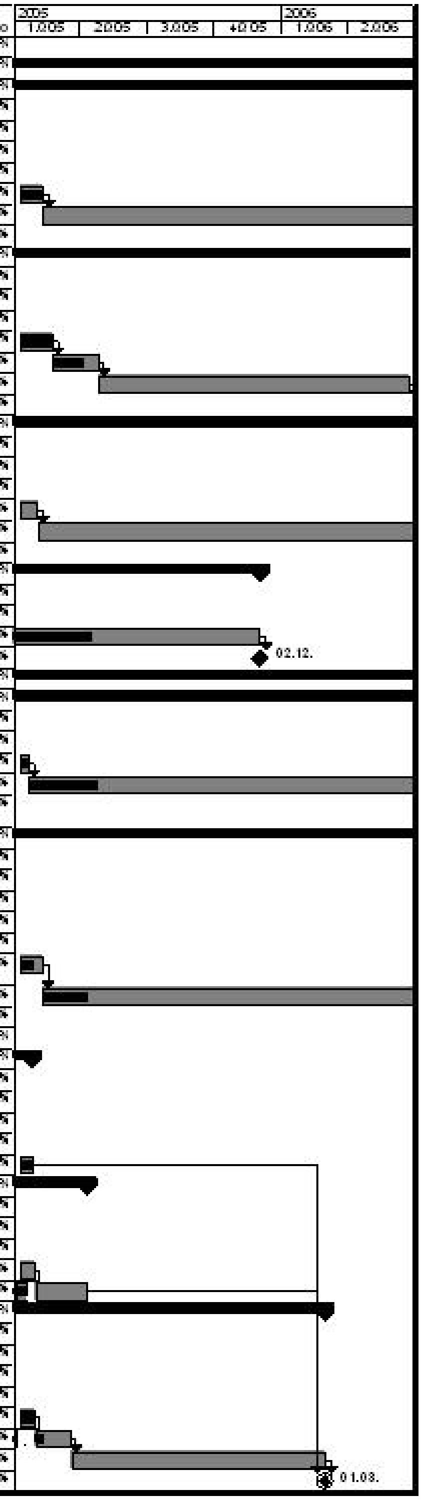

N°	Task Name	MS, Deliverable	Contactor	% :schlo
9.4	Software		TUL/WUT-ISE	64%
9.4.1	Data management development		TUL/WUT-ISE	67%
9.4.1.1	Specification		TUL/WUT-ISE	100%
9.4.1.2	Conceptional design with DOOCS		TUL/WUT-ISE	100%
9.4.1.3	Prototype		TUL/WUT-ISE	100%
9.4.1.4	User evaluation		TUL/WUT-ISE	100%
9.4.1.5	Finalize design		TUL/WUT-ISE	100%
9.4.1.6	Implementation in TTF		TUL/WUT-ISE	20%
9.4.1.7	Report on data management developments	Final Report	TUL/WUT-ISE	0%
9.4.2	RF gun control		PSI/WUT-ISE	47%
9.4.2.1	Write specification		PSI/WUT-ISE	100%
9.4.2.2	Design of controller		PSI/WUT-ISE	100%
9.4.2.3	Procurement and assembly		PSI/WUT-ISE	100%
9.4.2.4	Installation and test		PSI/WUT-ISE	30%
9.4.2.5	Report on RF gun control tests	Final Report	PSI/WUT-ISE	0%

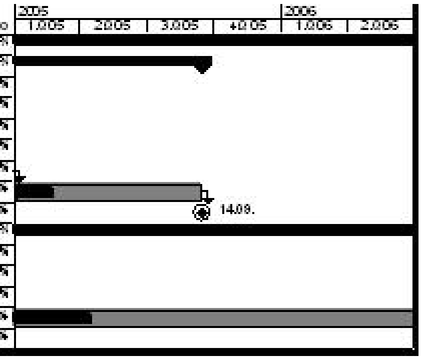

N°	Task Name	MS, Deliverable	Contactor	% :schlo
10	WP10 CRYOSTAT INTEGRATION TESTS			46%
10.1	Displace CRYHOLAB		CEA	0%
10.2	CRYHOLAB adaption to 9 cell		CEA	90%
10.2.1	Mechanical adaption		CEA	100%
10.2.2	Low performance cavity and coupler		CEA	100%
10.2.3	Assembly in CRYHOLAB and cryogenic test		CEA	100%
10.2.4	High performance coupler - High pow er pulsed test		CEA	75%
10.2.5	Magnetic shielding with cryoperm		CEA	0%
10.3	Integration tests in cryostat (1st test)		CEA	0%
10.3.1	CEA Cold Tuning System + Piezo (Assembly + warm test)		CEA	0%
10.3.2	Installation of 9-cell & coupler - Cooldow n		CEA	0%
10.3.3	Cold test in CryHoLab		CEA	0%
10.3.4	**Evaluate experimental results**	Status repor	CEA	0%
10.4	Integration tests in cryostat (2nd test)		CEA	0%
10.4.1	Magnetostrictive tuner		CEA	0%
10.4.2	Evaluate experimental results	Status repor	CEA	0%
10.5	**Integration tests in cryostat (3rd test)**		CEA	0%
10.5.1	Piezoelectric tuner		CEA	0%
10.5.2	Evaluate experimental results	Status repor	CEA	0%
10.6	**Integration tests in cryostat (4th test)**		CEA	0%
10.6.1	**New coupler from LAL**		CEA	0%
10.6.2	**Evaluation of results**		CEA	0%
10.6.3	Final evaluation	Final Report	CEA	0%

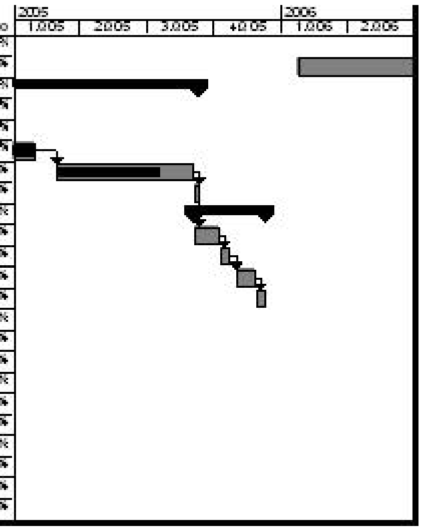

N°	Task Name	MS, Deliverable	Contactor	% :schlo
11	WP11 BEAM DIAGNOSTICS			49%
11.1	Beam position monitor			46%
11.1.1	Present BPM installed in TTF module	Start Measuremen		100%
11.1.2	Cryogenic measurements on BPM			100%
11.1.3	Beamtests of BPM on TTF			60%
11.1.4	Design of BPM Cavity			100%
11.1.5	**Design of BPM cavity ready**			100%
11.1.6	Fabrication of BPM Cavity			0%
11.1.7	**BMP cavity ready**			0%
11.1.8	Development of new hybrid coupler and electronics			100%
11.1.9	Design of Digital Signal Processing			80%
11.1.10	New BPM ready for installation	BPM Prototype		0%
11.1.11	Beam tests with new BPM			0%
11.1.12	Evaluation of BPM operation	Final Report		0%
11.2	Beam Emittance Monitor			64%
11.2.1	Slit width simulations			100%
11.2.2	Slit design			100%
11.2.3	Optics simulations			100%
11.2.4	Optics appropriations			100%
11.2.5	System assembly and tests			100%
11.2.6	Mechanical assembly at TTF			100%
11.2.7	Optical assembly at TTF			100%
11.2.8	Integration of controls into TTF			100%
11.2.9	Ready for beam test in TTF	Start Measuremen		100%
11.2.10	Beamtests at TTF			0%
11.2.11	Evaluate first beamtest result	Status Repor		0%
11.2.12	Successive measurements			0%
11.2.13	Final evaluation	Final Report		0%

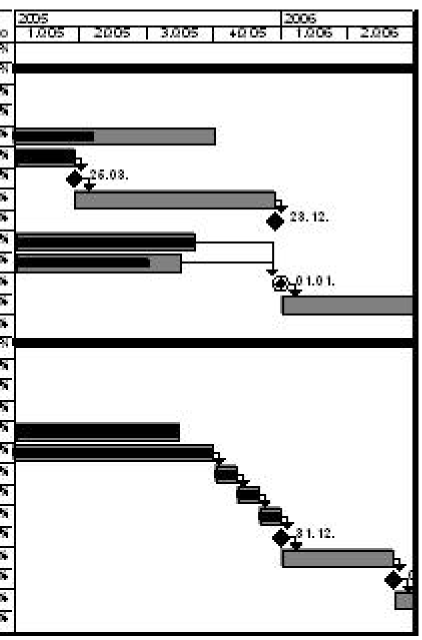

Status of Milestones and Deliverables

			2005 (2nd 12 months)	**Status:**	**Care Annual Meeting 05**			
No.	Task	Milestones and Deliverables	Title	planned end	expected end	Reference	task leader	contrac
1	**2.1.7**	**Final Report (D)**	**Final report on reliability issue**	**31.12.05**	31.12.05	under preparation	L.Lilje	DESY
2	2.2.1.9	Design Report	Report about new design for components	16.09.05	01.11.05	Report Sept. 16, 2005	P.Michelato	INFN-M
3	2.3.2.6	Tools Ready	Tools fabrication finished	11.03.05	01.10.05	Quarter Report 2-05	J.Tiessen	DESY
4	2.3.3.3	Commissioning	Start production welding of components	11.03.05	01.05.05	Quarter Report 1-05	J.Tiessen	DESY
5	3.1.2.5	Commissioning	Spinning machine ready	10.11.05	15.08.05	Quarter Report 2-05	E.Palmieri	INFN-LNL
6	3.2.2.5	Commissioning	Hydro forming machine ready	01.07.05	01.06.05	Quarter Report 2-05	W.Singer	DESY
7	3.2.3.5	Design report	Construction tube necking machine finished	24.02.05	31.19.05	SRF Annual Meeting 05[1]	W.Singer	DESY
8	3.2.4.3	Design report	Seamless tubes ready	01.07.05	15.07.05	Quarter Report 2-05	W.Singer	DESY
9	4.1.1.6	Apparatus ready	Coating apparatus operational	14.03.05	31.07.05	Quarter Report 2-05	J.Langner	IPJ
10	4.1.1.7.3	Hardware ready	Droplet filter ready	31.12.05	30.06.06	Quarter Report 2-05	J.Langner	IPJ
11	4.2.2.4	Status Report	Summary report on quality of planar arc coating	27.05.05	25.05.05	SRF Annual Meeting 05[1]	S.Tazzari	INFN-Ro2
12	**5.1.1.4**	**Final Report (D)**	**Best EP parameters**	**31.03.05**	28.02.06	unexp. results, not finished	C.Antoine	CEA
13	5.1.2.2	Cavities ready	3 cavities fabricated	31.03.05	01.06.05	AnnRep-05	C.Antoine	CEA
14	5.1.3.4	Commissioning	First operation of EP set-up	31.12.05	01.02.06	Lab safety problems	C.Antoine	CEA
15	5.2.1.1.3	Status Report	Proof-of-Principle experiment hot water rinsing	01.11.05	31.01.06		A.Matheisen	DESY

16	5.2.1.2.3	Design report	Electrode design fixed	01.12.05	31.03.06		A.Matheisen	DESY
17	**5.2.1.3.5**	**Final Report (D)**	**Process parameters fixed**	**01.12.05**	31.03.06		A.Matheisen	DESY
18	5.3.1.4	Commissioning	First operation of automated EP	08.02.05	31.07.05	Quarter Report 1-05	E.Palmieri	INFN-LNL
19	5.3.2.4	Status Report	Software ready	21.02.05	31.07.05	Quarter Report 1-05	E.Palmieri	INFN-LNL
20	5.3.4.2	Report	Proposal for alternative electrolytes	24.05.05	31.05.06	work in progress	E.Palmieri	INFN-LNL
21	5.4.1.5	Commissioning	Installation finished	11.04.05	28.02.06	heating to modify	D.Reschke	DESY
22	**5.4.2.4**	**Final Report (D)**	**Cleaning parameters fixed**	**06.10.05**	30.06.06		D.Reschke	DESY
23	6.1.3.5	Commissioning	Scanning apparatus operational	16.12.05	31.07.05	Quarter Report 2-05	W.Singer	DESY
24	6.2.1.3	Status Report	Calibration defects finished	01.01.05	01.01.05	SRF Annual Meeting 05¹	M.Valentino	INFN-LNL
25	6.2.3.6	Start operation	Flux gate detector operational	19.12.05	19.12.05	SRF Annual Meeting 05¹	M.Valentino	INFN-LNL
26	6.3.1.7	Interim Report	First report on BCP/EP and DIC surface	10.06.05	10.06.05	SRF Annual Meeting 05¹	D.Reschke	DESY
27	6.3.2.2	Start Measurements	Start strong emitter evaluation	30.11.05	30.11.05	AnnRep-05	D.Reschke	DESY
28	8.1.5	Design report	Report UMI tuner	10.08.05	01.09.05	SRF Annual Meeting 05¹	A.Bosotti	INFN-
29	8.3.4	Tuner Prototype(D)	Start of Integrated Experiments	01.06.05	31.12.05	AnnRep-05	Boslan,P	CEA
30	8.4.2		Report on actuator/piezo sensor	21.03.05	21.03.05	SRF Legnaro-05	M.Fouaidy	CNRS
31	8.4.4		Report on radiation hardness tests	15.08.05	15.08.05	PAC05	M.Fouaidy	CNRS
32	9.1.4.4	Status Report	Report on exceptional handler operation	02.12.05	02.12.05	AnnRep-05	S.Simrock	DESY
33	9.4.1.7	Final Report	Report on data management	14.09.05	15.12.05	AnnRep-05	T.Jezynski	WUT-

		(D)	developments					ISE
34	10.3.4	Status report	Evaluate experimental results	09.12.05	09.12.05	SRF Annual Meeting 05¹	B.Visentin	CEA
35	11.2.9	Start Measurements	Ready for beam test in TTF	31.12.05	31.12.05	TTF (schedule) delay	M.Castellano	INFN-Fras

SRF Annual Meeting 05¹
= http://www.JRA1-Annual-Meeting-2005.de/

Meetings and Conferences

Date	Title/Subject	Location	Number of attendees	Website address
Jan 24, 2005	WP4	Rome		
Jan 24, 2005	WP8: Magnetostrictive tuner development	DESY, Hamburg	5	

Feb 02, 2005	Telephone Meeting			
Feb 08-09, 2005	WP4	Swierk		
Feb 15, 2005	WP9	DESY		
March 11, 2005	WP8: Preparation of magnetostrictive test characterization	IPN, Orsay	5	
Mar 18, 2005	WP7	Orsay		
Mar 30-Apr 01	Tesla meeting	DESY		
Apr 01, 2005	WP8	Lodz		
May 11, 2005	EP Parameters and Experiences	Argonne USA		none
May 20-21, 2005	WP4: Problems of the current reduction and stabilization, design of new magnetic filters	Rome	6	none
May 16-20, 2005	PAC 2005	Knoxville, Tennessee, USA		http://www.sns.gov/pac05/
May 23-24, 2005	EP Parameter and Experiences	TJNF USA		none
May 30-June 5 2005	WILGA Symposium	Wilga, Poland	120	http://wilga.ise.pw.edu.pl/2005/eng/
June 7, 2005	WP5: Parameters of electro polishing	Saclay		none
June 22-25 2005	12th International Conference MIXDES	Cracow, Poland	150	www.mixdes.org
June 19-23, 2005	ILC European Meeting	London	134	http://www.pp.rhul.ac.uk/workshop/
July 10-15, 2005	SRF Workshop	Cornell, Ithaca. USA	251	http://www.lns.cornell.edu/public/SRF2005/
August 14-27, 2005	ILC Workshop	Snowmass,USA	650	http://www.linearcollider.org/cms/

Aug 13-Sept 2	SPIE 2005	Warzaw, PL	100	http://www.eurocongress.home.pl/Spie2005/
Sept. 19 -	IMAPS 2005	Darlowo, PL	90	http://imaps2005.man.koszalin.pl/

21,2005				
Okt 19-21	Annual SRF Meeting	Legnaro	45	http://jra-srf.desy.de/
Nov 23-25, 2005	Annual CARE05 Meeting	CERN	190	http://hep-lab.web.cern.ch/HEP-lab/CARE05/JRANA.htm
Dec 5-7, 2005	TESLA-Technology Collaboration Meeting	Frascati		http://tesla-new.desy.de/content/index_eng.html

Talks

Title	Speaker/Lab	Event	Date	Web site
Mechanical Vibration Measurements on TTF Cryomodules	A. Bosotti (INFN/LASA)	PAC 05	May 20	http://www.sns.gov/pac05/
Full Characterization at Low Temperature of Piezoelectric Actuators Used for SRF Cavities Active Tuning	M. Fouaidy IPN-Orsay	PAC 05	May 20	http://www.sns.gov/pac05/
Variety of electromechanical Lorentz force compensation systems dedicated for superconducting high field resonant cavities	P. Sekalski DMCS-TUL	Wilga Symposium	May 31	http://wilga.ise.pw.edu.pl/2005/eng/index.ph
Modelling of magnetic channels for micro-droplets filtering and tests of their efficiency in UHV arc-discharges.	P.Strzyzewski, IPJ, Swierk	The 5th International Workshop and Summer School"Towards Fusion Energy – Plasma Physics, Diagnostics, Spin-offs", Kudowa, Poland	June 6-10, 2005	None
Invited talk	W.Singer, DESY	ISOHIM 2005	14.06.05	http://www-conference.slu.se/ISOHIM/
Oral presentation	S. Anakhov, DESY	ISOHIM 2005	16.06.05	http://www-conference.slu.se/ISOHIM/
The Cold Re-entrant Q-BPM Design		ILC Meeting, London	June 2005	http://www.pp.rhul.ac.uk/workshop/
Baking for ILC	B. Visentin / CEA	ILC Meeting, London	June 21st 2005	http://www.pp.rhul.ac.uk/workshop/
Performance of Magnetostrictive Elements at LHe Environment	P. Sekalski DMCS-TUL	MIXDES	June 22	www.mixdes.org

Static and dynamic properties of piezoelectric actuators at low temoerature and integration in SRF cavities cold tuning systems	M. Fouaidy, IPN-Orsay	MIXDES	June 23	www.mixdes.org

Title	Speaker/Lab	Event	Date	Web site
Invited talk	W. Singer, DESY	SRF2005	11.07.05	http://www.lns.cornell.edu/
Piezoelectric stack based system for Lorentz force compensation	P. Sekalski, DMCS-TUL	SRF 2005	July 12	http://www.lns.cornell.edu/public/SRF2005/
High quality Niobium films produced by Ultra High Vacuum Cathodic Arc	R.Russo, INFN-RM2 & Napoli	TFSRF 2005	July 17, 2005	http://www.jlab.org/intralab/calendar/archive05/TFSRF/program.html
Coupler review	T. Garvey / LAL	SRF-2005	July 2005	http://www.lns.cornell.edu/public/SRF2005/
Q-Slope	V.Palmieri	SRF2005	July 12th	http://www.lns.cornell.edu/public/SRF2005/
Flux gate magnetometry	C. Bonavolontà	SRF2005	July 12th	http://www.lns.cornell.edu/public/SRF2005/
Cleanliness techniques	Detlef Reschke, DESY	SRF workshop 2005, Cornell	July, 10th	www.lns.cornell.edu/SRF2005/program.html
Improved Standart Cavity Fabrication	P.Michelato, INFN-Mi	SRF Annual Meeting 05	Oct., 19th	
Automatized EP	Rampazzo, INFN-LNL	SRF Annual Meeting 05	Oct., 19th	
Thin film cavity production	M.Sadowski,	SRF Annual Meeting 05	Oct., 19th	

Seamless by hydroforming	W.Singer, DESY	SRF Annual Meeting 05	Oct., 19th	
Electropolishing in Saclay	Eozenou, CEA	SRF Annual Meeting 05	Oct., 19th	
Surface preparation	A.Matheisen, DESY	SRF Annual Meeting 05	Oct., 19th	
Spinning of seamless cavities	E.Palmieri, INFN -LNL	SRF Annual Meeting 05	Oct., 19th	

Title	Speaker/Lab	Event	Date	Web site
DC Field emission measurements	A.Dangwal, DESY/Univ. Wuppertal	SRF Annual Meeting 05	Oct., 20th	
GMR sensors and Eddy Current techniques applied to cavities	C. Bonavolontà, INFN-LNL/Univ. Naples	SRF Annual Meeting 05	Oct., 20th	
Development of a Piezoelectric Tuner - Preliminary tests on C45 TTF 9-cells Cavity	P.Bosland, CEA	SRF Annual Meeting 05	Oct., 20th	
UMI Tuner for SCRF resonators Design and Fabrication	A.Bosotti, INFN-Milano	SRF Annual Meeting 05	Oct., 20th	
Emittance monitor	M.Castellano, INFN-Frascati	SRF Annual Meeting 05	Oct., 20th	
The Cold Re-entrant BMP	C.Simon, CEA	SRF Annual Meeting 05	Oct., 20th	

Low Level RF	W.Koprek	SRF Annual Meeting 05	Oct., 20th	
R&D on Fast Activ Cold tuning System for SRF cavities	M.Fouaidy, LAL	SRF Annual Meeting 05	Oct., 20th	
Magnetostrictive tuner development and recent results with CTS tuner	P.Sekalski, DMCS-TUL	SRF Annual Meeting 05	Oct., 20th	
Radiation Effects on Electronics	S.Simrock, DESY	SRF Annual Meeting 05	Oct., 20th	
Squid Scanning	S.Singer, DESY	SRF Annual Meeting 05	Oct., 20th	
Power Couplers	A.Varioila, LAL	SRF Annual Meeting 05	Oct., 20th	

Title	Speaker/Lab	Event	Date	Web site
Cryostat Integration Test	B.Visentin, CEA	SRF Annual Meeting 05	Oct., 20th	
Design of a tuning system for high gradient superconducting accelerating cavities	P.Sekalski, DMCS-TUL	CARE Annual Meeting 05	Nov., 23th	http://indico.cern.ch/conferenceDisplay.py?confId=a059
Superconducting RF Cavities for Electron Linear Accelerators	B.Visentin, CEA	CARE Annual Meeting 05	Nov., 23th	http://indico.cern.ch/conferenceDisplay.py?confId=a059
Advances of the Low Level RF control (LLRF) for VUVFEL	S.Simrock, DESY	CARE Annual Meeting 05	Nov., 24th	http://indico.cern.ch/conferenceDisplay.py?confId=a059
Report on SRF Activities	D.Proch, DESY	CARE Annual Meeting 05	Nov., 25th	http://indico.cern.ch/conferenceDisplay.py?confId=a059
Application of multilayer piezoelectric elements for resonant cavity deformation in VUV- FEL DESY accelerator	A.Napieralski, P. Sekalski, DMCS-TUL	IMAPS 2005	Sept., 20th	http://imaps2005.man.koszalin.pl/

Publications

CARE-Pub	Title	Authors	Journal/Conf.
	Research activities within a frame of the CARE-JRA1 Thin film cavity production work-package	J. Langner, M.J. Sadowski, s. Tazzari	ELEKTRONIKA 2-3/2005 p.76
	High quality super-conducting niobium films produced by ultra-high vacuum cathodic arc	R. Russo, L. Catani, A. Cianchi, J. Langner, S. Tazzari	Supercond. Sci. Technol. **18** (2005) L41–44
	Modelling of magnetic channels for micro-droplets filtering and tests of their efficiency in UHV arc-discharges	P. Strzyżewski, J. Langner, R. Mirowski, M.J. Sadowski, S. Tazzari, J, Witkowski	Physica Scripta (2005), in print
	Research on deposition of thin superconducting films for RF accelerator cavities (in Polish)	J. Langner, R. Mirowski, M.J. Sadowski, P. Strzyzewski, J. Witkowski, S. Tazzari, L. Catani, A. Cianchi, J. Lorkiewicz, R. Russo,f. Tazzioli, D. Proch	Elektronika Vol. 50, Nos. 7 (2005) pp. 6 - 11

	Przegląd prac Politechniki Łódzkiej realizowanych w programie CARE - Research overview realized by Technical University of Lodz in CARE framework -	A. Napieralski, M. Grecki, P. Sekalski, D. Makowski, M. Wojtowski, W. Cichalewski, B. Koseda, B. Swiercz,	Elektronika 2/2005, ISSN 0033-2089
	Systemy elektromechaniczne do kompensacji odkształcenia wnęk rezonansowych stosowanych w technologii - TESLA Electromechanical systems for shape compensation of TESLA technology based cavities -	P. Sekalski	Elektronika 7/2005, ISSN 0033-2089
	Single Bunch Transient Detection for the Beam Phase Measurement in Superconducting Accelerators	P.Pawlik, M. Grecki, S. Simrock	DIPAC 2005, Lyon, France, 6th-8th June 2005
	Super–conducting niobium films produced by means of UHV arc	J. Langner, M. J. Sadowski, K. Czaus, R. Mirowski, J. Witkowski, L. Catani, A.Cianchi, R. Russo, S. Tazzari, F.Tazzioli, D. Proch, N.N. Koval, Y.H. Akhmadeev	CARE-Pub-04-004
	Thin superconducting niobium-coatings for RF accelerator cavities; progress in CARE-JRA1-WP4	J.Langner, L.Catani, A.Cianchi, R.Mirowski, J.Lorkiewicz, D.Proch, R.Russo, M.J.Sadowski, P.Strzyżewski, S.Tazzari, J.Witkowski	Proc. SPIE Int. Soc. Opt. Eng. 5948 (2005)

CARE-Pub	Title	Authors	Journal/Conf.
	UHV arc deposition of superconducting niobium filmes for RF application	J.Langne, R.Mirowski, M.J.Sadowski, P.Strzyżewski, J.Witkowski, S.Tazzari, L.Catani, A.Cianchi, J.Lorkiewicz, R.Russo	Advances in Applied Plasma Sciences Vol. 5 (2005)
	Modelling of distributions of magnetic fields used for guiding of plasma stream produced in arc discharges (in Polish)	P.Strzyżewski, J.Langne, R.Mirowski, M.J.Sadowski, S.Tazzari, J.Witkowski	Przegląd Elektrotechniczny (2005) - in print
	System for High Resolution Detection of Beam Induced Transients in RF Signals	P. Pawlik, M. Grecki, S. Simrock	MIXDES 2005, Kraków, Poland, 22-25 June 2005
	The application of SRAM chip as a novel neutron detector	D. Makowski, M. Grecki, B. Mukherjee, S.Simrock, B. Swiercz, A. Napieralski	2005 NSTI Nanotechnology Conference and Trade Show Nanotech 2005, May 2005
	Interpretation of the single event upset in static random access memory chips induced by low energy neutrons	B. Mukherjee, D. Makowski, D. Rybka, M. Grecki, S. Simrock	12th Mixed Design of Integrated Circuits and Systems, MIXDES 2005, June 2005
	SEE induced in SRAM operating in a superconducting electron linear accelerator environment	D.Makowski,B.Murkherjee, M. Grecki, S. Simrock	XIV IEEE-SPIE 2004, May 2004
	SRAM-based passive dosimeter for accelerator environments	D. Makowski, M. Grecki, B. Mukherjee, S.Simrock, B. Swiercz, A. Napieralski	7th European Workshop on Diagnostics and Instrumentation for Particle Accelerators, DIPAC2005, June 2005
	Dosimetry of high energy electron linac produced photoneutrons and the bremsstrahlung gamma rays using TLD-500 and TLD-700 dosimeter pairs	B. Mukherjee, D. Makowski, S. Simrock	Nuclear Instruments and Methods in Physics Research, 2005
	IaradSim - IA32 architecture under high radiation environment simulator	B. Swiercz, D. Makowski, A.Napieralski	2005 NSTI Nanotechnology Conference and Trade Show, Nanotech 2005, Smart Sensors and Systems, May, 2005
	The sCore - Operating System for Research of Fault-Tolerant Computing	B. Swiercz, D. Makowski, A.Napieralski	12th Mixed Design of Integrated Circuits and Systems, Mixdes 2005

Conferences

CARE-Conf	Title	Authors	Journal/Conf.
	Cathodic Arc Grown Niobium Films for RF Superconducting Cavity Applications	A. Cianchi, L. Catani, J. Lorkiewicz, S. Tazzari, J. Langner, R. Mirowski, M.J. Sadowski, P. Strzyżewski, J. Witkowski, A.Andreone, G.Cifariello,E. Di Gennaro, G. Lamura, R. Russo	Proc. SRF2005 Intern. Workshop, Cornell, USA, July 2005 (in print)
	Thin superconducting niobium-coatings for RF accelerator cavities; Progress in CARE-JRA1-WP4	J. Langner, L. Catani, A. Cianchi, R. Mirowski, D. Proch, R. Russo, M.J. Sadowski, P. Strzyżewski, S. Tazzari, and J. Witkowski	Proc. SPIE Intern. Congress on Optics and Optoelectronics, Warsaw, Poland, Aug. 28 – Sept. 2, 2005 – *in print*.
	Improvement of the Blade Tuner Design for Superconducting RF Cavities	Carlo Pagani, Angelo Bosotti, Paolo Michelato, Nicola Panzeri, Paolo Pierini	PAC 05
	Quality Control of the Electro Polishing Process at DESY	N. Steinhau-Kühl, A.Matheisen, B.Meyer, B.Petersen, M.Schmoekel	PAC 05
	Electro-polishing Surface Preparation for High Gradient Cavities at DESY	A.Matheisen, H.Morales, B.Petersen, M.Schmökel, N.Steinhau-Kuehl	PAC 05
	Performance of Magnetostrictive Elements at LHe Environment	M. Grecki, P. Sekalski, DMCS-TUL, C.Albrecht, DESY	12th International Conference MIXDES 2005, pp. 799-802, ISBN 83-919289-9-3.

	The Fast Piezo-Blade Tuner for SCRF Resonators	Carlo Pagani, Angelo Bosotti, Paolo Michelato, Nicola Panzeri, Rocco Paparella, Paolo Pierini, INFN	SRF2005
	Electromechanical, Thermal Properties and Radiation Hardness Tests of Piezoelectric Actuators at Low Temperature	M. Fouaidy, G. Martinet, N. Hammoudi, F. Chatelet, A. Olivier, S. Blivet, H. Saugnac, A. Le Goff, IPN-Orsay	SRF2005 poster
	Progress on spun seamless cavirties	V. Palmieri	Submitted for publication in the Proceedings of SRF2005

CARE-Conf	Title	Authors	Journal/Conf.
	Modelling of magnetic channels for micro-droplets filtering and tests of their efficiency in UHV arc-discharges	P. Strzyżewski, J. Langner, R. Mirowski, M.J. Sadowski, S. Tazzari, J, Witkowski	Proc. 5th Inter. Workshop and Sommer School "Towards Fusion Energy - Plasma Physics, Spin-offs", June 2005
	UHV arc deposition of superconducting niobium films for RF application	J.Langner, R.Mirowski, M.J.Sadowski, P.Strzyżewski, J.Witkowski, S.Tazzari, L.Catani, A.Cianchi, J.Lorkiewicz, R.Russo	Proc. 5th Inter. Symp. on Applied Plasma Sciences, Hawaii, USA, Sept. 2005
	Cold tuning system for 700 MHz elliptical superconducting Cavity for proton accelerator	M. Fouaidy, N. Hammoudi, N. Gandolfo, S. Rousselot, M. Nicolas, P. Szott, S. Blivet, H. Saugnac, S. Bousson, IPN-Orsay	SRF2005 poster
	Advancement in comprehension of the Q-slope for superconducting cavities	V. Palmieri	Submitted for publication in the Proceedings of SRF2005

	Further improvement with dry-ice cleaning on SRF cavities	Arne Brinkmann, Jens Iversen, Detlef Reschke, Jörg Ziegler	SRF 2005 poster
	Efficiency of Electropolishing Versus Bath Composition And Aging: First Results	F. Éozénou, C. Antoine, A. Aspart, S. Berry, JF. Denis, B. Malki	SRF2005, submitted to Physica C
	Aluminium and Sulphur Impurities in Electropolishing Baths	A. Aspart, F. Eozénou, C. Antoine	SRF2005, submitted to Physica C
	RRR of Copper Coating and low temperature electrical resistivity of material for TTF couplers	M. Fouaidy, N. Hammoudi, IPN Orsay S. Prat, LAL	SRF 2005 poster
	Update on the Experiences of Electro Polishing of Multi-Cell Resonators at DESY	N.Steinhau-Kühl, A.Matheisen, L.Lilje, B.Petersen, M.Schmökel, H.Weitkämper	Submitted for publication in the Proceedings of SRF2005
	Quality Control Update of the Clean room for Superconducting Multi Cell Cavities at DESY	N.Krupka, K.Escherich, M.Habermann, K.Harries, A.Matheisen, B.Petersen	Submitted for publication in the Proceedings of SRF2005
	Clean-room facilities for high gradient resonator preparation	K.Escherich, A.Matheisen, N.Krupka, B.Petersen, M.Schmökel	Submitted for publication in the Proceedings of SRF2005
	Full Characterization at Low Temperature of Piezoelectric Actuators used for SRF Cavities Active Tuning	M.Fouaody, G.Martinet, N.Hammoudi, F.Chatelet, S.Blivet, A.Olivier, H.Saugnac	PAC 05

CARE-Conf	**Title**		**Journal/Conf.**
	Fluxgate magnetometry	C.Bonavolontà, V.Palmieri, V.Rampazzo, M. Valentino	Submitted for publication in the Proceedings of SRF2005
	Modelling of the distribution of magnetic fields used for guiding plasma stream produced in vacuum arc discharges (in Polish)	P. Strzyżewski, J. Langner, R. Mirowski, M.J. Sadowski, S. Tazzari, J, Witkowski	Proc. XV General Symposium on Applications of Electromagnetisme in Modern Techniques and

			Informatics, Ciechocinek, Poland, Sept., 2005
	High quality niobium films produced by ultra-high vacuum cathodic arc	R. Russo	First Thin Films Applied to Superconducting RF Workshop, July 17-18, 2005, Jefferson Lab, Newport News,USA
	Application of multilayer piezoelectric elements for resonant cavity deformation in VUV-FEL DESY accelerator	A. Napieralski, P. Sekalski DMCS-TUL	IMAPS 2005
	Research on the use of UHV arc discharges for deposition of superconducting layers	J.Langner, L.Catani, A.Cianchi, J.Lorkiewicz, R.Mirowski, D.Proch, R.Russo, M.J.Sadowski, P.Strzyżewski, S.Tazzari, J.Witkowski	Proc. Inter, Conf. PLASMA-2005, Opole, Poland, Sept. 2005
	Behaviour of gas conditions during vacuum arc discharges used for deposition of thin films	P.Strzyżewski, L.Catani, A.Cianchi, J.Langner, J.Lorkiewicz, R.Mirowski, R.Russo, M.J.Sadowski, S.Tazzari, J.Witkowski	Proc. Inter, Conf. PLASMA-2005, Opole, Poland, Sept. 2005
	CARE activities on superconducting RF cavities at INFN Milan	A. Bosotti, P. Pierini, P. Michelato, R. Paparella, N. Panzeri, L. Monaco, R. Paulon, M. Novati, INFN, C. Pagani, DESY	SPIE Conference, Warsaw, Poland
	Piezoelectric stack based system for Lorent force compensation caused by high field in superconducting cavities	P. Sekalski, A. Napieralski, DMCS-TUL, S.Simrock, DESY	SRF 2005 poster

Notes

CARE-Note	Title	Authors	CARE-Note
	SC Cavity SIMCON User's Manual	K. T. Pozniak, T. Czarski, W. Koprek, R.S. Romaniuk	TESLA Report 2005-02
	Design of eight channel 81 MHz IF downconverter board in digital RF feedback system for TTF2	T. Filipek, G. Moeller, H. Weddig, S. Simrock, R. Romaniuk, K. Pozniak	TESLA Report 2005-03
	Modular & reconfigurable common PCB-platform of FPGA based LLRF control system for TESLA test facility	K. T. Pozniak, R. S. Romaniuk K. Kierzkowski	TESLA Report 2005-04
	Software Layer for SIMCON ver. 1.1 FPGA based TESLA cavity control system User's Manual	W. Koprek, P. Kaleta, J. Szewinski, K.T. Pozniak R. S. Romaniuk	TESLA Report 2005-05
	First Generation of Optical Fiber Phase Reference Distribution System for TESLA	K. Czuba, F. Eints, M. Felber, J. Dobrowolski, S. Simrock	TESLA Report 2005-08
	FPGA based,full-duplex,multi-channel, optical Gigabit, synchronous Data transceiver for TESLA technology LLRF control system	K.T. Pozniak,R.S. Romaniuk,W. Jalmuzna, K. Olowski, K. Perkuszewski, J. Zielinski, K. Kierzkowski	TESLA Report 2005-07
	DSP Integrated, Parameterized, FPGA based Cavity Simulator&Controller for VUV-FEL	W. Koprek, P. Pucyk, T. Czarski, K.T. Pozniak, R.S. Romaniuk	TESLA Report 2005-06
	CHECHIA cavity driving with FPGA controller	T. Czarski, W. Koprek, K.T. Pozniak, R.S. Romaniuk, S. Simrock	TESLA Report 2005-12
	Milestone Report: Construction tube necking machine (WP Task 3.2, 3.5)	W. Singer	SRF Annual Meeting 05

	DOOCS environment for FPGA-based cavity control system and control algorithms development	P. Pucyk, W. Koprek, P. Kaleta, J. Szewinski, K.T. Pozniak, T. Czarski, R.S. Romaniuk	TESLA Report 2005-13
	Design of the Re-entrant Cold BPM	M. Luong, G. Congretel, M. Jablonka, C. Magne, C. Simon	CARE-Note-2005-002-SRF
	Improved standard cavity fabrication	P. Michelato, L. Monaco, R. Paulon	CARE-Note-2005-003-SRF

CARE-Note	Title	Authors	CARE-Note
	Mechanical study of the “Saclay piezo tuner” PTS (Piezo Tuning System)	P. Bosland, Bo Wu, DAPNIA - CEA Saclay	CARE-Note-2005-004-SRF
	DC Field Emission Scanning Measurements on Electropolished Niobium Samples	Arti Dangwal DESY/Uni Wuppertal, Günter Müller Uni Wuppertal, Detlef Reschke DESY	SRF2005, to be published
	FPGA based, DSP integrated, 8.channel SIMCON, ver.3.0	W.Giergusiewicz, W.Koprek, W.Jalmuzna,K.T.Kpozniak.R.S.Romaniuk	TESLA Report 2005-14
	Report on Fast Piezo Blade Tuner (UMI Tuner) for SCRF Resonators Design and Fabrication **(8.1.5 Milestone)**	C.Pagani, A.Bosotti, P.Michelato, R.Paparella, N.Panzeri, P.Pierini, F.Puricelli, INFN Milano, G.Corniani, ZANON, Schio,Italy	CARE-Note-2005-XXX-SRF
	Final Report for New Components: Cold Flanges	P.Michelato, L.Monaco, N.Panzeri	CARE-Note-2005-XXX-SRF
	PI piezo Life Time Test Report	A. Bosotti, R. Paparella, F. Puricelli, INFN	CARE-Note-2005-XXX-SRF
	Revue des tolerances geometriques et cotation fonctionelle sur les ensembles froid ez chaud du coupleur de puissance de type TTF-3	A. Gonnin	CARE-Note-2005-XXX-SRF

Report of the review conducted by the International Advisory Committee for JRA-SRF

(Review conducted at the annual JRA-SRF meeting in Legnaro, 19-21 October, 2005).

The composition of the committee is as follows:

Hasan Padamsee (Cornell, chair)
Isidoro Campisi (Oak Ridge National Laboratory)
Peter Kneisel (Thomas Jefferson National Laboratory)
Jens Knobloch (BESSY)
Wolfgang Weingarten (CERN), not present for this meeting.

We reviewed 10 work packages (plus management) spanning three classes of projects with different ranges of benefits. Projects with a short-term impact are designed to benefit TTF-II operation. These are low-level RF, beam diagnostics. Projects likely to have a medium term impact are squid and magnetometer pre-scanning of niobium sheets, studies to improve the understanding of electro-polishing, and optimize parameters, dry-ice cleaning, field emission scanning of monitor samples, analyzing the performance of existing cryo-modules, advances in couplers and tuners, and Cryoholab to test tuners and couplers. Projects that are likely to have a long-term impact include development of spinning and hydroforming multi-cell cavities, and vacuum-arc deposition of Nb films on copper cavities with an even a longer outlook.

Among the several highlights there were impressive low-level RF accomplishments to complete the next generation prototype with tests, basic electropolishing studies to improve understanding, tuner studies to characterize the piezo and magnetostrictive devices, and the procurement of new couplers from industry.

The committee was pleased to see many projects cross important milestones for success. 14 milestones were successfully completed. The average delay of the remaining 13 milestones is about 5 months. All deliverables to date are complete except one. A new CARE website will be a useful server for reports, publications and other documents

The committee was pleased to see contributions from many new and young talented scientists and engineers all over Europe. A special effort will be needed to keep the LLRF team from Poland strongly engaged in future implementation and development.

Some work packages have completed commissioning of new apparatus, such as field emission scanning, spinning and vac-arc deposition. These projects are now ready to start needed studies. We recommend careful thought be given to prepare a list of studies that will now be most useful to carry out. For example since the scan rate of field emission is slow, we recommend scanning a careful selection of samples, for example those which will follow the preparation sequence of cavities that show strong field emission. Many of the long-term studies will require single cell tests, and good planning will be necessary to avoid a bottleneck. We eagerly await the results of such studies.

Detailed Comments

Reliability analysis of WP2 remains important to improve our understanding of variations in cavity performance and module performance. These studies deserve an additional impetus because of their far-reaching consequences.

Flange sealing studies increase confidence in the adopted geometry of the gaskets and the bolting procedures. Although nuts/bolts flanges may be workable for the X-FEL (1000 cavities) in the longer range (for ILC) it may be worthwhile to explore new flange options that will reduce the number of nuts and bolts.

Beam position monitoring is making good progress. There is a clear need for clean compatible and compact devices. Using dipole HOMs as BPM is also making good progress and should be pursued in further TTF studies.

The SQUID scanning system is nearing readiness. It should help provide a much cleaner scan to detect real defects and differentiate these from surface scratches and pits. The less expensive magnetometer scanning with new device has passed the proof-of-principle stage,and shows promise.

New apparatus for spinning and hydroforming 3-cell units are in place. Both techniques have benefited and can continue to benefit from each other's experience. For example, the hydroforming team has introduced "necking" in the iris region, which is actually spinning. They are also annealing (at 800 C) the Nb tube before hydroforming. The spinning team may benefit from the annealing step to reduce the formation of fissures.

With the new interest in large grain and single grain Nb, it may be of interest to try both spinning and hydroforming with these materials, especially in view of the large elongation properties.

There has been much progress in vacuum-arc deposition. A single cell 1500 MHz cavity has been coated for demonstration of the apparatus. The copper cavity needs to be cleaned by state-of-art methods, developed by CERN and others. Techniques to screen droplets have been devised on both set-ups and implemented on the planar set-up. First RF measurements have been made for planar arc samples.

Further Recommendations

Provide a template for a uniform reports for the various work-packages.

The LLRF has made excellent progress on the 3rd generation. But the main advances of this generation should be made clear.

Every effort should be made to carry out a test on the 9-cell spun cavity as soon as possible.

The suggestion of spinning stiffening rings into the cell should be tried out.

Hot water rinsing is carried out at Henkel Company. A definitive conclusion is needed about the pros and cons of this procedure.

The IAC needs to be expanded to include an expert in beam diagnostics and low-level RF.

Work Package 2: Improved Standard Cavity Fabrication.
Improved Standard Cavity Fabrication (ISCF) aims at improving the present cavity fabrication technology. It is based on the operating experience with superconducting cavities in the TTF test linac.
There is an obvious need to modify at least partially the cavity design and the preparation procedures to improve the performance and reliability of the SRF accelerating system. The tasks foreseen in WP2 are relative to reliability analysis, improved component design and electron beam (EB) welding procedures.

Activity status

Task 2.1: Reliability analysis

The activity relative to the reliability is progressing with some delays, primarily due to the time consuming phase of information retrieval and analysis. Correlations between the cavity performance degradation, from the vertical test to the string behavior in the cryomodule, with the number of problems encountered during the assembly procedure have been highlighted. This indicates that the reduction of problems during the cryomodule assembly would produce a reduction of this effect.

Task 2.2: Improved component design

An analysis of main ancillaries of SRF cavities has been done to highlight possible critical points in achieving both better performance and higher reliability for future large accelerator facilities such as like ILC (International Linear Collider). In February 2005, the milestone 2.2.1.3 was met with the delivery of the document "*Summary report on the status of art on ancillaries on the experience of various laboratories involved in SC RF*" (CARE-Note-2005-003-SRF).
Among the main ancillaries of a SRF cavity, cold flange connections play a crucial role and an improvement of their reliability is required for the future SRF accelerator structures where several thousands of cold flanges will be used. Therefore, the reliability of the seal, the reduction of costs of flanges and seals, the decrease of seal assembly and tightening time, the shortening of the junction dimensions and the increase of the machine filling factor are key points.
A critical analysis of the TESLA beamline connection flanges at room and at cryogenic temperature, with dedicated experimental measurements and the development of a model for FEM analysis has been performed this year. Results so far obtained give information on their behavior, on the leak tightening limit etc. The main result, after the experimental validation of the model, is the possibility to study the joint behavior changing the compression force, the groove and seal geometry, the gasket material, etc. The milestone 2.2.1.14, -Final report for new components-, can be considered fulfilled with the delivery of the CARE Note "Final Reports for new components: Cold Flanges" (October 25, 2005).
A description of the activities performed for the analysis of the TESLA beamline flange behavior is presented.
During the flange assembly, the torque of bolts and nuts produce the load on the sealing gasket. The force applied on the seal depends on the friction coefficients between bolts, nuts and washers. In order to decouple the applied load from the friction coefficient, we load, in a controlled way, the seal with a material testing machine (Instron, maximum load 200 kN) measuring the leak rate and the mechanical properties of the gasket. Two different aluminum alloys have been used for the gaskets: Al5754 (also called AlMg3) and Al6060. The alloys composition has been verified by ICP spectrophotometry.

Some pictures and a sketch of the measurement set up are shown in Figure 2.1.

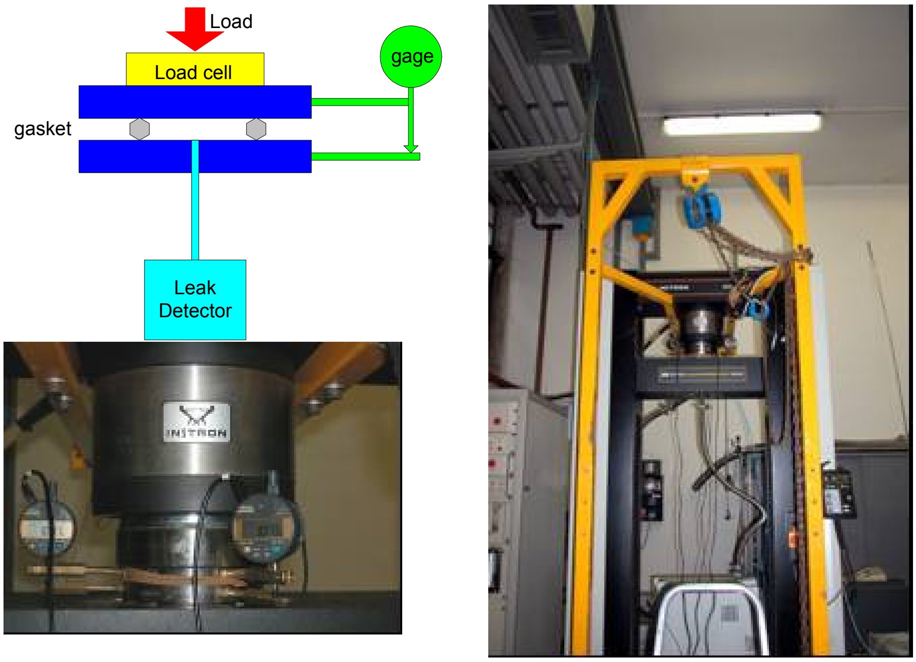

Figure 2.1: Sketch and pictures of the apparatus used for compression and leak tests of TTF flange and gasket. Maximum load 200 kN. The leak detector is connected to the bottom flange

The mechanical properties of the gasket are summarized in the displacement vs. load graphs shown in **Erreur ! Source du renvoi introuvable.**.2. Due to the different material, G18 and G20 (Al5754) gaskets show, for the same load, larger compression.

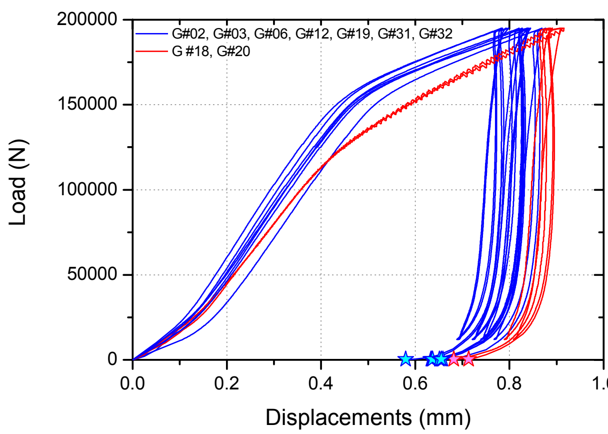

Figure 2.2: comparison of different seals during the load test

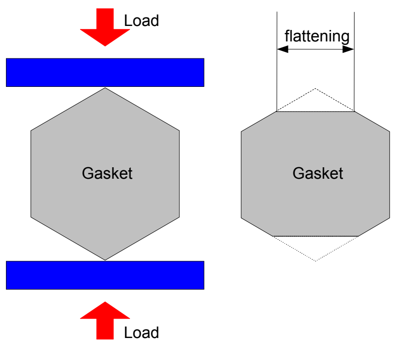

Figure 3: gasket flattening

Usually the linear force and the pressure applied to the seal are the parameters that have to be carefully investigated to characterize the quality of a seal. For this purpose, we perform a series of tests to evaluate the gasket flattening (see **Erreur ! Source du renvoi introuvable.**) as a function of the applied load. Using these data we calculate the pressure applied on the gasket.

Figure 2.4 shows typical data for the two aluminium alloys considered. The gasket flattening increases linearly with the load and hence the pressure stays constant. At about 30 kN, the tightness of the seal is generated (the pressure on the seal is about 560 MPa).

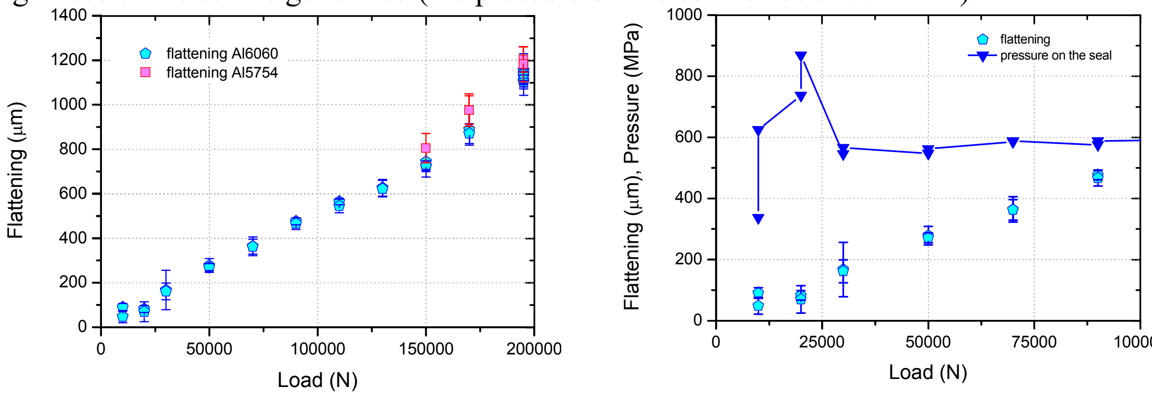

Figure 2.4: Gasket flattening and pressure on the seal.

During compression measurements, leak tests have been performed in order to study the generation of the seal and the behavior of the leak rate vs. the load applied to the flanges. The leak test starts at the early beginning of the seal generation, and, in these conditions, the leak rate is quite high: this produces in some measurements a strong He background signal, whose subtraction reflects some uncertainty in the leak test. As an example the leak behavior during a compression test is shown (gasket G #03 - Al6060) in Figure 2.5.

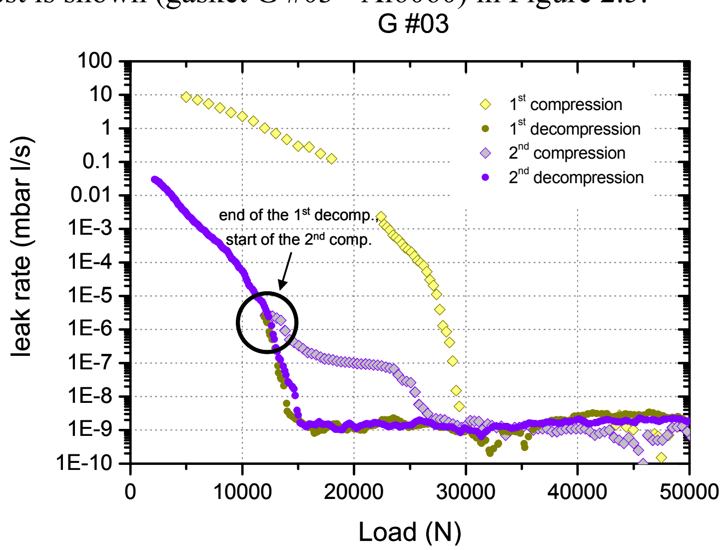

Figure 2.5: leak rate measurement during compression and decompression test.

The results obtained applying the mechanical test machine have been used to predict the behavior of the joint (flange/gasket system) under standard operation, where bolt and nuts are used. Figure 2.6 shows the experimental setup for these measurements.

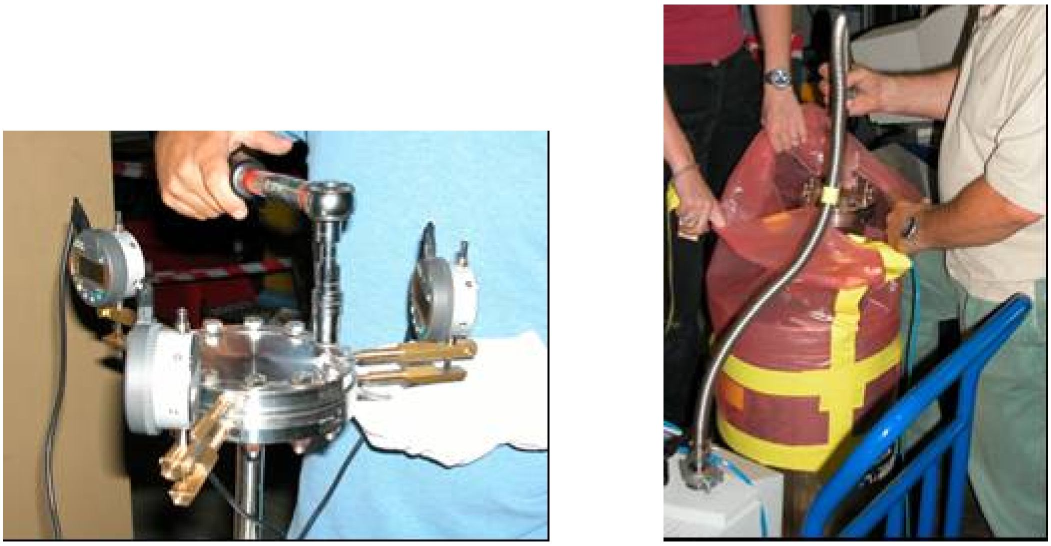

Figure 2.6: bolt tightening with torque meter and liquid nitrogen temperature leak test.

By comparing the measurement of the permanent squashing produced during the Instron tests with the one obtained from the manual tightening of the flange, we were able to obtain the torque-compression - force relation and therefore the friction coefficient between the stainless steel bolts and CuNiSil nuts in our particular conditions (see Figure 2.7).

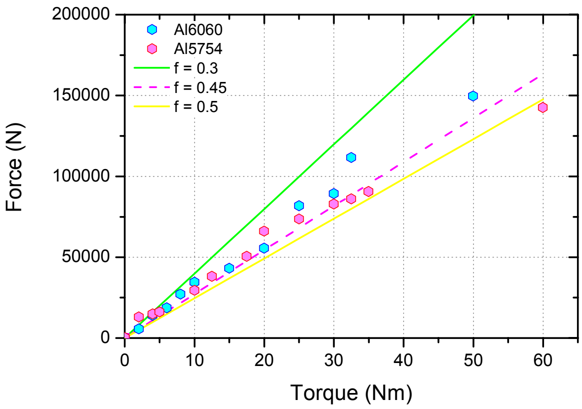

Figure 2.7: experimental relation between torque and compression force.

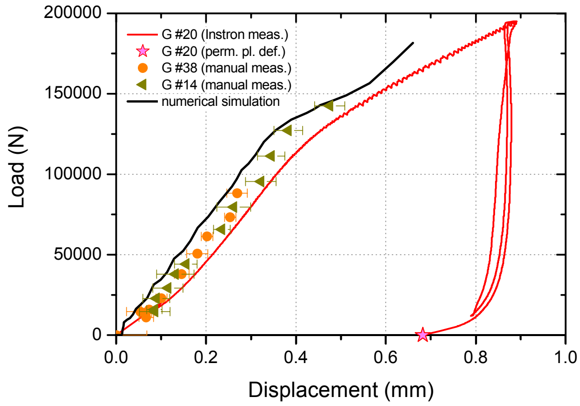

Figure 2.8: comparison between the numerical model results and the experimental data.

The test results allowed to validate a finite element model of the connection (see Figure 2.8). This can be used for future study and optimization of new seal geometry and material.

Task 2.3 Electron Beam welding

The UHV-Motor has been delivered and tested for UHV-capability. The desorption rate after 100 h pumping is $5{\cdot}10^{-6}$ mbar·l/s. We judge the residual gas analysis as good. The construction for the mechanical conversion is in the final phase.
In the first stage of expansion the y-drive will be operated by hand. The integration in the PLC will be the next step.

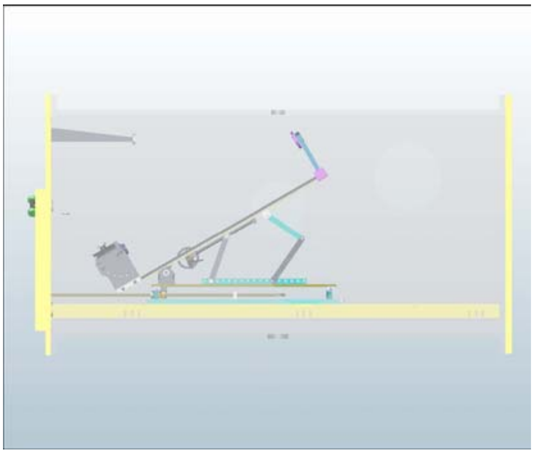

Figure 2.9: tilt fixture for 45°-seams

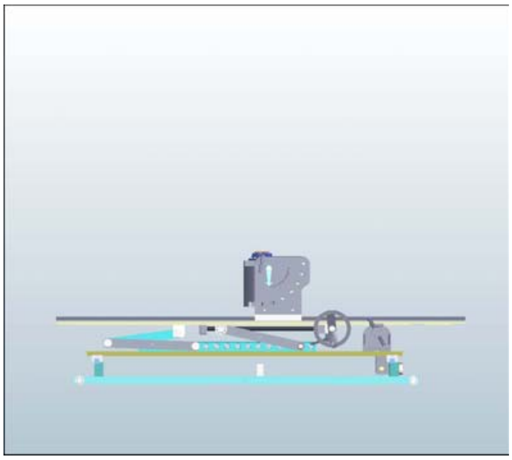

Figure 2.10: carousel operation for front seams

Work package 3: Seamless Cavity Production

Task 3.1 Seamless cavity production by spinning

The spinning machine has been finished and it is working perfectly. The new set of rollers still need to be done, but since the material used for rollers is very expensive, the rollers will be fabricated after the end of the machine commissioning. This will allow us to do some modifications to the rollers on the basis of the acquired experience.
The new machine is equipped with a more powerful hydraulic station, in order to achieve higher values of pressure between the lathe tailstock and headstock. This enables us to get a higher wall thickness at the cavity iris. Indeed, for long time, a thin wall at the cavity iris has represented a problem for seamless fabrication.
Since the machine is more powerful, all the spinning parameters must be changed. Higher values of the pressure applied to the rollers, and higher compression pressure along the axis of the cavity require a lower number of spinning steps. Indeed, through the standard procedure developed before, we helped the plastic deformation process increasing the number of spinning steps. However, the higher is the number spinning steps, the more the material hardens, increasing the risk of fracture propagations. The evaluation of spinning parameters is a long procedure and a lot of attention must be paid on the preparation of samples.
The support system and turning mechanism, while swaging the cavity, is working but it is only temporary, since we are evaluating the possibility of using different rollers with a cavity-roller contact area that is much higher than the standard one. Of course, this will dramatically change the spinning parameters.
In short, the milestones of a drawing spinning machine was reached already some time ago; the milestone of having the spinning machine ready is almost achieved apart from the commissioning, as the assembly of the machine is already finished but is still suitable for modifications. The evaluation of spinning parameters has only started and it will be the longest operation of the whole of task 3.1.

Fig. 3.1: Phase of the double turret necking process during the spinning parameter definition action.

Task 3.2: Seamless cavity production by hydroforming

Activity status
The tube necking machine was successfully constructed according to schedule. A photograph and a schematic are shown in Fig. 3.2 and Fig. 3.3.

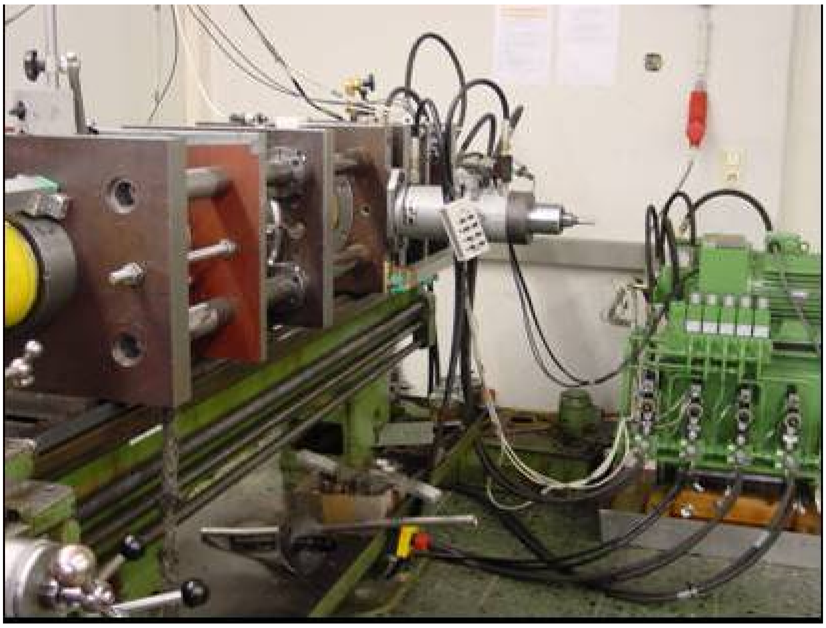

Fig. 3.2: View of the tube necking machine

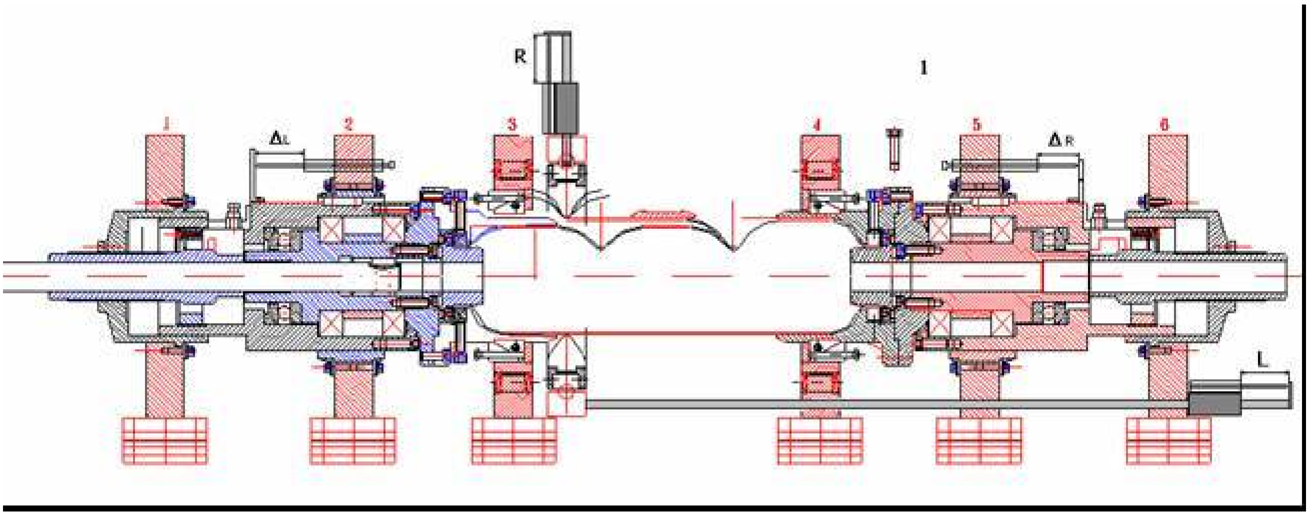

Fig.3.3. Schematic of the tube necking machine (cross section)

The machine is foreseen for necking of Nb and NbCu tubes with internal diameters (ID) of 130 and 150 mm. The diameter should be reduced to 75.6 or 83.6 mm.
The machine consists of seven transversally oriented plates. Several hydraulic cylinders are fixed on the plates:

- Left and right cylinder for the application of axial pressure. Cylinder parameters: diameter 150 mm, stroke 125 mm, pressure 200 bar
- Cylinder for movement of the central plate. Cylinder parameters: diameter 100 mm, stroke 600 mm, pressure 200 bar

- Cylinder for movement of the instrument. Cylinder parameters: diameter 100 mm, stroke 45 mm, pressure 200 bar

All plates connected to each other using four bars of diameter 50 mm. Bars fixed on end plates. All cylinders equipped with position and pressure sensors.
The necking machine is fixed on the lathe. The tube rotation is caused by lathe mechanism. The machine is PC controlled. Two options of the software are created for two types of the tube necking (see Appendix 1 and 2):
Option 1: necking of the tube end to diameter of 75.6 or 83.6 mm (Software Neckend)
Option 2: necking of the tube middle (iris) to diameter of 75.6 mm (software Neckiris)
The first experiments have shown a good function of the machine. The necking of the Cu tubes both at the tube end and at the tube middle (iris) was successfully implemented (see figure 3.4). The optimization of the necking parameters is going on.

Fig. 3.4. Necking at the tube end and tube middle implemented by necking machine.

Fig. 3.5: View of the hydroforming machine

In the frame of the task 3.2 the hydroforming machine was provided with new moulds for fabrication of multi cells and also with water hydraulic system for the internal pressure in the tube and with oil hydraulic system for the cylinder movements. The developed computer control system for the hydroforming allows the hydraulic expansion in stepwise as well as in continuous regime. A view of the machine can be seen in Fig. 3.5. The construction of the hydroforming machine is finished and first tests for commissioning of the machine are going on.

The multi cell seamless cavities are planned to be fabricated starting both from the tube with inside diameter ID=130 mm and ID=150 mm.

The main principles for the production of seamless niobium tubes for hydroforming are developed in cooperation with scientific institutes and industrial companies.

Fig. 3.6 Seamless niobium tubes for cavity fabrication by hydroforming

The seamless tubes are built starting from the thick sheet having already rather small and uniform grain structure. Tubes are produced by combination of spinning and flow forming (Fig. 3.6). Combination of spinning with flow forming allows improving the surface and significantly reducing the wall thickness variations. Flow forming was done in forward direction (Fig. 3). This method allows producing tube with wall thickness tolerances of +/- 0.15 mm what should be sufficient for subsequent hydroforming.

Fig. 3.7. Flow forming of the seamless niobium tubes

Work Package 4: Thin Film Cavity Production

Task 4.1 – Linear Arc Cathode Coating

Milestones and deliverables of the reporting period

No milestones were planned for the year 2005.

Activity status

Task 4.1 is focused on the development of an UHV arc system with the linear (cylindrical) cathode configuration. The principal scheme of the cavity coating by means of the linear (cylindrical) arc discharge and the modified linear-arc facility, which was put into operation in 2004, is presented in Fig. 4.1.

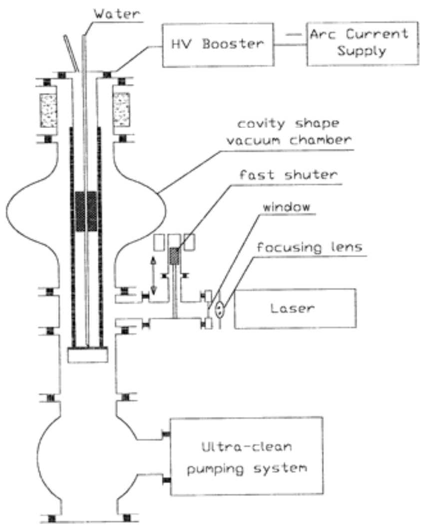

Fig.4.1. Scheme of the linear-arc UHV system and modified linear-arc facility at IPJ (Swierk).

In 2005 studies of the arc-current reduction and stabilization were performed with the use of a stainless-steel chamber of the shape and dimensions similar to an original single TESLA RF-cell. That chamber was equipped with two main flanges, which are used as connections with the UHV pumping stand (at the bottom) and a magnet driving system (at the top); and four side-on (radial) diagnostic ports distributed symmetrically in the central symmetry plane of the cell, where the distance between the cathode and wall of the cell is the largest.

Since the cleanliness of deposition processes plays a crucial role during the formation of thin superconducting niobium layers, in order to achieve high-quality superconducting films particular attention was paid to the initial vacuum conditions. The residual gas pressure, and particularly the partial pressures of water, nitrogen, oxygen, CO_2, hydro-carbides etc., were reduced by the construction and operation of the linear-arc facility according to requirements of the UHV technology. The vacuum pumping stand was constructed as a completely oil-free system and the whole facility was equipped with appropriate heaters and supply units for baking. Due to the baking it was possible to achieve a final pressure of 1.5×10^{-10} mbar, and to reduce the amount of impurities, as shown in Fig. 4.2.

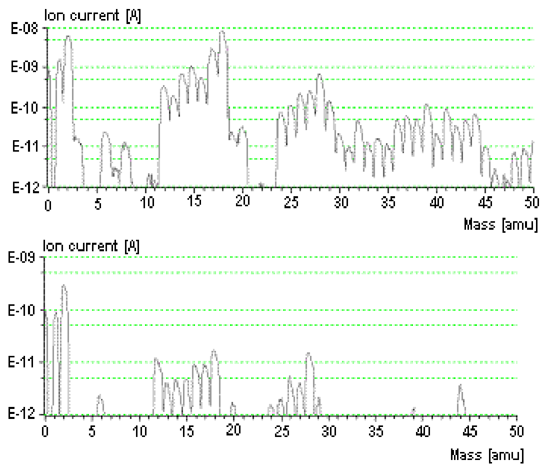

Fig. 4.2 Typical RGA mass-spectra recorded within the linear-arc facility, as recorded before and after 24-hour baking at 150 ^{0}C.

Studies of the current reduction and stabilization have been performed by means of a new power supply unit and a special solid-magnet system, which was placed inside the cathode tube in order to drive the arc discharge along the cathode surface. These studies have been completed (according to the updated schedule), and stable discharges can be produced at a current reduced to about 70 A. Measurements performed with the ion-current collector, placed at a distance corresponding to the cell wall, have shown that, for the investigated operational conditions, the ion-current density amounts to 50-80 mA/cm^2.

The optimization of the powering system was performed and the apparatus for single cell coating was put into operation in July 2005. The parameters of this power-supply are as follows: the maximum current I_{max} = 350 A, booster voltage V_b = 200 V, PC control, and DC or pulsed-operation. A general view of a new DC/pulse supply unit is presented in Fig. 4.3.

Fig 4.3. A new DC/pulse power-supply for the linear-arc facility.

In order to make the linear-arc facility operational for the single-cavity coating, two TESLA-type cavities made of pure copper have been prepared by means of EB welding. They have been equipped with standard flanges and installed at the modified UHV linear-arc facility, as shown in Fig. 4.4.

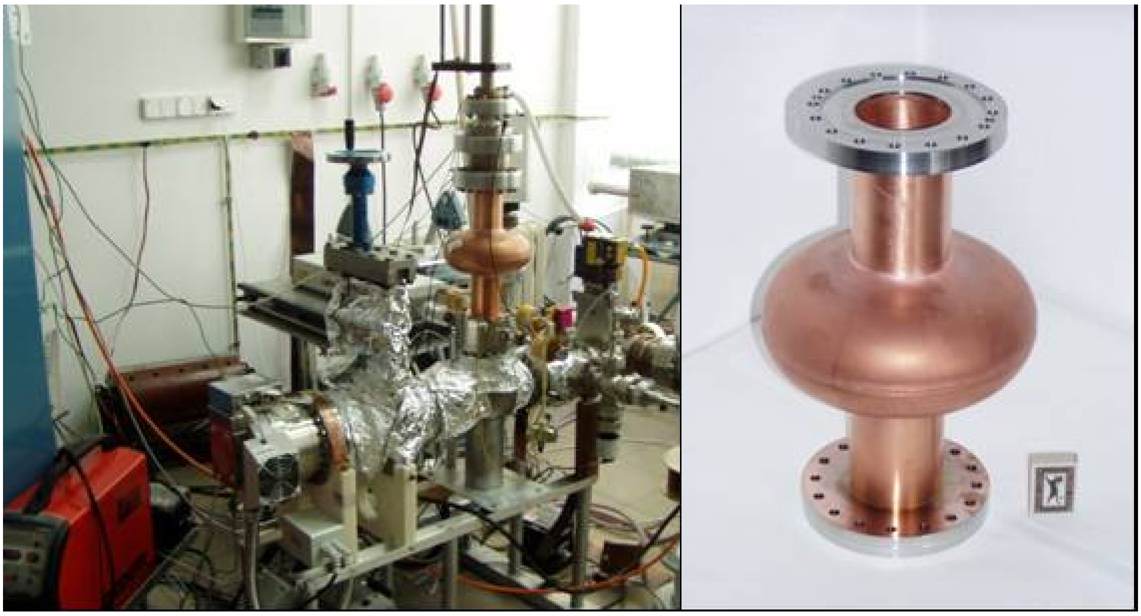

Fig. 4.4. Single copper-cavity with end flanges and the modified UHV linear-arc system during laboratory tests of the single-cavity coating.

The temporal behavior of the discharge current in the UHV linear-arc facility without magnetic filtering was studied. The maximum arc current amounted to about 100 A, and the period of the cathode-spot motion (around the cylindrical cathode) was found to be 20 ms. Oscillogrammes of the arc current were recorded, as shown in Fig. 4.5.

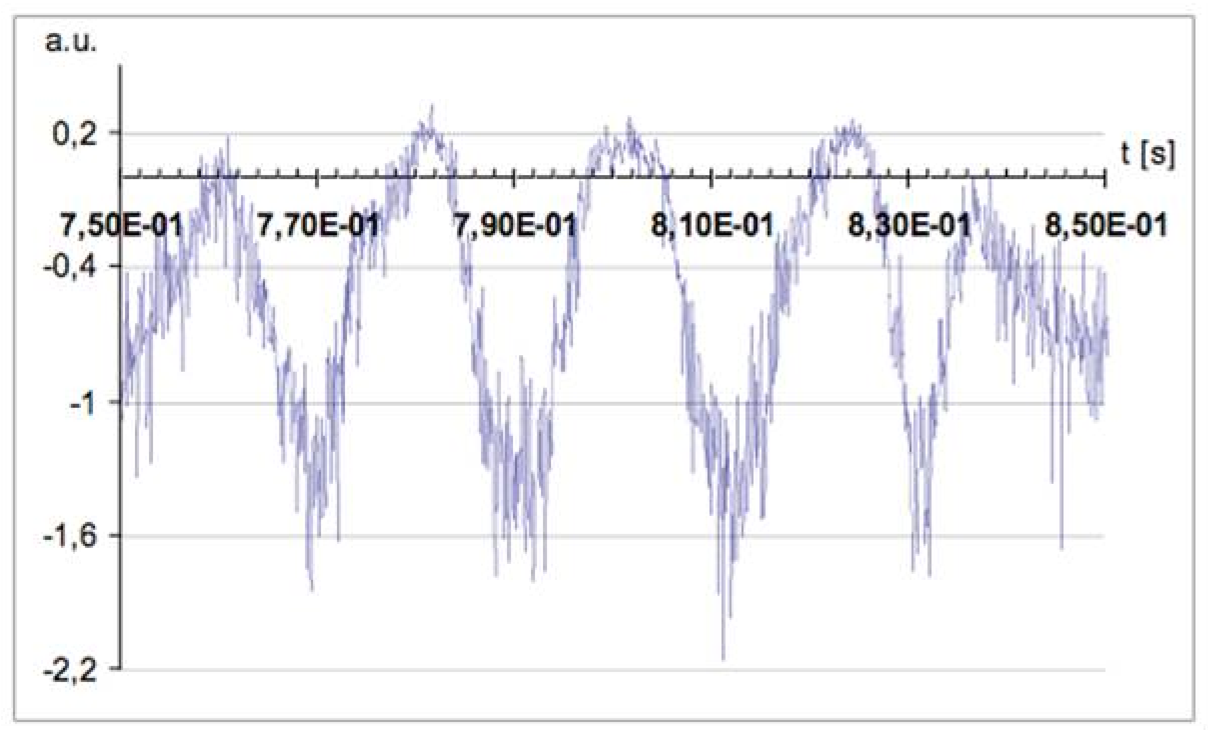

Fig.4.5. Waveforms of the discharge current, as recorded during laboratory tests of the UHV linear-arc facility.

In order to perform coating of single cells a special arc-driving system, equipped with a miniature permanent magnet, was designed and manufactured at IPJ. A magnetic field, which is produced by the permanent magnet placed inside the niobium cathode tube, can stabilize the arc discharge and focus it on the cathode surface near the magnet position. The construction facilitates the control motion of the arc discharge along the z-axis and the coating of the inner surface of an RF-cavity more uniformly. A general view of the top part of the magnet drive system is shown in Fig. 4.6.

Fig. 4.6. Top part of the magnet-drive system used in the modified UHV linear arc facility.

Using the equipment described above, the single copper-cavities (taken from a TESLA test-bed) have been coated without micro-droplet filtering. After the coating, these cavities were cut along the symmetry axis in order to perform an analysis of the inner surfaces. A general view of the cut cavity is shown in Fig. 4.7.

Fig. 4.7. Two parts of the coated single-cell, which was cut in order to perform an analysis of the inner surfaces.

Several samples were cut out of the Nb-coated surface and an analysis of their surfaces was performed by means of SEM, as shown in Fig. 4.8.

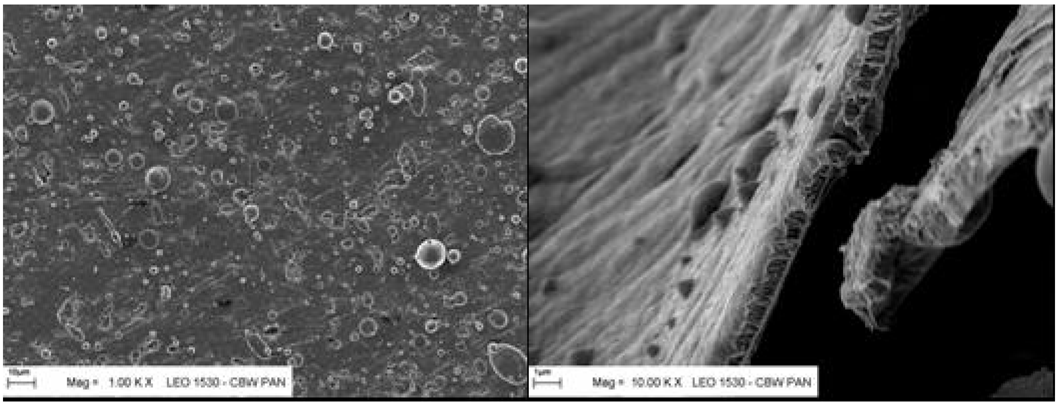

Fig.4.8. SEM pictures showing a relatively large population of the deposited micro-droplets (left), and the edge and thickness of the deposited niobium layer (right, larger magnification).

For a comparison, several samples of pure sapphire were also coated within the UHV linear-arc facility under similar experimental conditions, and they were analyzed with the same SEM, as shown in Fig. 4.9.

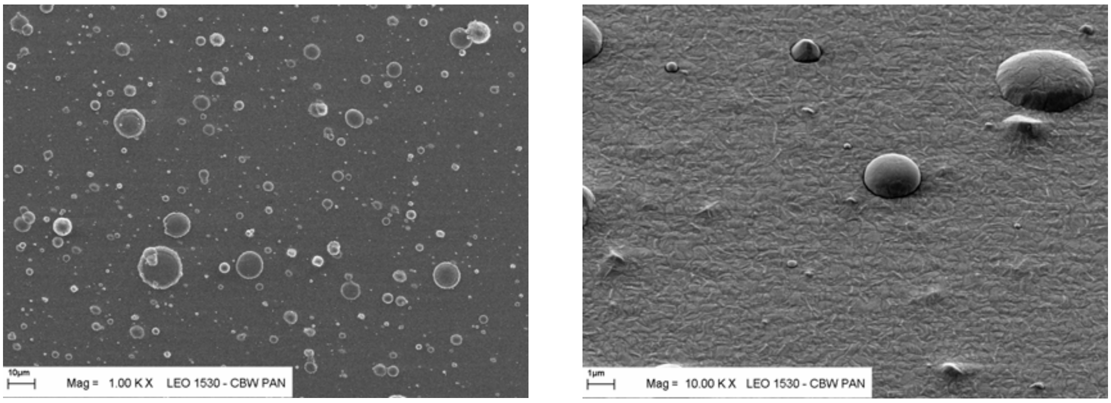

Fig. 4.9. SEM pictures showing the population of the deposited micro-droplets (left), as well as the structure of the niobiumlayer and shapes of the micro-droplets (right, larger magnification).

An analysis of the micro-droplets deposited upon the sapphire samples was performed within the frame of the IPJ-Tor Vergata University collaboration, and some exemplary results are presented in Fig. 4.10.

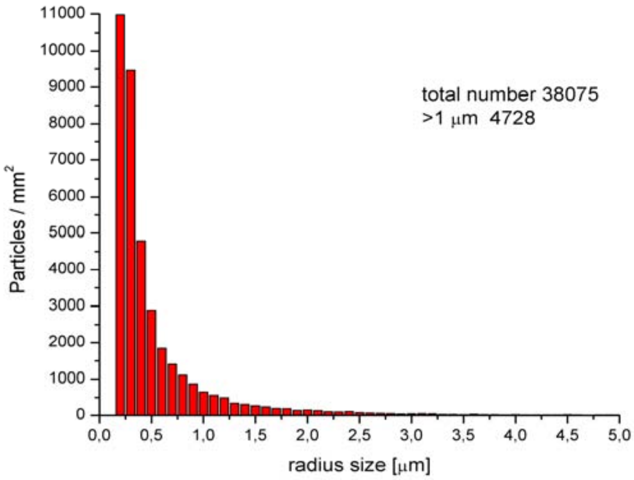

Fig. 4.10. Histograms of the micro-droplet population, as measured upon the sapphire sample coated within the UHV linear-arc facility.

In order to reduce a number of the micro-droplets within the linear-arc facility, a special cylindrical magnetic filter was designed and constructed. It consisted of a set of thin copper tubes distributed symmetrically around the cylindrical surface and joint at the ends by special connectors. This construction enables an appropriate magnetizing-current and cooling-water flow to be realized. Since the cylindrical magnetic filter is a new concept, it requires extensive theoretical studies and experimental tests. Model computations of the magnetic field distribution have been performed for different configurations. An example is shown in Fig.4.11.

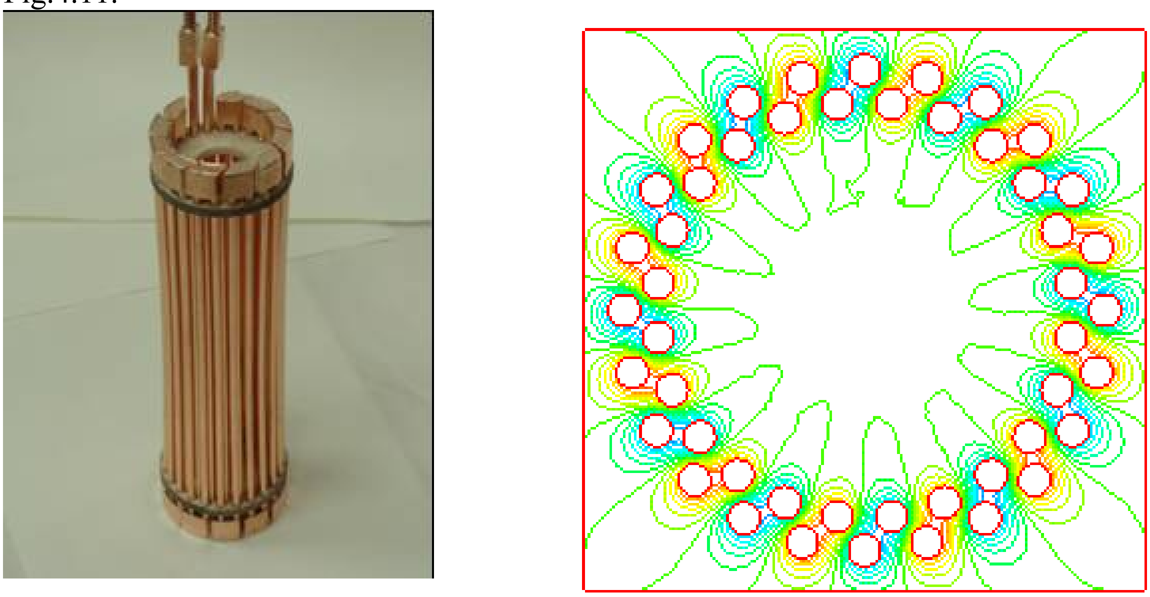

Fig. 4.11. General view of the cylindrical magnetic filter and the corresponding distribution of magnetic field lines in the horizontal cross-section.

Preliminary tests of the cylindrical magnetic filter have been performed within an auxiliary experimental stand. The vacuum tightness, cooling efficiency and resistance of the filter to arc discharges, were investigated. It was demonstrated that the prototype cylindrical filter can be used under the required experimental conditions, as shown in Fig. 4.12.

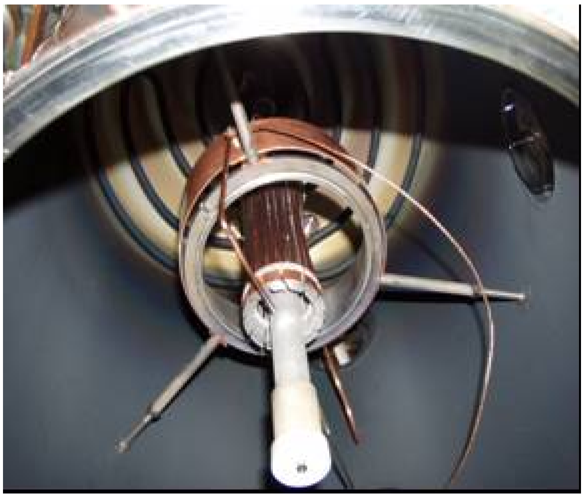

Fig. 4.12. Picture of the cylindrical magnetic filter and an additional anode after the exploitation tests.

The ion current density, as measured by means of the ion collector placed at a distance of 7.4 cm from the filter surface, amounted to 10 mA/cm^2 only. It means that the application of the cylindrical filter requires further studies in order to solve all construction problems (the design, the selection of materials, manufacturing technique, etc.) as well as some operational problems (the ignition of arc, the resistance of the system, etc.)

Further tests of the single-cavity coating (even without any filtering) should be performed with original cavities, which should be delivered from the partner laboratories (e.g. DESY or INFN-Legnaro) as soon as possible

Task 4.2 – Planar-Arc Cathode Coating

Milestones and deliverables of the reporting period

A summary report on quality of planar arc coating was prepared and delivered as Annex 1 to CARE/JRA1 Quarter report 2/2005 on WP4, published on August 15, 2005.

Activity status

Task 4.2 is focused on the development of an UHV cathodic arc-system in the planar cathode configuration. The principle scheme of a planar arc discharge system for coating of samples and a photograph of the actual, un-filtered system presently in operation, are shown in Fig. 4.13.a) and Fig. 4.13.b) respectively.

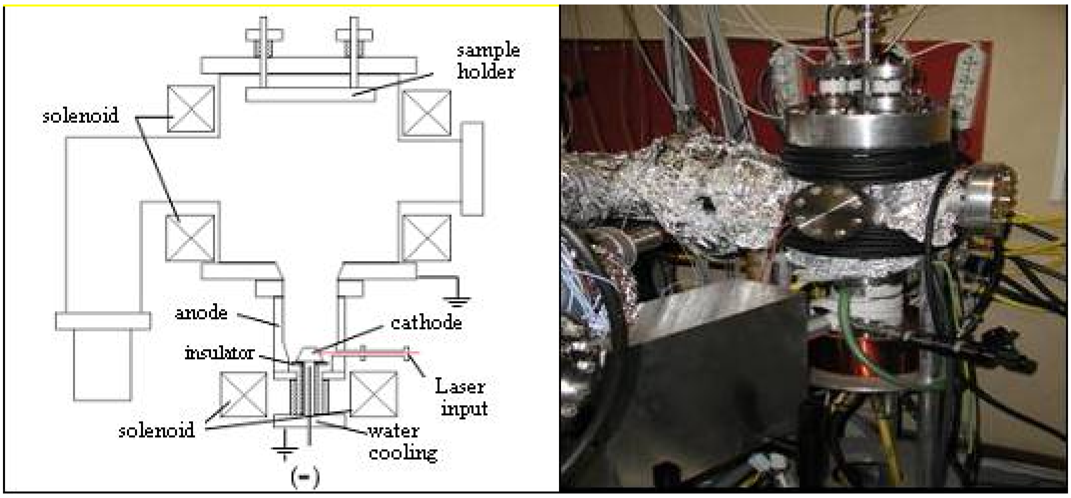

(a) (b)
Fig. 4.13. Scheme of the linear-arc UHV system and modified planar-arc facility in Rome.

The present non-filtered system is equipped with coils to focus the plasma ion stream and with a new laser for triggering the arc discharge. A second planar-arc facility, equipped with an ion energy analyzer (on loan from CERN) and a magnetic macro-particle filter of the Aksenov type (L-type), is shown in Fig. 4.14.

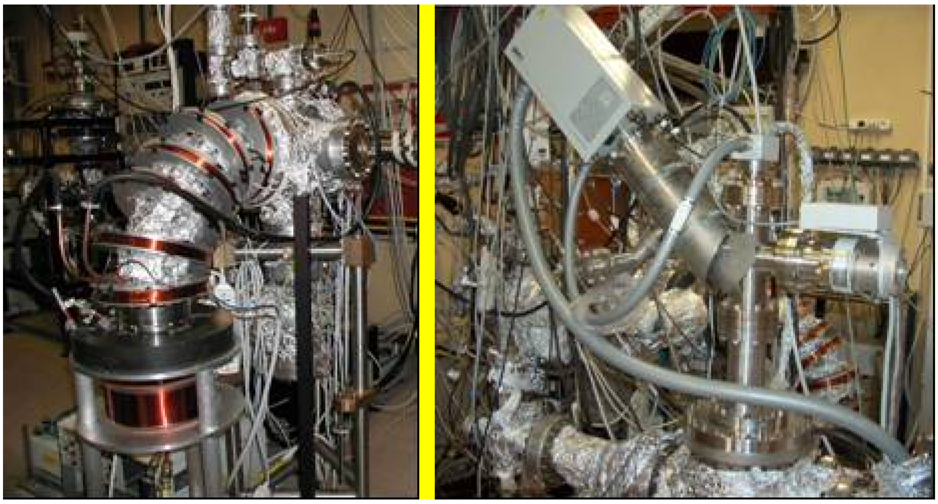

Fig. 4.14. Ion energy analyzer (left) and the magnetic filter (right), as installed upon the second planar-arc facility, which was put in operation in 2005.

In 2005 an important task was the upgrading of the magnetic filter, with the aim of improving both the particle rejection and the deposition rate, by improving the spatial distribution of magnetic field lines. Different T-type filters have been designed at IPJ and constructed in both Rome and Swierk. Examples of the magnetic field distribution computations performed in Swierk are presented in Fig. 4.15.

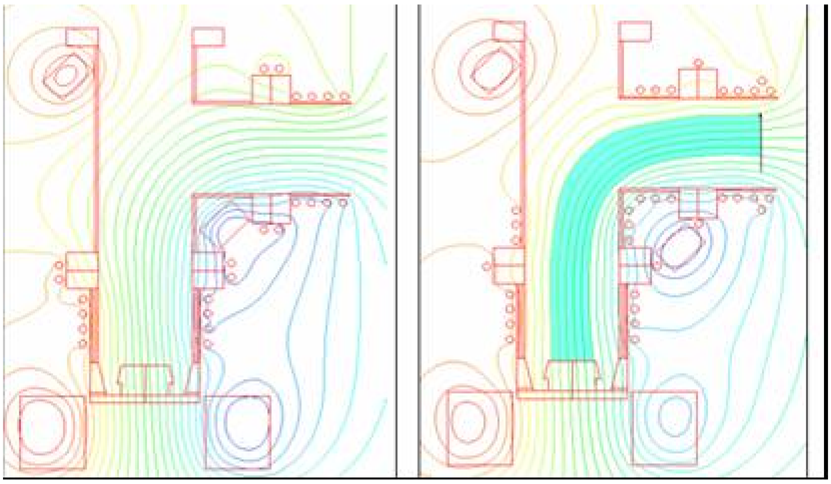

Fig. 4.15. Distributions of magnetic filed lines within the filter channel depend strongly on the configuration of coils and values of magnetizing currents.

Based on the model computations, a new magnetic filter of the T-type has been designed and is being fabricated. It is better cooled, so as to tolerate higher arc-currents, and its magnetic field configuration should allow for better plasma transport and therefore for a higher deposition rate and an improved uniformity of the deposited layers. The filter shape should also lead to improved macro-particle (micro-droplet) rejection.

A planar, un-filtered system version was also designed, fabricated and put into operation in 2005, to study deposition on a cavity-shaped substrate. It is presently used to study the problems on such a substrate, in particular how to obtain, inside it, a uniform thickness film. The systems stainless-steel vacuum chamber consists of two separable parts, whose shape is close to that of a TESLA-type cavity half cell, equipped with a set of sample holders located at different positions, as shown in Fig. 4.16.

Fig. 4.16. General view of the unfiltered planar-arc facility for the single-cell deposition (left) and a picture of the inner surface of the upper half-cell with sample holders (right).

Fig. 4.17 shows, as an example, the measured ion currents on samples as a function of their position on the chamber surface, for different magnetic field configurations.

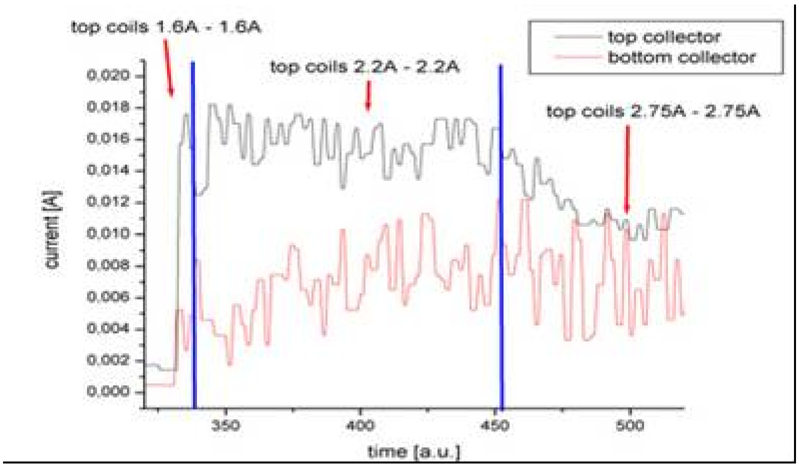

Fig.4.17. Changes of the ion current measured for different collectors and magnetic fields.

In order to improve the operation of all planar arc devices new automatic control systems were implemented: a laser control panel, shown in Fig. 4.18,

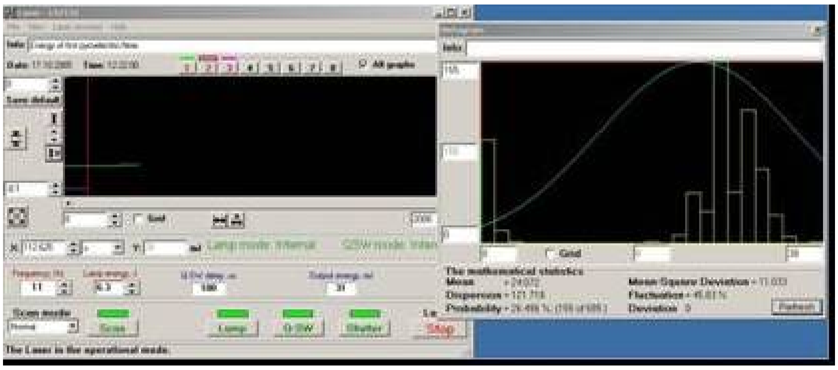

Fig. 4.18. Laser control-panel.

and computer-controlled arc ignition electronics allowing automatic recovery after extinction, as shown in Fig. 4.19.

Fig.4.19. Example of arc current values recorded during operation showing automatic arc recovery.

According to the updated program of task 4.2 on sample characterization, samples coated under different conditions were studied. The subtask concerning the characterization of Nb-coated sapphire samples from the UHV planar-arc facility was performed by measuring their residual resistivity ratio (RRR), critical temperature (T_c) and critical current (J_c) using an

inductive method. The RRR values of Nb films on sapphire samples kept close to room temperature, typically ranged from 20 to 50, as reported in a paper published in Supercond. Sci. Technol.**18** (2005) L41-L44).
Typical measured critical temperatures and critical current densities of early UHV arc deposited Nb film samples are shown in Fig. 4.20.

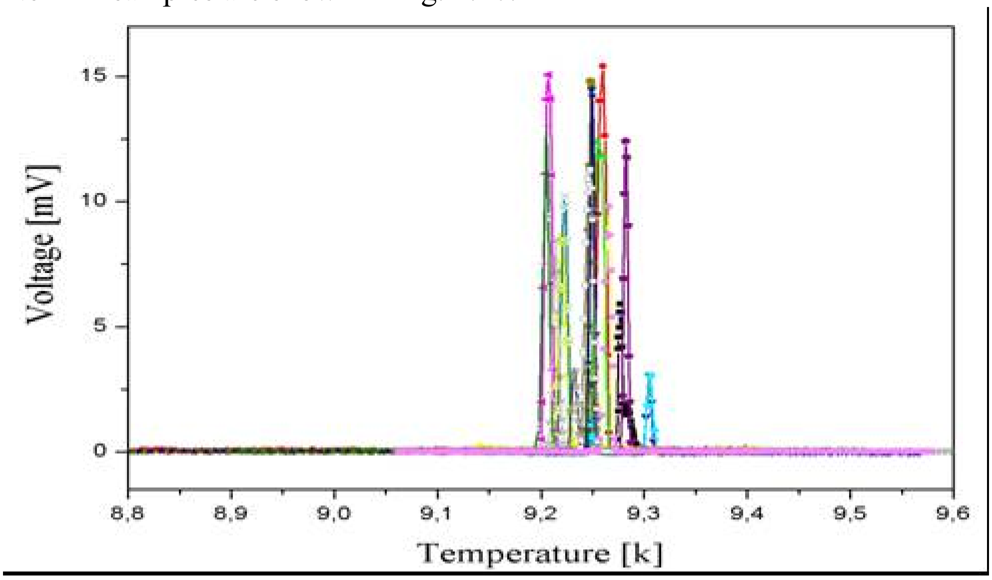

Fig. 4.20. T_c measurements on various samples

The measured T_c values, close to those of bulk Nb, were an indication that stresses in the film are relatively low while the narrow transition widths (<0.02 K) suggested that the deposited Nb-films are uniform and clean.

A summary report on the quality of UHV planar-arc Nb coating (the 2005 milestone) was prepared and delivered together with the CARE/JRA1 Quarter Report 2/2005. According to this report the critical temperature (T_c), transition width (ΔT_c) and surface current density (J_c) values of our best film samples are close to those of bulk Nb, i.e. $T_c = (9.26 \pm 0.03)$ K, $\Delta T_c \approx 0.02$ K and $J_c = 3x10^7$ A/cm^2. An example is shown in Fig. 4.21.

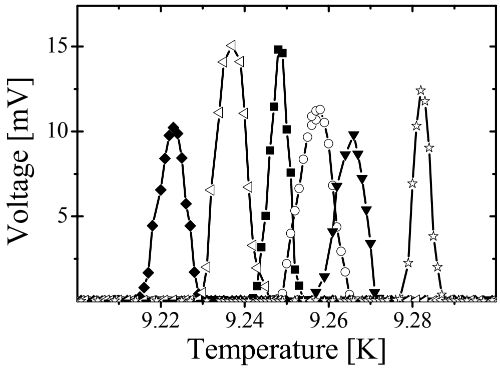

Fig. 4.21. Measurement of the critical temperature T_c of the Nb-coated sample (see Annex 1 to CARE/JRA1 Quarter Report 2/2005).

The structure of Nb films was also analyzed using X-ray diffraction, atomic force microscopy and SEM.
The lattice parameter resulting from X-ray diffraction spectra, collected using Cu–K radiation with filtered K_β line in the $\theta-2\theta$ configuration, ranged from 0.3306 to 0.3318 *nm* (close to

0.3306 *nm* of the bulk Nb), which again is an indication of low stresses. Atomic Force Microscopy pictures of films on copper showed an average Nb grain size of about 200 nm, and a film roughness comparable to that of the Cu substrate. The roughness of films deposited on sapphire substrates was instead much smaller. In some cases the growth of columnar structures of about 1.5 μm in height, e.g. at the bottom and walls of micro-craters left by larger micro-droplets, was observed (see Annex 1 to CARE/JRA1 Quarter Report 2/2005). The most important result was the demonstration that the UHV-arc Nb-coated samples show the same type of behavior as bulk Nb, and that the Nb-layers obtained with magnetic filtering appear to be the best ones.

Detailed 3D-profilometry on unfiltered and filtered Nb films samples deposited on sapphire substrates are being performed in the framework of a collaboration with Jefferson Laboratory, USA to study the efficiency of our present magnetic filter. A very first result is shown in Fig. 4.22: while on the unfiltered sample one finds $\approx$ 10 large signals, clearly to be attributed to Nb droplets, over the explored area while on the filtered one only a few very small signals – to be better classified - are seen.

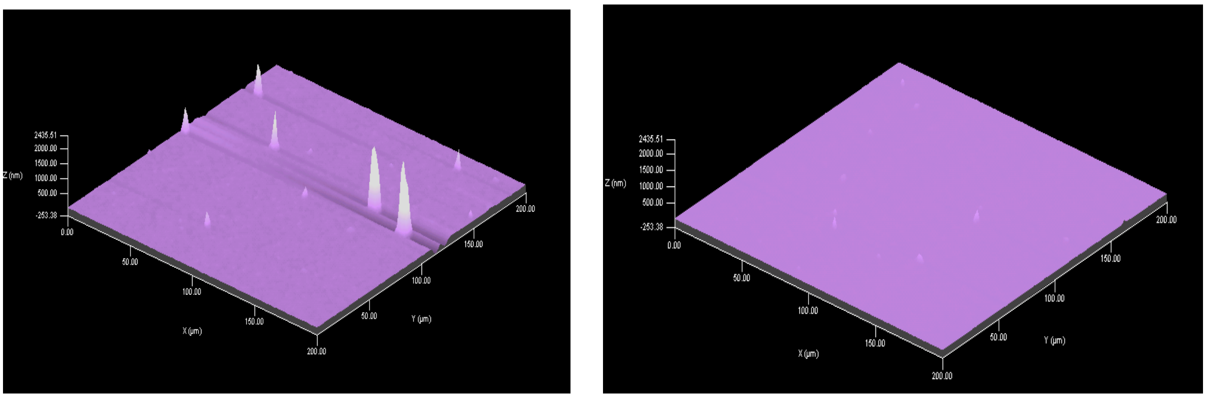

Fig. 4.22. Profile-diagrams of unfiltered- and filters-samples of the 200 μm x 200 μm size (courtesy of A. Wu, Jefferson Lab).

Low field RF measurements were also performed on (small) sapphire coated samples by our collaborators at INFN-Napoli. The film RF surface impedance $Z_s(T, H)$ was measured as a function of temperature, using the 22 GHz resonant Cu cavity shown in Fig. 4.23.

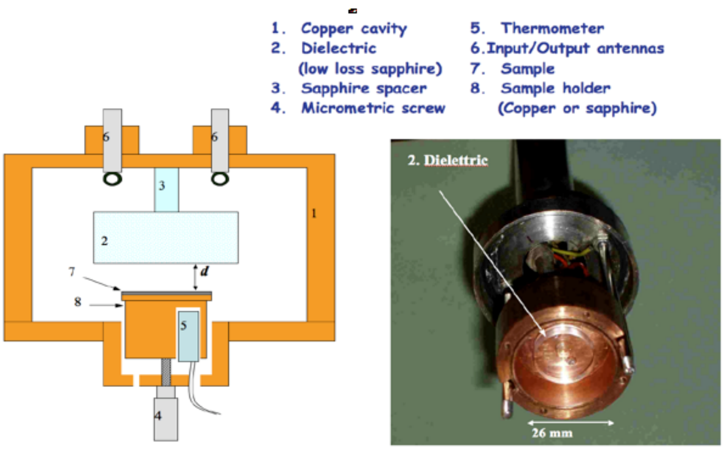

Fig. 4.23. Schematic drawing of the system and view of the (opened-up) cavity used for low-field RF measurements at INFN-Napoli .

Results (Fig. 4.24) show that, within the explored parameter range, the filtered film behaves like the bulk Nb reference sample to within the experimental errors.

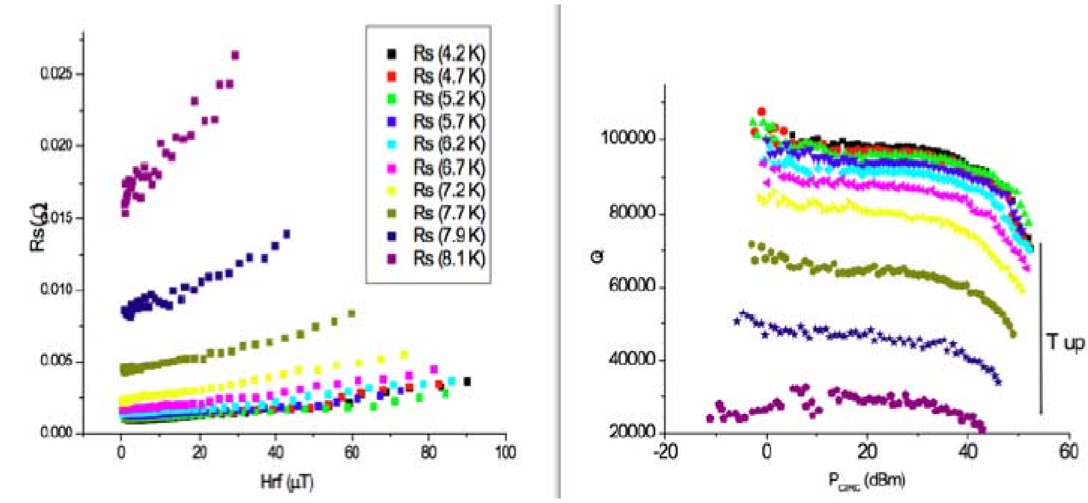

Fig. 4.24. Residual resistance and Q values of the investigated samples as a function of temperature (see Proc. SRF-2005 and Annex-1 to CARE/JRA1 Quarter report 2/2005 on WP4).

The subtask concerning the characterization of Nb films on copper was performed through collaboration with researchers at Cornell University, USA, who carried out high field measurements on our (large) samples (Fig. 4. 25). The first high-field RF measurements of filtered Nb-coated, large Cu-samples were performed at 6 GHz, and the results were reported by A. Romanenko and H. Padamsee at SRF-2005. The quality factor (Q) of the best sample, which sustained a magnetic field value of 300 Oe, possibly limited by the host cavity quench, was comparable within the errors to the present limit value (≈ 3 x 10^8) of the host cavity.

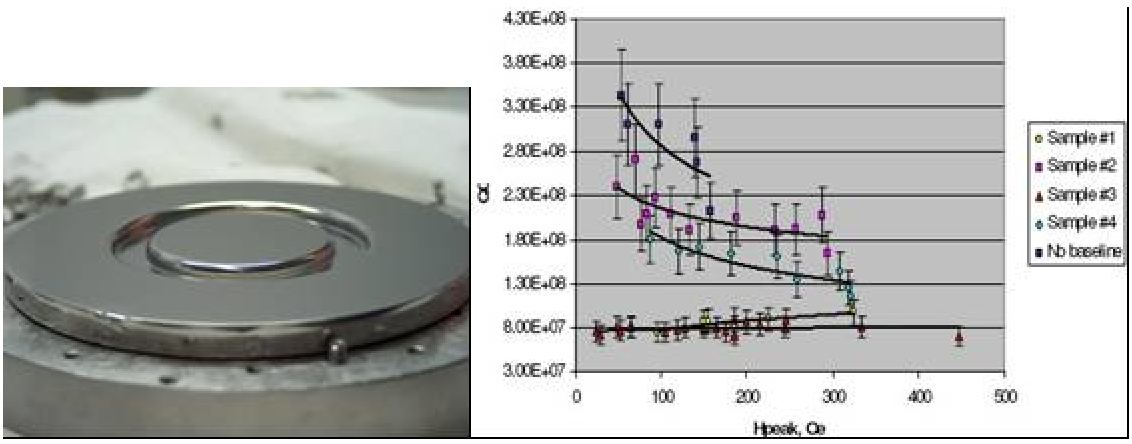

Fig. 4.25. One of the ≈10 cm diameter Nb coated Cu samples measured in Cornell (left) and measurements of the Q_o versus H_{peak} of four such samples (A. Romanenko and H. Padamsee, Proc.SRF 2005, Cornell, July 2005).

As regards studies of other HTC superconducting coatings, the UHV-arc apparatus to study the production of NbN films, equipped with a system to finely control the gas flow rate into the arc chamber, has been assembled. Commissioning has been started but is being delayed because of problems with arc stability as a function of the gas pressure, which need further investigation.

Work package 5: Surface Preparation

Task 5.1: Electro-polishing on single cells

Activity status

Sub-task *5.1.1 EP on Samples*

Work on samples has allowed us to identify the key role of fluorine ion concentration in the ageing of the EP solution, as well as in the prevention of the production of solid sulphur. We have been able to quantify the ageing of the polishing solution and to identify conditions for safer use. Attempts to enhance the HF concentration showed that even if this produces a longer lifetime and less sulphur production, unfortunately this approach will not be applicable to cavities due to its Cathode-Anode distance sensitivity. Several tracks are now explored like enhancing F- content via a salt instead of fluoric acid, or changing the viscosing agent. As lifetime and pollution of the EP solution is certainly a key issue toward a gain of reproducibility, we shall pursue this program.

Sub-task 5.1.2 Single cell cavities: completed

The cavities have been delivered and have been tested (standard RF measurement).

5.1.3 Build EP chemistry for single cell cavities

Construction of lab hoods has been completed, and acquisition system has been studied and developed. Security authorizations have been obtained and commissioning is underway (still test with water). First cavity treatment is expected for the beginning of next year.

Figure 5.1 : EP set-up for single cells

All the results from these 2 last years will be gathered in a global report (namely Deliverable # 8), now in draft form, which will be produced at the beginning of next year.

Task 5.2 - EP on multi cells

Activity status

The EP stet up is running continuously. First information on ageing of system components is available. Due to this information some re-design is necessary and shifts the expected end dates of task 5.2.
Data on acid ageing are available now and a system for online control and to replenish the acid by adding HF acid automatically is under development. This part of the WP is complete.
The parameters for continuous runs are fixed and quality control is established. Some modifications and additional quality control steps are needed due to new results showing up during the last 100 h of operation. This will lead to an extension of the work on bath ageing.
The software for electrode optimization is ordered and installed on a DESY computer. Training of personal is in progress and parameters for input data of the software are ordered
A laser roughness instrument is under installation at the University of Wuppertal. This system looks to be the relevant one for the measurements. The roughness measurement system will be tested on samples.
Industrialization of the EP will be made in parallel to the study of industrialization of the electro-polishing funded under the XFEL preparation investigations.

Remarks
For the realization of an industrial prototype of the electro-polishing system, the time foreseen under this work package is not enough to build up and operate such a system

Fabricate EP multi-cell industrial prototype
Commission EP multi-cell industrial prototype
EP multi-cell industrial prototype ready
Operate EP multi-cell industrial prototype

Discussion needed:
Actually no relevant data are available for salt mixtures. The information from sub-task 5.1.1.3 gives a variation in the existing EP bath mixture. It has to be discussed who and under which activity the test of this mixture will be done. Actually the single cell infrastructure is not available. On the other hand industrial companies should have the capability to change the mixture in use for the single cell test program at DESY.

Task 5.3: Automated Electro-Polishing

Activity status

The Automated EP System has been tested on copper and given satisfaction. The program has been written in LabView and has been installed onto PLC Field point. This has the big advantage of not loosing the control of the working point during the locking procedure around the minimum of the EP bath differential conductivity. That was indeed the main problem we faced during our preliminary attempts of dynamic control of the EP differential conductivity by a simple PC, due to the fact that standard PCs often interrupt the process just while refreshing so that the dynamic control is often lost. The operation on niobium is more critical, not only from the DATA processing point of view, due to the presence of plateau oscillations, but also from the security aspect. Therefore, the application of the Automated EP to the

niobium is in progress. The EP design control architecture is finished and the software has been already tested successfully. While testing, however, we decided to improve the algorithm trying to insert the possibility of self-recognition of the minima by the program itself. Moreover, we decided to add a few more buttons to work manually, semi-automatically and totally automatically. This last possibility is very complex; so, reaching this milestone requires further investigation.
As far as the new electrolytes are concerned, we have found alternative recipes based on oxalic and boric acids instead of sulphuric acid. Hydrofluoric is still present; we are evaluating the possibility to get rid of it, which means that the milestones are not complete and that it will be finished by December.

Task 5.4: Dry ice cleaning.

Activity status

During the commissioning of the system the efficiency of the heater unit was identified, suprisingly, to be insufficient. The heater unit shall prevent strong cooling of the cavity during the dry-ice treatment. After some preliminary tests on niobium material, a bid for a new high efficiency infra red heater unit is on hand and the order is under preparation.
In addition the complex control system is further delayed. Main reason is a man power problem caused by unexpected repair and maintenance work for the HERA accelerator at DESY. The gas alarm system for the personal interlock system is ordered.

Work package 6: Material Analysis

Task 6.1 - Development of SQUID based equipment for detection of defects in Nb

Activity status.

The construction of the system for non-destructive inspection of niobium sheets, based on SQUID sensor is finished.

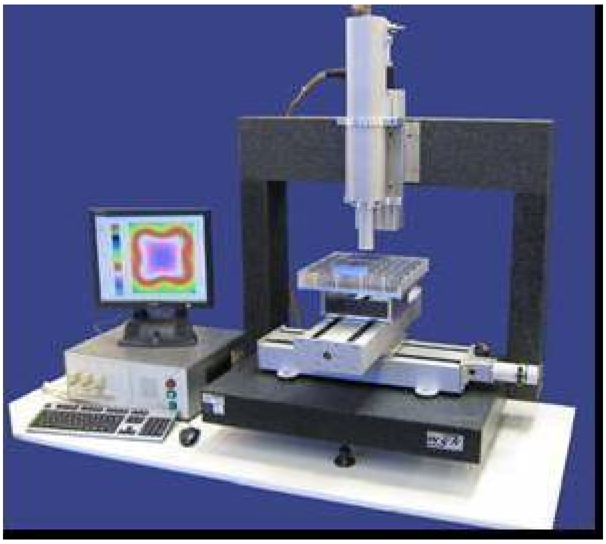

Fig. 6.1: View of a SQUID scanner for Nb sheets

Fig. 6.1 shows the main components of the SQUID scanner. The scanner is based on a xyz table with ca. 300mm x 300m travel area. The SQUID sensor is electronically controlled by a flux modulation and control loop, in order to keep the magnetic flux through the SQUID constant. Compensation current is controlled by the flux measurement. Different filters are implemented into the lock in amplifier to improve the Signal/Noise ratio. The system works in a non-shielded environment.
The first testing of functionality was done at the end of June 2005. The specially prepared test sample was used in measurements. Eleven tantalum spheres with diameters of about 0.1 mm were embedded into a 30 x 30 cm2 niobium sheet by electron-beam melting of the surface. First test results can be seen in Fig. 6.2

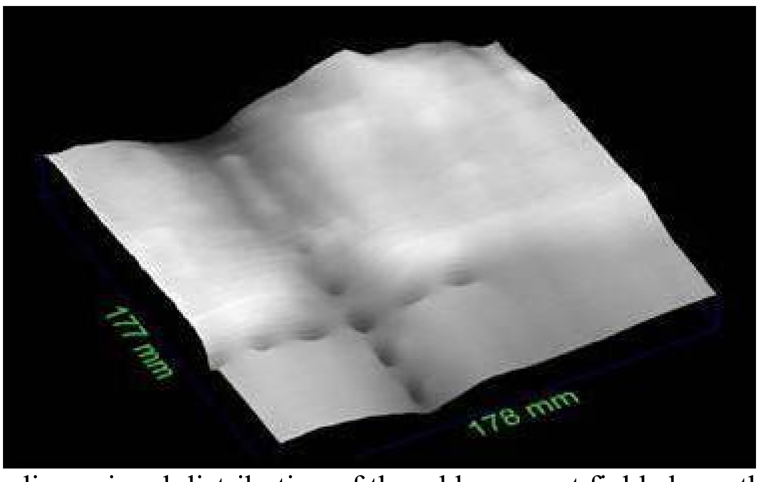

Fig. 6.2: Three-dimensional distribution of the eddy-current field above the niobium test sampl

The eddy-current frequency was 6 kHz. Nine of eleven embedded Ta inclusions are clearly detected. The system is in position to detect defects in niobium. Further optimization of the system set up is in progress.

Task 6.2 - Flux gate magnetometry

Activity status

The flux gate scanning apparatus has been designed and built, so that it can perform:

i) A tomography of the electrolytic cell, in order to configure the effect of cathode geometry on Electropolishing,
ii) The distinction of Niobium with different RRR by relative measurements of conductivity by detecting the eddy current decay.

Referring to tomography of the electrolytic cells, we have fabricated a few elementary rectangular cells for the procedure calibration and several shaped electrolytic cell having the possibility to test different cathode shapes.

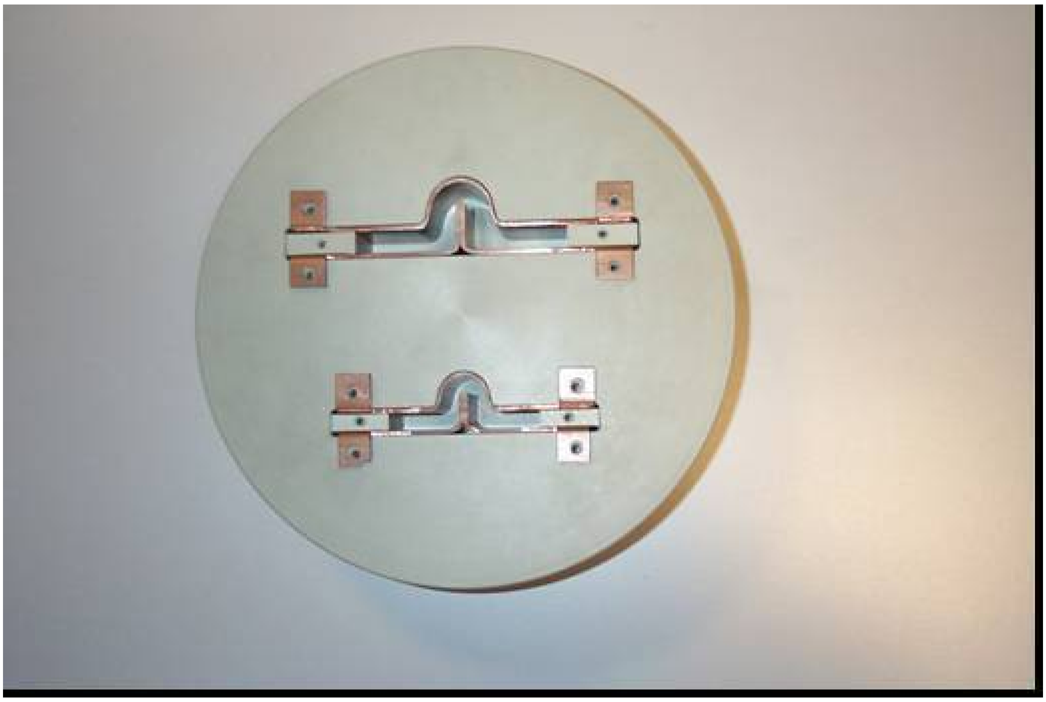

Fig. 6.3 The cavity shaped electrolytic cells with a cathode that totally enters into the cell.

Due to the large dimensions (around 5-6 mm diameter) of the flux gate, the quality of the tomography done up to now is not excellent. We have then bought fluxgates of much more reduced dimensions, which are at the moment under test.

In the meanwhile, is it ready for testing the inversion program that extracts the current distribution from the magnetic field inverting the three-dimensional Biot –Savart law.

Referring to the problem of detecting the defects onto
Niobium slabs, we have also designed the experiment to monitor two different kind of defected samples:

- Physical defects like surface scratches and foreign particle embedded onto Niobium
- Samples with degraded RRR to distinguish from samples with RRR 300.

Fig. 6.4 The scanning flux gate apparatus.

Work Package 6: Material Analysis

Task 6.3 - DC field emission studies of Niobium samples

The automated field emission scanning measurements (FESM), programmed in LabVIEW, have been successfully started in the beginning of the year 2005 at University of Wuppertal. Two Nb samples electropolished (EP) at Saclay (SEP1&2) were systematically scanned at electric surface fields of 40-120 MV/m before and after high pressure rinsing (HPR) at DESY. Both EP samples showed an onset of FE at surface fields around 40 MV/m and emitter number densities up to 30/cm^2 at 120 MV/m. After HPR, the FE of SEP2 was clearly improved, i.e. the onset field increased to 60 MV/m and the emitter number density reduced to 14/cm^2 at 120 MV/m (Fig. 6.5).

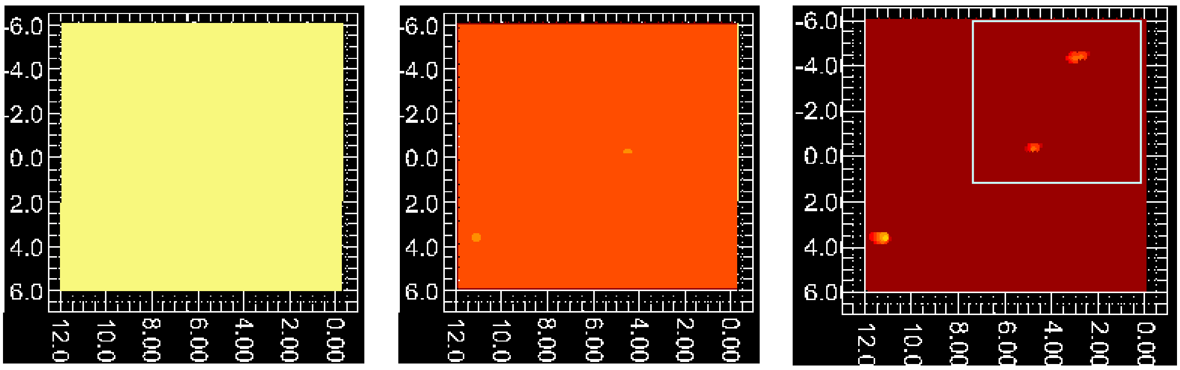

(g) E = 40 MV/m, 0 emitter (h) E = 60 MV/m, 2 emitters (i) E = 90 MV/m, 3 emitters

3rd Series: Φ_{Anode} = 300 µm, Δz = 50 µm (± 5 µm), A = 12 mm×12 mm

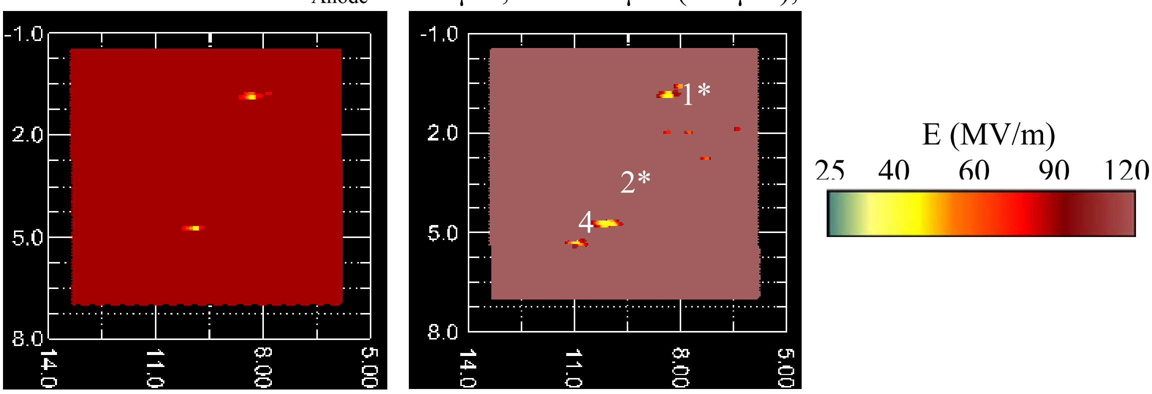

(k) E = 90 MV/m, 3 emitters (l) E = 120 MV/m, 8 emitters

4th Series: Φ_{Anode} = 100 µm, Δz= 40 µm (± 5 µm), A = 7.5 × 7.5 mm^2

Fig. 6.5: Regulated voltage maps of EP-Nb sample SEP2 after HPR at various field levels showing the onset field of emitters (color bar). The maps k and l correspond to the marked area in map i.

In order to learn more about the nature of these emitters, local measurements with the FESM (Fig. 6.6) and surface analysis with SEM and EDX (Fig. 6.3) were performed for some strong emitters. The I-V curves showed nearly stable Fowler-Nordheim (FN) behavior with local field enhancement factors between 17 and 231 which are typical for particulates and surface irregularities. High resolution SEM and EDX measurements revealed three types of emitters: a thin conductive object with submicron protrusions, a scratch-like surface defect and a crystlline particle with S, Cl and K content.

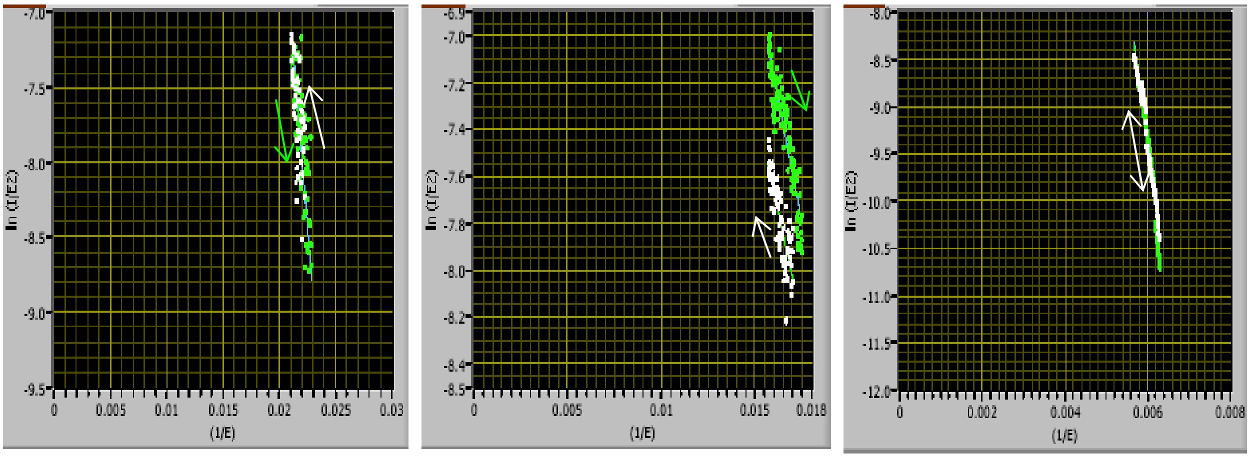

#1* E_{on} (1 nA) = 68.7 MV/m
$\beta\uparrow = 75.1$, $S_1 = 1.6 \times 10^{-15}$ m^2
$\beta\downarrow = 64.6$, $S_2 = 2.4 \times 10^{-13}$ m^2

#3* E_{on} (1 nA) = 48.5 MV/m
$\beta\uparrow = 166.6$, $S_1 = 1.6 \times 10^{-20}$ m^2
$\beta\downarrow = 147.6$, $S_2 = 7.2 \times 10^{-20}$ m^2

#4 E_{on}(1 nA) = 76.9 MV/m
$\beta\uparrow = 19.3$, $S_1 = 1 \times 10^{-13}$ m^2
$\beta\downarrow = 17.9$, $S_2 = 5 \times 10^{-13}$ m^2

Fig 6.6: I-V curves and FN parameters of single emitters # 1, 3 and 4 as marked in Fig. 1(l).

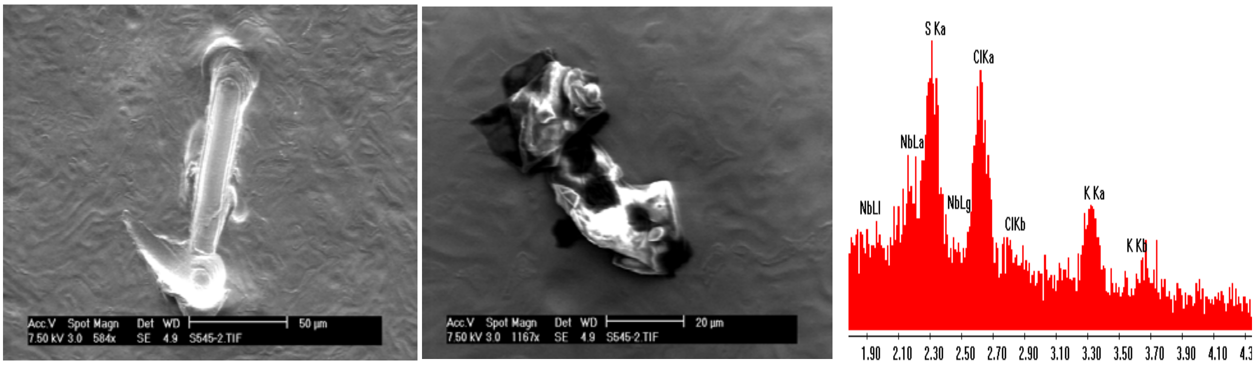

Fig 6. 3: SEM images of emitter #3* (left) and #4* (middle). The EDX spectrum of #4* (right) shows S, Cl, K contents.

These results have been summarized in the MS report (6.3.1.7), presented as a poster contribution at the International Workshop on RF Superconductivity at Cornell University in July 2005 and submitted to the Workshop Proceedings.

As the next step, the dry ice cleaning (DIC) of these two Nb samples was performed at DESY. Most recent scans on SEP2 have shown no emitters up to about 90 MV/m, i.e. much reduced FE after DIC as compared to HPR, but have to be confirmed with sample SEP1.

A series of new high-purity Nb (RRR=300) samples of 28 mm diameter has been fabricated at DESY which provides improved mechanical strength for assembly inside 9-cell cavities for the regular quality control of the standard EP and HPR processes at DESY. FESM investigations of these samples will start in January 2006.

Work package 7: Couplers.

Work-package 7 of JRA1 concerns the development of power couplers. This WP is broken down into three main tasks:

7.1 – New proto-type couplers.
7.2 – Fabrication of a titanium-nitride coating bench for the coupler ceramic windows.
7.3 – Conditioning studies of proto-type couplers.

For task 7.1 we have designed two new-proto-types named TTF-V and TW60 respectively. The RF design of these couplers was completed in 2004. The TTF-V coupler is inspired from the TTF-III couplers used on the TTF VUV-FEL, however, the "cold" part of the coupler has its outside diameter increased to 62 mm with the aim of allowing higher power operation and pushing multipactor limits to higher levels. The coupler then has a 50 Ω impedance for both warm and cold assemblies. Such a coupler may be of interest for a 'superstructure' version of the TESLA cavity (i.e. a 2 x 9 cell cavity). The TW60 coupler (TW for **T**ravelling **W**ave) has a radically different window geometry. The warm and cold windows are thin ceramic disks brazed into the co-axial coupler line. The impedance mismatch of the warm ceramic is compensated by a reduced height wave-guide section in front of the wave-guide to co-ax transition. The cold window impedance is matched to the travelling wave via inductive elements on the outer co-axial line. This implies some standing wave field component however, calculations show that the RF fields are not excessive. The return loss of the TTF-V coupler, as calculated with the code HFSS is shown in Fig. 7.1. Schematic drawings of the couplers are shown in Figures 7.2.a and 7.2.b.

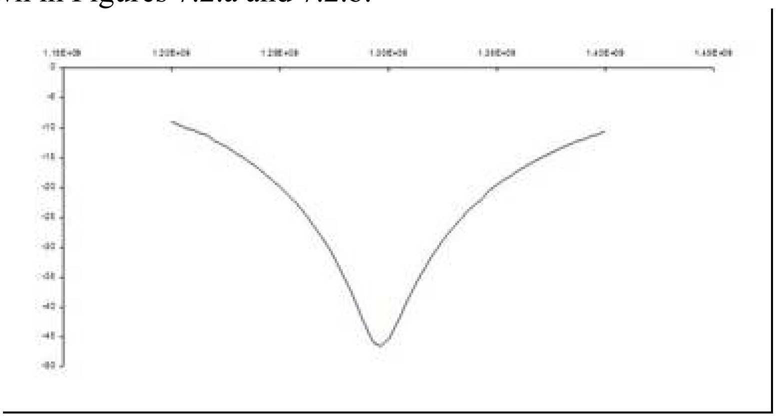

Fig. 7.1 Calculated frequency dependence of the return loss of the TTF-V coupler.

Engineering drawings of the couplers, prepared during the last reporting period, were used in calls for tenders for both proto-types to be manufactured as "equipment built to specification". Detailed technical specification documents were prepared for each of these calls. Four copies of each coupler have been ordered. In the case of the TW60 coupler, a wave-guide test box will also be built. The time required for the company to deliver the proto-types is approximately one year. Consequently, the TTF-V couplers are expected in May of 2006 and the TW60 couplers in August of 2006. Following the recommendations of the International Scientific Advisory Committee from the 2004 annual CARE meeting, we have started to perform thermal simulations of the proto-types. For this purpose we have purchased a fixed-term licence for the ANSYS code. These calculations are in progress (Fig. 7.3).
A significant effort from the drawing office has been made to provide a complete set of drawings of a modified TTF-III coupler. These drawings incorporate new, relaxed, fabrication tolerances which hopefully will result in reduced manufacturing costs. The drawings also

include an automated movement of the central antenna of the coupler via a stepping motor. This improvement is necessary for a coupler to be used on any long super-conducting linac such as the European XFEL or the International Linear Collider.

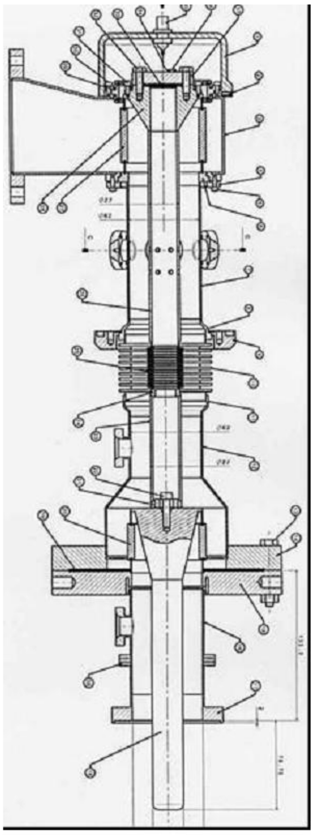

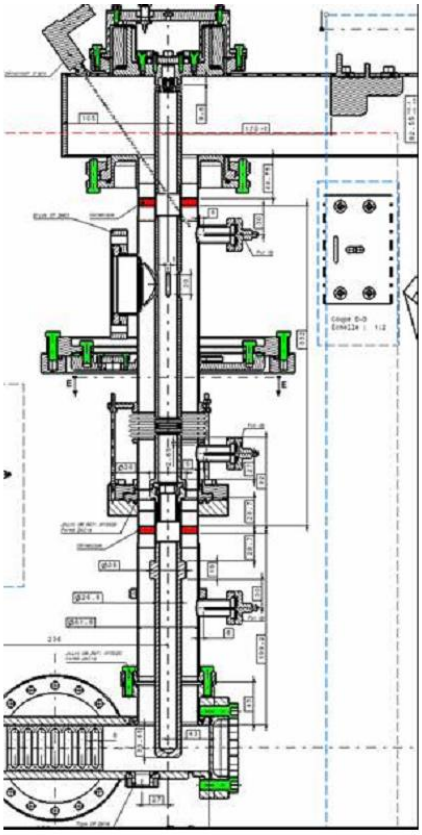

Figure 7.2.a Schematic of the TTF-V Coupler. Fig. 7.2.b Schematic of the TW60 Coupler.

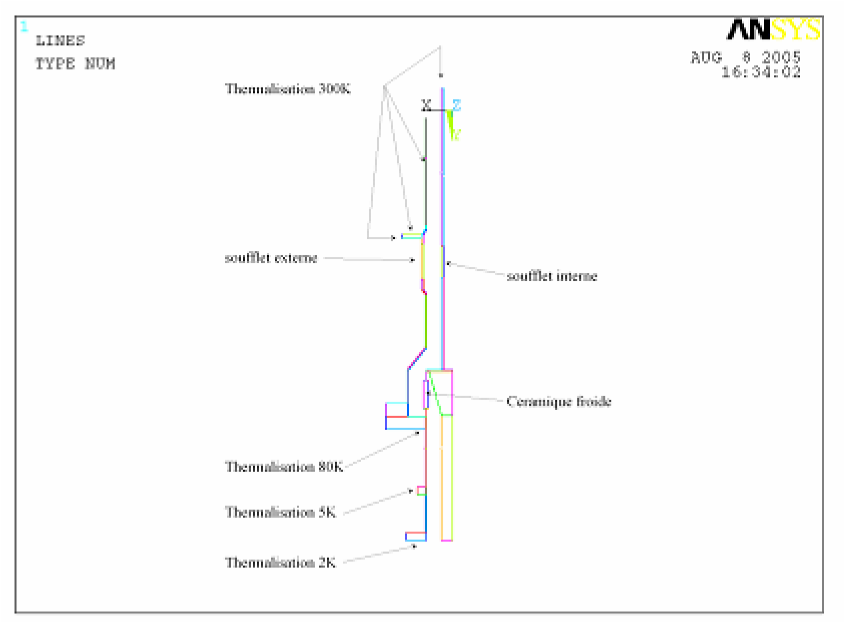

Figure 7.3. ANSYS model for the thermal calculation of TTF-V.

A significant effort from the drawing office has been made to provide a complete set of drawings of a modified TTF-III coupler (Fig. 7.4). These drawings incorporate new, relaxed, fabrication tolerances which hopefully will result in reduced manufacturing costs. The drawings also include an automated movement of the central antenna of the coupler via a stepping motor. This improvement is necessary for a coupler to be used on any long super-conducting linac such as the European XFEL or the International Linear Collider.

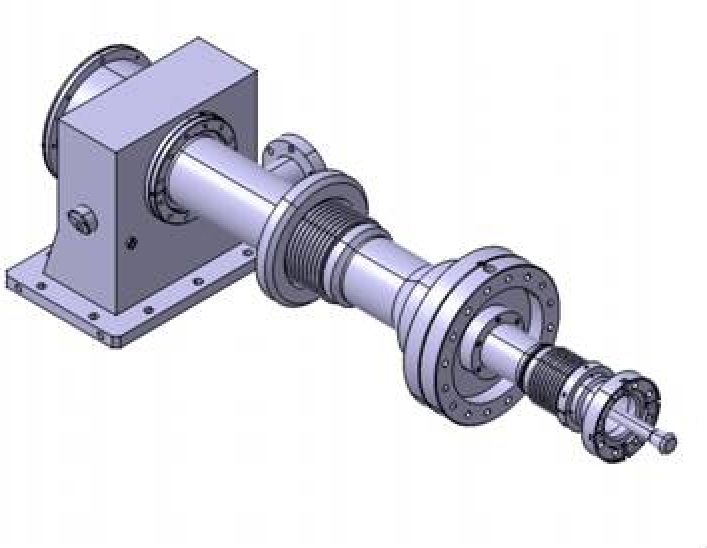

Figure 7.4. Computer Aided Design image of the modified TTF-III coupler.

Two couplers of the TTF-III type, but fabricated using a different method from that used habitually, have been delivered. The windows of these couplers have not yet received their anti-multipactor coating as it was feared that a brazing operation during their fabrication may have removed or damaged the coating. They will be coated later at DESY or by industry and will be tested under high power in 2006. For Task 7.2 we have already begun to perform some bibliographic research on coating benches. A preliminary technical specification of the bench we wish to build is given in an internal technical note. The first contacts with three companies specialised in the fabrication of coating benches have taken place. Preliminary enquiries indicate that we can purchase an industrially built sputtering system well adapted to the ceramic geometry. Construction would require six months. To date, the coupler ceramics have been coated using an evaporation technique and we are concerned that the quality of the coating may be poorer with a sputtering system. We intend to perform comparative tests on ceramic samples before making a firm decision on the choice of bench. This may result in some delay in the construction of the bench with respect to the initial schedule.

Task 7.3, conditioning studies, has represented a considerable part of our effort in 2005. In principle, we wish to perform conditioning studies on the prototypes TTF-V and TW60. While awaiting delivery of these couplers we have started conditioning tests with TTF-III couplers purchased in the context of a LAL-DESY collaboration. These tests provide us with valuable experience of the operation of our conditioning bench along with its associated diagnostics and control system. Before conditioning, the couplers have to undergo a rigid procedure of ultra-sonic cleaning, with ultra-pure water (electrical resistivity = 18 MΩ.cm), rinsing (again with ultra-pure water) drying in a class 10 clean room (Fig. 7.5), baking in vacuum, assembly in the class 10 clean room and finally mounting to the RF bench under a mobile laminar flow providing class 100 conditions. The couplers, tested in pairs (Fig. 7.6), undergo an in-situ bake-out at 150 °C for 24 hours before the RF is applied. The rigorous application of this procedure is indispensable if one wishes to obtain good coupler performance. A *quality assurance* document has been established to guide the technical staff in the application of these procedures.


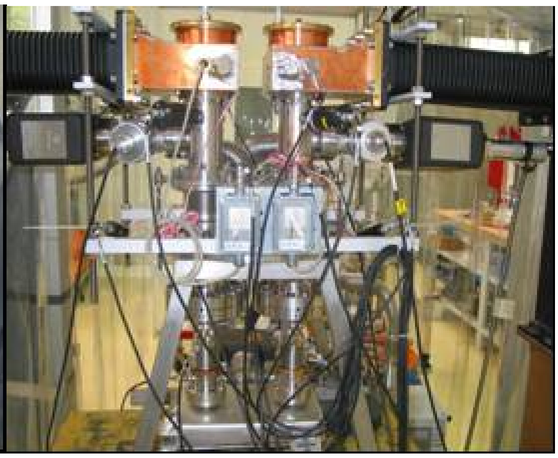

Figure 7.5. Coupler assembly in class 10 clean room. Figure 7.6. TTF-III couplers being conditioned.

A histogram showing conditioning times for different pairs of couplers is shown in Figure 7.7. The spread in conditioning times, for couplers having received an in-situ bake-out, (40 ~ 90 hours) is lower, in general, than that observed at DESY. Nevertheless, we still have relatively few pairs conditioned. The reason for the spread will be the subject of further studies (differences in coupler manufacturing, differences in preparation), in the hope that eventually all couplers can be conditioned faster or at least as fast as the shortest conditioning time observed to date. Note the coupler pair which exhibits the shortest conditioning time (~ 22 hours) was conditioned using higher vacuum threshold levels within the automated conditioning routine (threshold levels which determine if the power level can be incremented. Electronic racks for diagnostic devices (electron pick-ups, photo-multiplier, temperature sensor) have been built which will allow couplers to be safely tested at low temperature in CryHoLab.

The work of WP7 has been presented at the following scientific meetings during 2005: The International Workshop on RF Superconductivity (Cornell); The 2nd International Linear Collider Workshop (Snowmass); *Les Journées Accélérateurs de la Societé Francaise de Physique* (Roscoff).

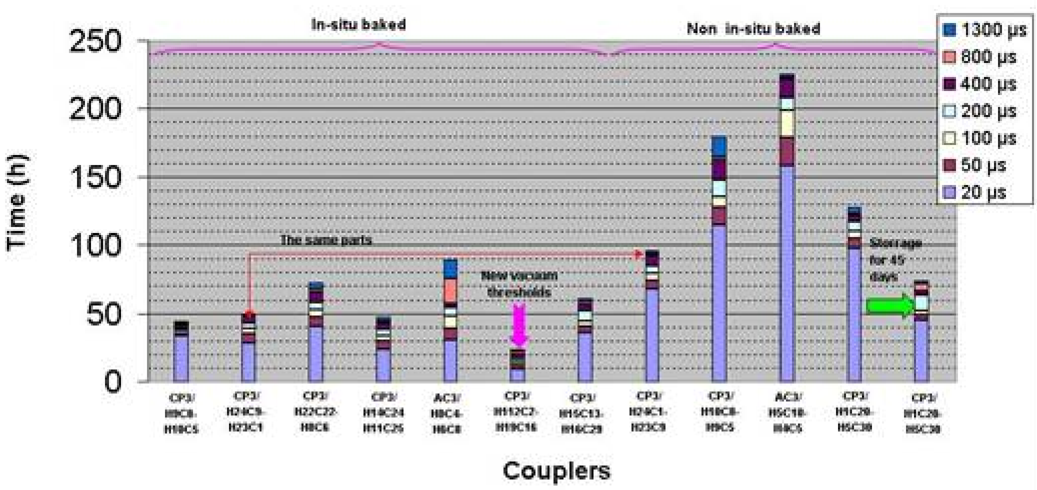

Figure 7.7. Histogram of conditioning times for different coupler pairs.

Work Package 8: Tuners

Activity status

Task 8.1 UMI Tuner

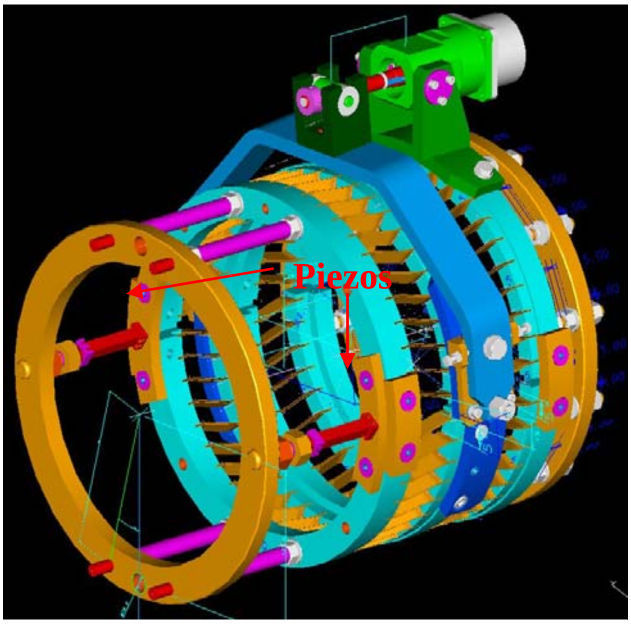

Figure 8.1. The INFN Blade Tuner provided with piezo actuators for fast tuning activity.

The new INFN coaxial blade tuner construction is nearly finished. All the parts have already been constructed by ZANON, where the assembly of two complete prototypes, including the modified helium tank, is well in progress.

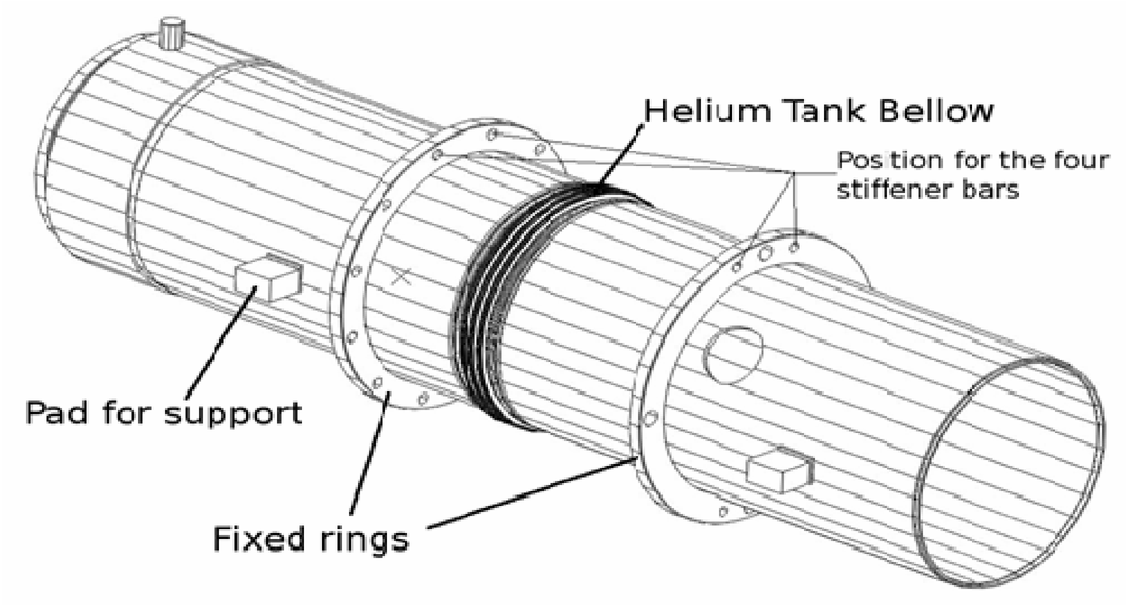

Figure 8.2. Helium tank showing the bellow, the fixed rings and the support pads.

The integration of piezostacks for Lorentz forces and microphonics compensation is completed for what concerns the tuner prototypes. Many piezo models from different manufacturers have been deeply characterized relating to their main extensive properties, such as blocking force, maximum stroke, length, maximum load. The final choice, the Noliac SCMA/S1/A/10/10/40/200/60/4000, fits all the requirements. Moreover, the tuner is designed to be compatible with other active elements, be they other kind of piezostacks (ad-hoc devices have been designed so that piezostacks of different section and length up to 72 mm can be accommodated) or even magnetostrictive actuators. The cavity elasticity is used to provide the piezo preload. Two cold tests are foreseen at the DESY and BESSY facilities at the beginning of 2006. In figure 8.1 you can see the coaxial blade tuner assembly, showing the leverage arm, the Ti ring welded on the tank and the two piezostacks. There is the possibility to use both piezostack as actuators, or to use one as a sensor.

The tuner assembly is mainly composed of three parts: the movement leverage, the bending rings (three rings) and the piezo actuators (see Figure 8.2). Two Ti fixed rings are welded to the helium tank to support the coaxial blade tuner, which is fixed to one of them by means of twelve bolts, while the other ring can receive up to four piezo actuators.
Because the tuner is fixed to the helium tank, a bellow is needed between the two fixed rings. The number of convolutions has been computed in order to avoid any non-elastic strain in the bellow for a maximum axial displacement of 1.8 mm.
Due to the change of the helium tank with the introduction of the bellow, a bending analysis has been performed in order to check the vertical displacements of the cavity subject to its weight and to the weight of the tuner (Figure 8.3). The maximum sagging computed (0.12 mm) is less than the admissible tolerance of concentricity of dumb bells (0.6 mm); therefore the new configuration can be accepted with confidence.

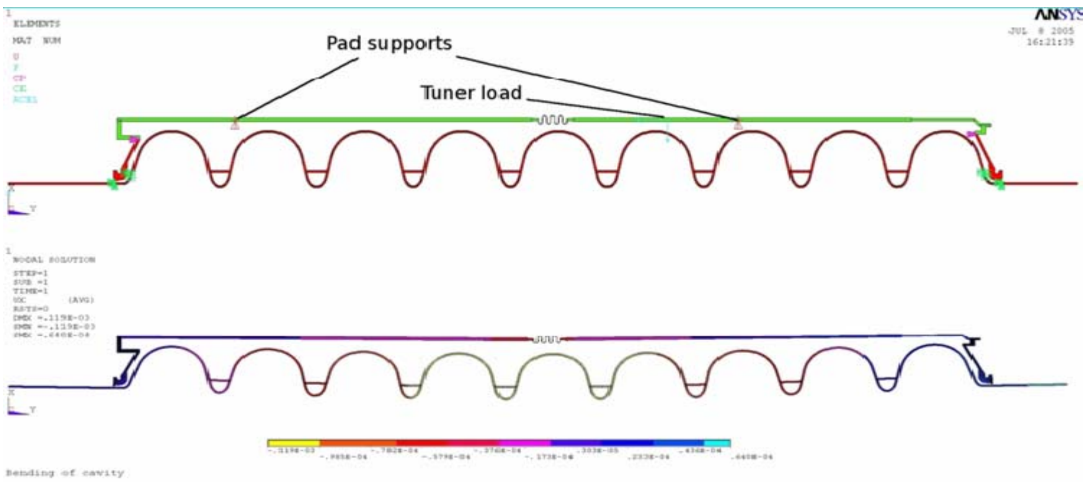

Figure 8.3. FEA evaluation of the cavity vertical displacement.

In parallel to the tuner design and construction, the activity of piezo characterization is still in progress. A load cell working in a LHe environment has been designed and successfully tested. The purpose of this device is the measure of the pre-load force to be applied to piezoelectric ceramics placed in fast tuners, being the correct pre-load value application mandatory to maximize their lifetime. The test on a prototype, built by the Italian firm CELMI, has proved that the glue and strain gauge sensors used *can work* in LHe cryogenic environment with good *repeatability* and *sensitivity.* In Figure 8.4 you can see the load cell calibration curve, showing the good linear behaviour.

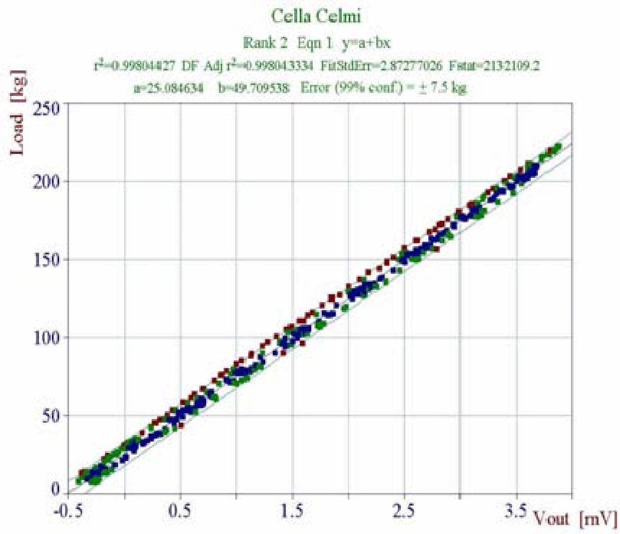

Figure 8.4. Cryogenic load cell

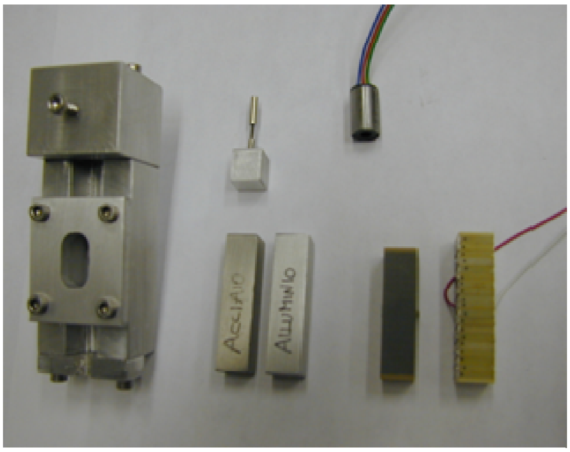

Figure 8.5: Device for measuring piezo shrinking in cryogenic environment

A lifetime test has been performed on a piezoceramic stack. The purpose of this test is to investigate the behaviour of piezoelectric ceramics in conditions equivalent to 10 years of operation as an actuator in active frequency tuners for ILC superconducting cavities. To do this a Physik Instrumente PI P-888.90 PIC255 piezoelectric actuator has been cooled down in LN_2 and has been excited uninterruptedly for a month up to its limits, sustaining about 1.5 10^9 cycles of switching, up to nearly the maximum stroke. After this working period in an extreme working environment, the PI P 888.90 piezo is still working fine and shows almost the same characteristics as measured before the test.
Other piezo properties such as thermal shrinking and the piezo working area (in terms of stroke and blocking force) at cryogenic temperatures are currently under investigation. In Figure 8.5 the device specially realized for the measurement of the thermal shrinkage is shown, based on the use of a LVDT position transducer and samples of well-known thermal shrinkages. Finally we are also making a great effort towards the use of the piezo itself as force sensor at cryogenic temperatures, calibrating some of its parameters (e.g.: capacitance and resonance frequencies) even involving the piezo modelling.

Task 8.2 Magnetostrictive tuner

The magnetostrictive tuner works in a LHe environment with success. It was tested in the vertical test stand, where the magnetostrictive tuner was assembled in series with a piezostack. The elongation of magnetic field driven actuator causes a shrinking of piezostack and as a consequence generation of voltage, which was measured. The results were published at the MIXDES conference. To measure more precisely the elongation as a function of applied current to the coil another test was designed. The detailed characterization of magnetostrictive rod is a main issue of the scheduled test. The experiment insert was planned (overview is shown below) and will be designed by IPN Orsay and fabricated in Poland or in France depending on the cost. The test will be performed at DESY.

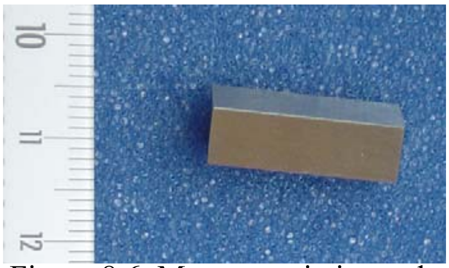

Figure 8.6. Magnetostrictive rod made of GALFENOL.

Three rods made of KELVIN ALL (1 rod) and GalFeNOL (2 rods – see Figure 8.6) materials will be evaluated. The second material is expected to have poorer properties in LHe, but it is cheaper even than the piezostack. Especially the following parameters will be investigated:

- elongation versus applied current, (magnetostriction coefficient) or/and displacement versus magnetic field applied for different preload settings
- max. stroke,
- slew rate of elongation (dynamics of motion),
- heat generation – coil is made of Nb_3Sn (critical temperature 18K),
- magnetic field distribution (if possible) – proper sensor need to be found,
- Young's modulus of magnetostrictive rod

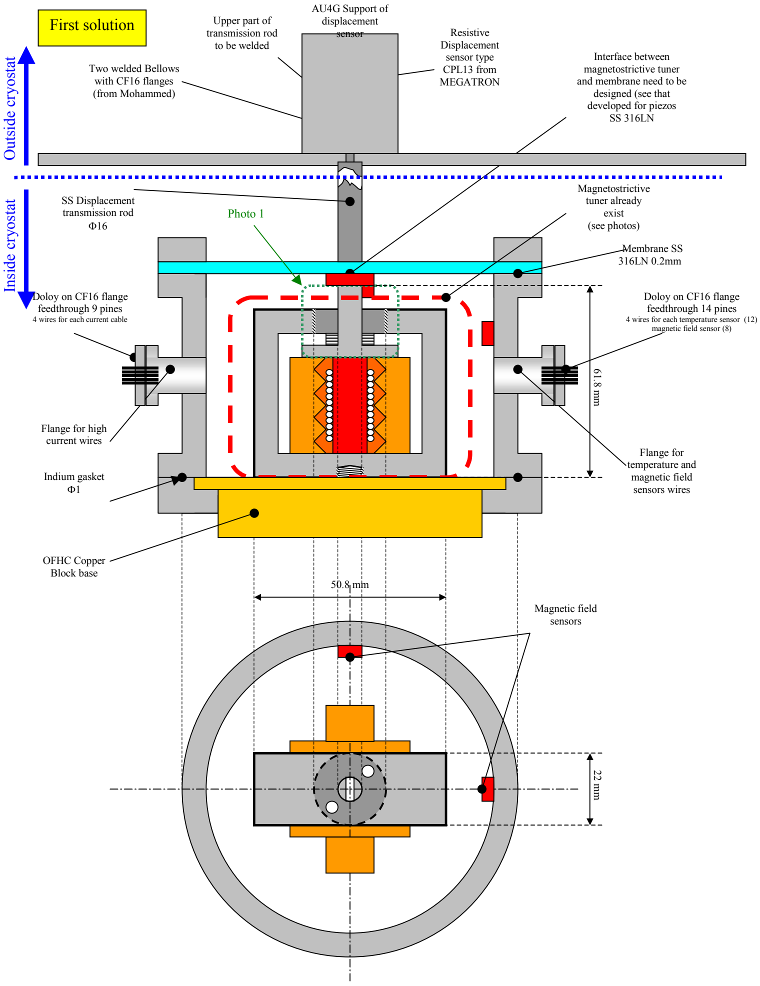

Figure 8.7. Overview of magnetostrictive element characterization experiment

At least there is a need to verify if the magnetostrictive rod might acts as a force sensor. To achieve this output current if rod is stressed, need to be measured.

The detailed characterization is slightly delayed due to the fabrication process of proper insert box for cryostat (see Figure 8.7). However, we decided to perform the test with cavity as it was scheduled.
Furthermore, some minor modification has been made in tuner itself (mechanical fixture has been changed to fit new helium tank).
There is also further research on driver for magnetostrictive element. Mainly the reliability is improving (due to high power supplied to active element a temperature distribution in amplifier is an issue). However current electronic system allows operating magnetostrictive elements in pulse mode with similar settings as the piezoelectric element is running.

Task *8.3 CEA Tuner*

Two (2) piezo tuners were designed and fabricated in the framework of CARE/SRF (see Figure 8.8). These new tuners were designed in such a way that they can be mounted on the present TTF cavities and cryomodules without any modification.

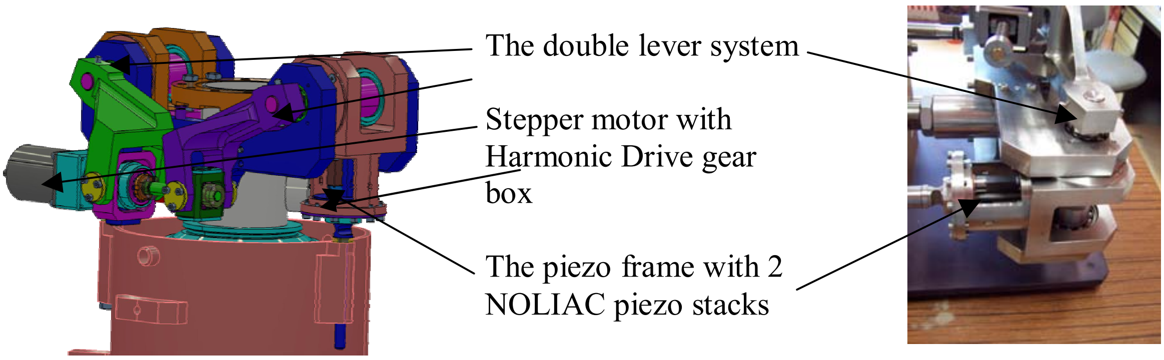

Figure 8.8. Overview of Piezo Tuner System (PTS) designed in CEA-Sacley.

First tests of the tuners were performed at 300 K on a test bench and on the TTF C45 cavity during summer and autumn 2005 (Figure 8.9 and 8.10). The electronics was specially developed for the integrated experiments in CRYHOLAB as scheduled in WP10.

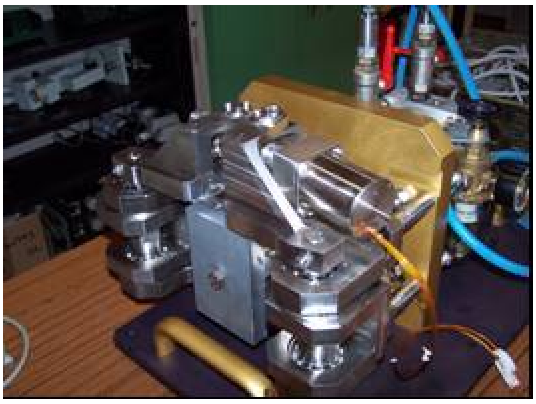

Figure 8.9. Measured stiffness on this test bench is 35 kN/mm, limited by mechanical plays in ball bearing

Figure 8.10. The piezo tuner is mounted on C45 TTF cavity with the electronics in the laboratory.

Commissioning of C45 TTF cavity power coupler was performed in CRYHOLAB before mounting the piezo tuner (WP10 work package). This commissioning demonstrated limitation of the 18 MV/m maximum gradient available with P_{max} = 950 MW in pulsed mode of 205 µs with 0.88 Hz repetition rate.

After RF power coupler commissioning and piezo tuner tests at 300 K, the cavity fully equipped was mounted in CRYHOLAB for integrated tests (Figure 8.11). Before cooling down, new measurements were performed at 300 K in this new environment, and which are summarized on the following figures and curves.

Figure 8.11. C45 TTF cavity in CRYHOLAB ready for integrated experiments.
The electronics on the left allows characterization of mechanical modes of the cavity assembly: F, Q, piezo to piezo and piezo to frequency transfer functions.

Typical transfer function curves obtained at 300 K in CRYHOLAB are shown in the following figures:

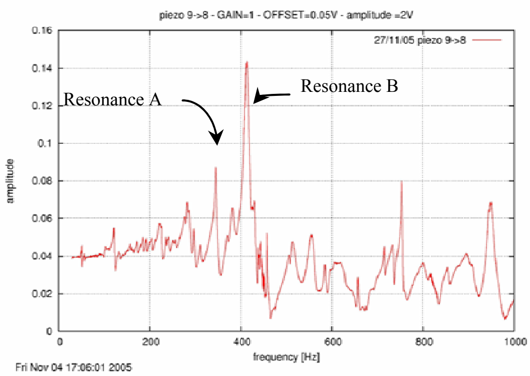

Piezo to piezo transfer function

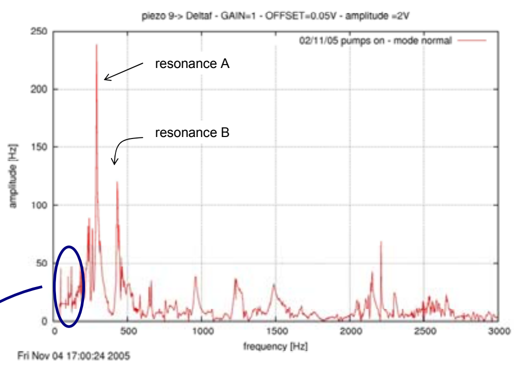

Piezo to frequency transfer function

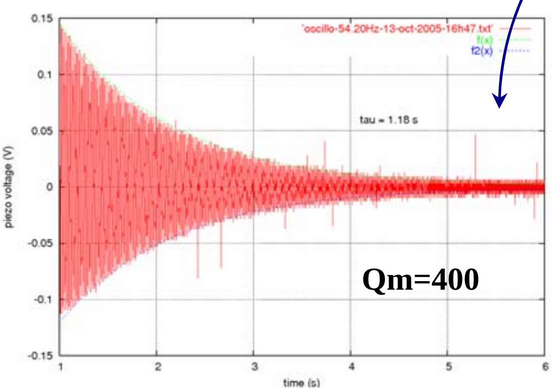

Figure 8.12. Comparison of these 2 curves shows the relative effect on the cavity frequency of the different mechanical modes detected by the piezo sensor. For example vibrations at around 400 Hz have less effect than the one at around 330 Hz.
Q value of the resonant mode at 54.2 Hz calculated with the exponential decreasing time τ=1.18 s shows high Q mechanical resonance

After cooling down, the transfer functions are modified, as is shown in the following curve corresponding to the piezo to piezo transfer function obtained at 4.2 K (Figure 8.13).

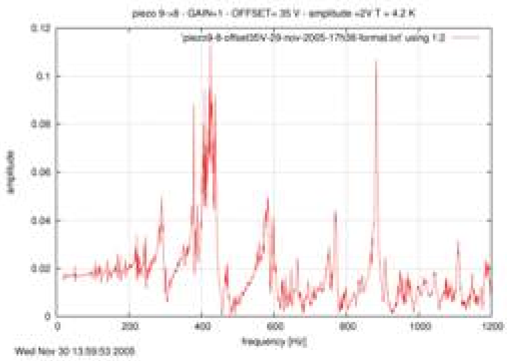

Figure 8.13. Piezo to piezo transfer function.

The preparation of the integrated experiment in CRYHOLAB is in progress. Last refinement in the electronics is still needed for beginning the experiments of Lorentz forces compensation that should be operational during future weeks.
These experiments are being performed with NOLIAC PZT29 stacks 30mm long. Future experiments in CRYHOLAB are foreseen at the beginning of year 2006 with the same tuner mounted with PI piezostacks (40 mm long) characterized by IPN-Orsay (task 8.4).

Task 8.4 IN2P3 Activity

The activities of IPN Orsay for the task 8.4 continue. Most of items of IN2P3 tasks for WP 8 are nearly completed: the corresponding results were reported in different conferences. Several piezoelectric actuators from three different companies were fully characterized at low temperature (e.g. full range displacement, dielectric and thermal properties). Radiation hardness tests with fast neutrons at low temperature (4.2 K – 300 K) were successfully performed. Three beam tests were carried out with three types of piezostacks: we tested four piezoelements of PICMA type from PI, four of NOLIAC type and three of JENA type from PIEZOSYSTEM JENA. The photographs of the experimental device and typical results are presented in Figure 8.14.

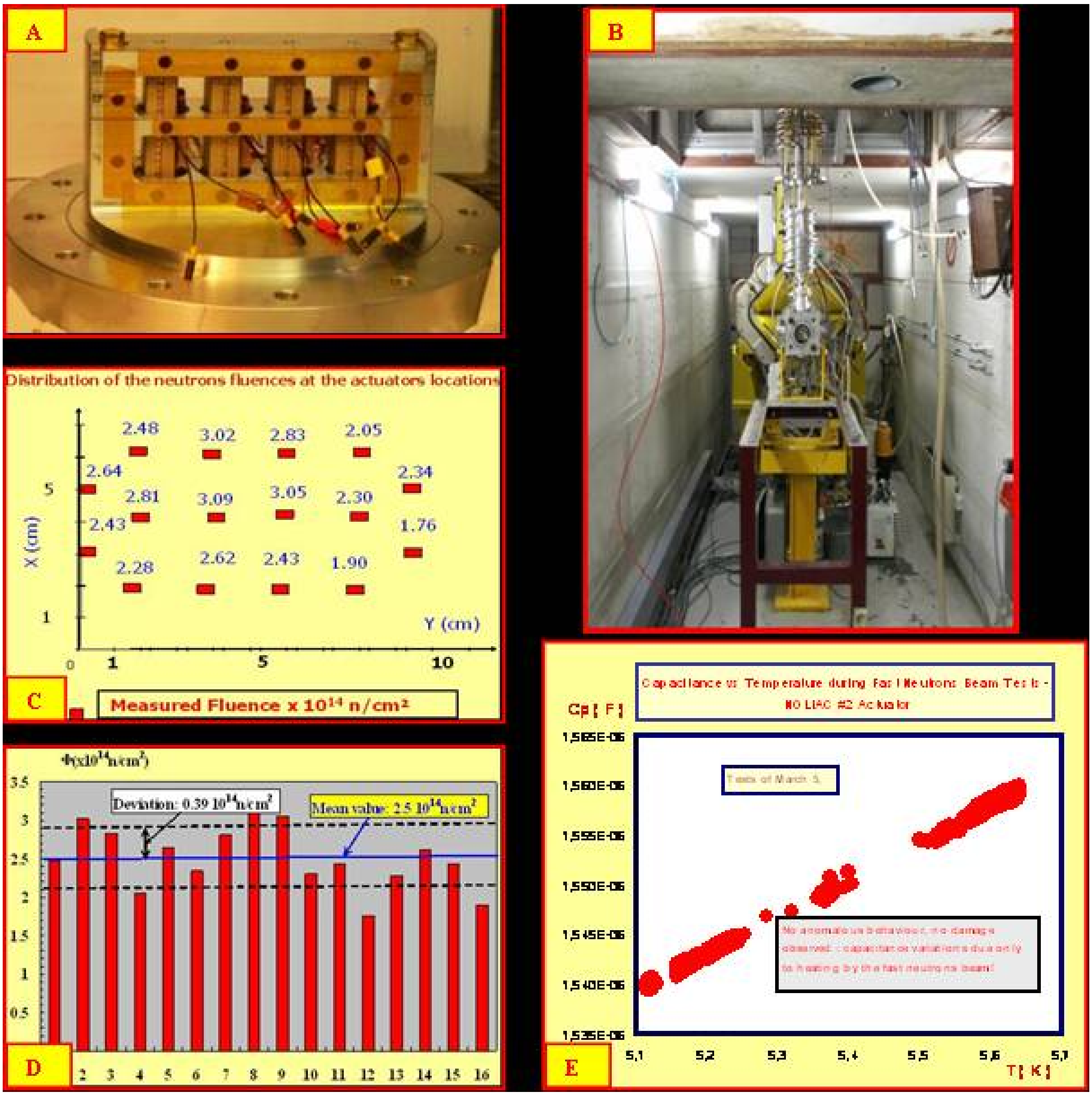

Figure 8.14. Irradiation test experiment: A) Test-cell : actuators equipped with nickel foils, B) Insert of the cryostat in front of the beam line, C) Map of the measured neutrons influence, D) Neutrons influence distribution, E) Actuator capacitance versus temperature.

Moreover, a preliminary room temperature measurement of resonant spectrum as function of the preloading force applied to piezostacks was successfully performed. Finally, a new experimental set-up dedicated to the study of preloading effect on the piezostacks electromechanical behavior at low temperature was developed and successfully tested: the main results are illustrated in Figure 8.15 and Figure 8.16. The sensitivity dC_p/dF of the piezoelectric actuator to preloading force F (F=733÷4022 N) was measured in the temperature range T = 1.68÷300 K: DC_p/DF decreases monotonously with T from 426nF/kN @ T=295 K down to 16nF/kN @ T=1.7 K.

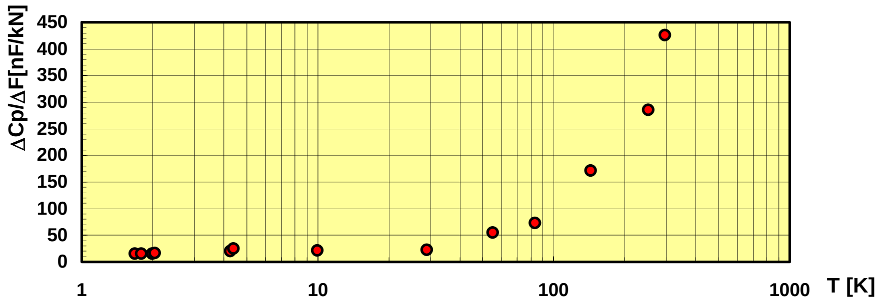

Figure 8.15: Sensitivity of piezoelectric actuator to preload force versus temperature

Moreover, the actuator capacitance increases linearly with the preloading force in the range 0.7kN- 4kN, at a given temperature (see Figure 8.16): the linear behaviour was observed in the whole temperature range (1.7 K- 300 K). Finally, a piezoelectric actuator was tested for its use as a force sensor at low temperature (i.e. capacitance variation, transient voltage, etc). A detailed report concerning this study is under preparation.

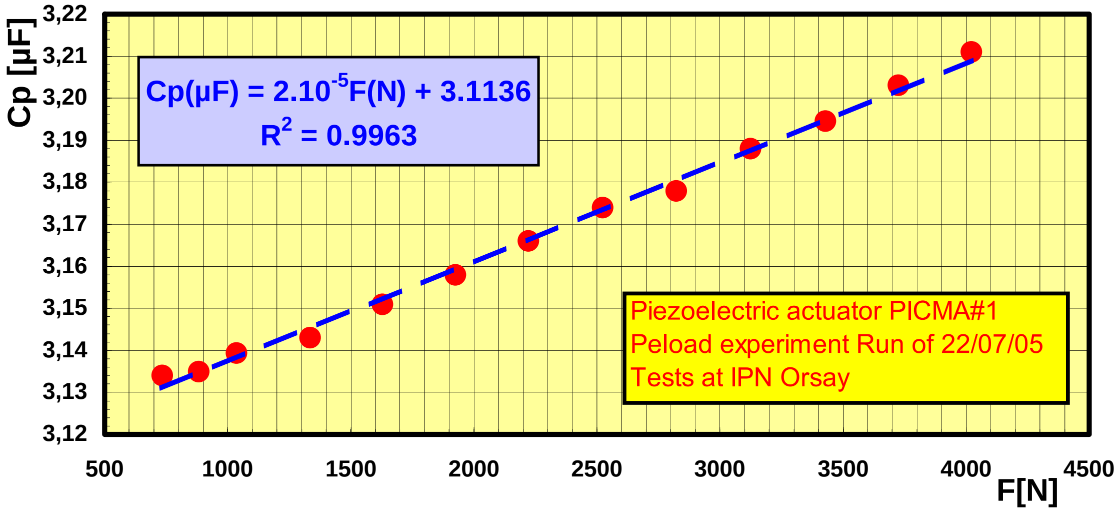

Figure 8.16. Piezoelectric actuator capacitance versus preloading force at T=4.4 K, vacuum pressure 10^{-5}mBar.

Work Package 9: Low Level RF

Activity Status

Task 9.1 Operability and technical performance

Sub-task 9.1.1 Transient detector

Progress: In line with schedule.

The goal of beam induced transient detection is to make beam phase measurement with respect to the RF field in the cavity and also to measure transient magnitudes during normal accelerator operation with beam charges from 0.5nC. This allows us to make easy and safe calibration and to monitor beam phase.
Since the beginning of the year 2005 large changes to the system have been done. The tests performed in January have proved that the applied method operates properly (http://ttfinfo.desy.de/LLRFelog/LLRFelog/data/2005/04 - 24.01.2005) and gives correct values.
During the past year transient detection system was redesigned and rebuilt focusing on automation and operability. Now it can be controlled remotely via DOOCS interface and can be calibrated automatically. The performed tests have proved that the system operates correctly (information about performed tests is available in TTF elogbook). Some design and data processing errors were found and fixed. Summary of a work done is presented below.

Completed hardware:
- Filter for transient detection
    - RF transient detection filter
    - Control circuitry for filter
- Circuitry for remote control of transient detection system
    - integration of the control system boards into VME crate with embedded SUN Sparc
    - DOOCS servers for ADC module, DAC module and digital IO module,
- Vector detector based on "The law of cosines"
- VME board with low noise 80dB variable gain amplifier
- VME board with signal distribution circuitry
- Automatic system calibration

Finished software:
- DOOCS server for transient detection
- DOOCS interface
- Matlab scripts for transient detection system control and transient measurement

Current system posseses ability to measure single bunch transient with accuracy of around 15 degrees at 1nC charge. This accuracy can be increased by averaging (Figure 9.9 – without averaging the peak to peak noise is around 35 degrees and with averaging of 30 samples this noise is reduced to roughly 7 degree.
The system accuracy will be improved by thermal stabilization of the filter. The filter has a big influence on accuracy of measurements and it is also very temperature sensitive (http://ttfinfo.desy.de/TTFelog/ - /TTFelog/data/2005/39/02.10_M - 02.10.2005 13:01). The preliminary tests obtained with thermally stabilized oven are presented in Figure 9.9. Phase

drift was reduced from 20 degrees (without temperature stabilization) to about 2 degrees (with temperature stabilization.
Finally the Transient Detection System will be installed in a thermally stabilized rack and additionally the RF transient detection filter will be mounted in thermally stabilized oven (placed inside thermally stabilized rack). The future plans also include improvement of the RF filter adjustment circuitry by replacing currently used circuit that has only one adjustment step with a circuit that has two adjustment steps for rough and precise tuning,

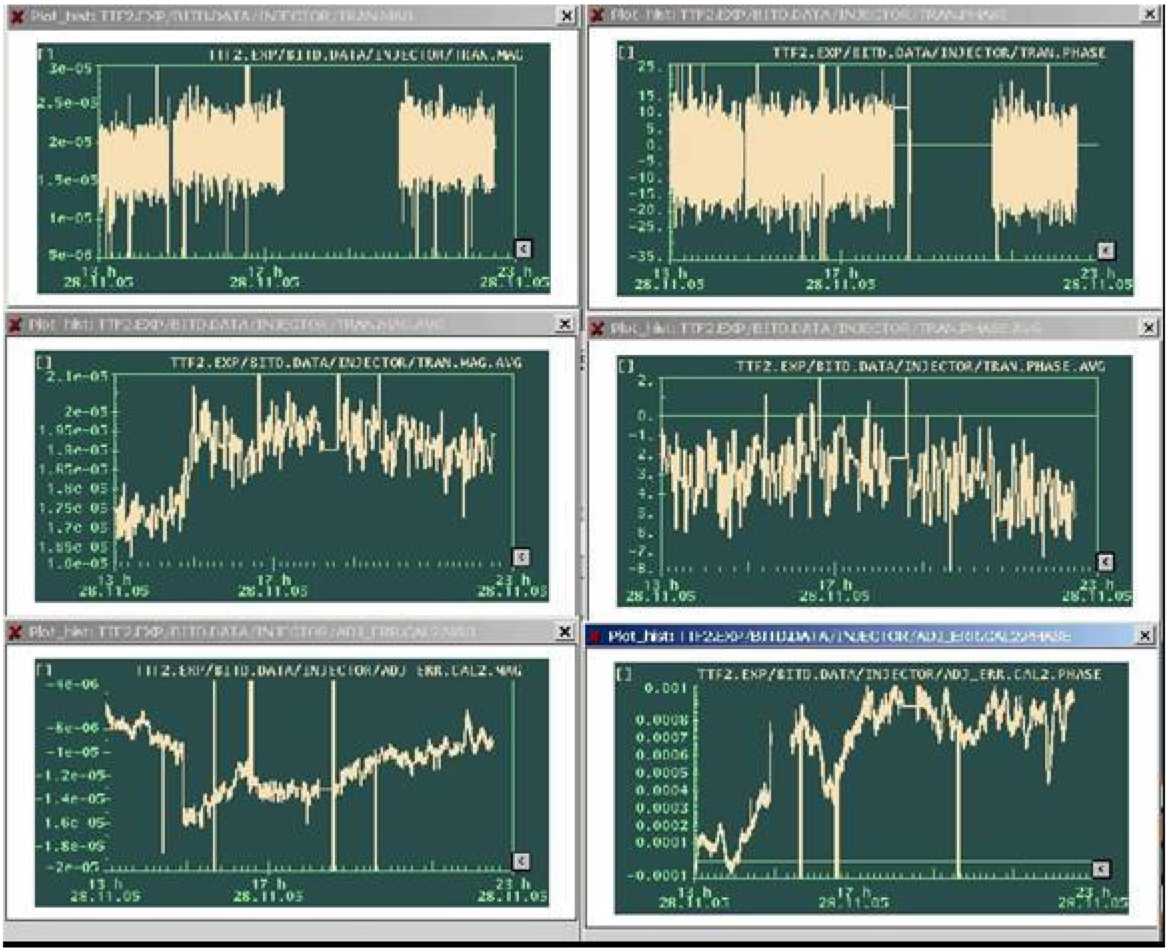

Figure 9.9 Transient detection system test with thermally stabilized oven

Figure layout: top left - transient magnitude, top right - transient phase, middle left - transient magnitude after averaging of 30 samples, middle right - transient phase after averaging of 30 samples, bottom left - filter adjustment magnitude error, bottom right - filter adjustment phase error. Magnitudes are in relative units (absolute magnitude is divided by RF field magnitude), phases are presented in degrees.

Milestones and deliverables: None defined in contract for this reporting period
Significant achievements and impact: accuracy improvement, integration of the system with operator panels
Deviations from schedule: None

Sub-task 9.1.2 LLRF Automation

Automation of RF-power station:

At the beginning of the year the monolithic solution has been designed, which was implemented as a single Finite State Machine. Unfortunately it has occurred, that this solution grew too much and operating became cumbersome to test and maintain. Therefore the design had to be changed. It was decided to split the design into two functional parts:

Exception handling part:
There has been implemented a set of several decision tables, which are listening to the environment constituted by DOOCS servers monitoring RF-power station parameters. The main purpose of these structures is to recognize and classify specific patterns of DOOCS signals, which can be called exceptions. If an exception is recognized it is marked with two identifiers (class and unique ID). There are three classes of exceptions distinguished (errors, warnings and actions). ID is a unique identifier allowing ascribing to actions human readable descriptions and corresponding procedures (only in case of actions).
After recognition an event is passed to the proper input buffer. For each class of the event one input buffer has been implemented. After placing in the buffer the event is picked up by the simple automat. This element takes care of further event processing.

Operator's assistance:
Due to the fact that exception-handling mechanism took over responsibility for many functions which formerly FSM dealt with. The scheme of the FSM driving single RF-power station has become strongly simplified and hopefully much easier to understand *test and maintain.*

Current status of present design:
Operator's FSM has been implemented and incorporated into DOOCS environment. It was preliminary tested (yet without connection with exception handling mechanism), but it proved its usability and after a few corrections it was able to drive the RF-power station according to preconfigured program.
Exception handling design is under development. Its main parts as set of decision tables, buffers and exception handling automata have been elaborated but have not been yet combined and tested together.
Applications:

- High power chain linearization,

In order to improve control efficiency of the LLRF system an application for linearization of the high power microwave klystron is necessary.

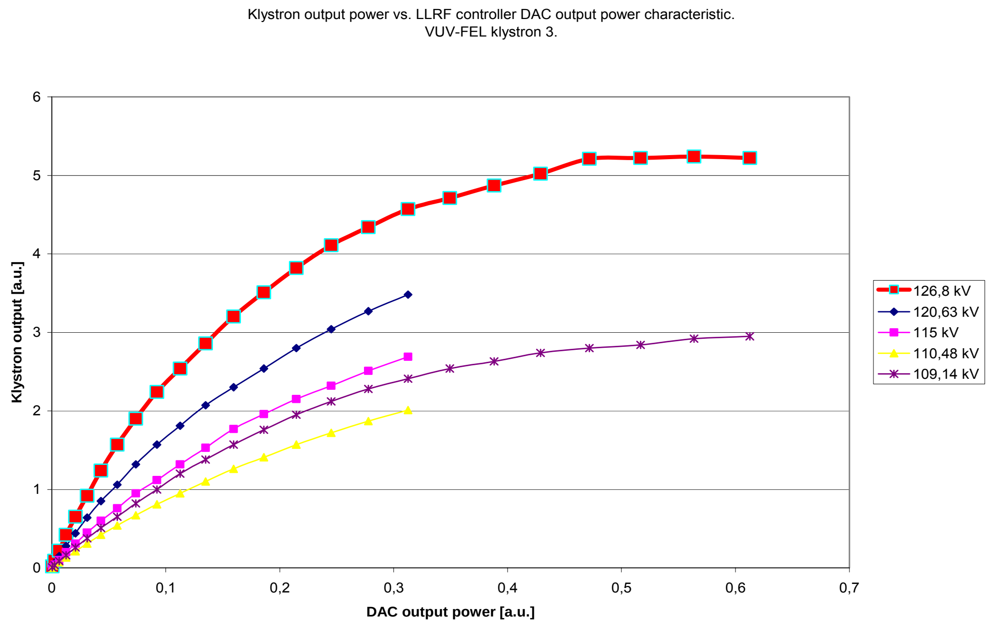

Figure 9.2. The klystron saturation phenomena in one of the VUV-FEL klystrons

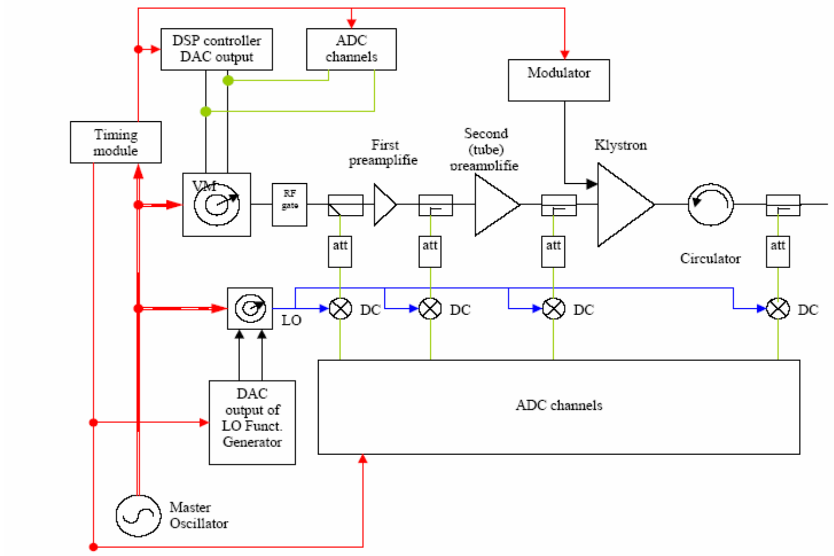

Figure9.3. Monitoring point (diagnostic) configuration for RF stations in the VUV-FEL. Data available from ADC channels is stored in the DOOCS environment and is used for further processing.

For choosing the linearization method which will fit in the present and future system requirements one has to examine the nature and quantity of the distortions introduced by high power pulse klystron. A monitoring points network needed for high power chain components nonlinearities diagnostics has been proposed and established for some of the VUV-FEL RF stations. To perform characterization of the nonlinearities of the HPC components a dedicated software tool created in Matlab is developed. Using proposed configuration and tool a number of studies (concerning response of the system for the different working parameters, nonlinearities detection, slow time drifts and phase errors induced by the components estimation) were performed for one of the VUV-FEL RF stations. Based on results achieved from present and upcoming measurements and taking into the consideration existing structure of the whole LLRF station as well as the system requirements a linearization method for the klystron will be proposed. The most promising approach (from those available on the market)

is linearization of the high power amplifiers chain using RF pre-distorer solution especially complex vector mapping.
In addition work on the software tool that will estimate nonlinearities of the klystron and the other HPC components in vicinity of the whole LLRF station operating point is under development and in the testing phase.

- Bouncer performance optimisation,

A very important issue that concerns also the klystron contribution to the whole superconducting module work performance is the high voltage pulse supply stability. As a change of the klystron HV level (eg. during the pulse) causes klystron output signal phase instability some compensation is compulsory. The Matlab tool (that co-operates with the DOOCS environment) is in testing phase for the bouncer system triggering optimization. Use of this tool during the regular machine operation will improve timing settings of the HV pulse shaping system for better voltage pulse slope cancellation during the signal plateau.

Progress: In line with schedule.

Milestones and deliverables: None for the reporting period.
Significant achievements and impact: FSM development and klystron linearization
Deviations from schedule: None

Sub-task 9.1.3 Control Optimization

Control Performance has been studied with a spread in operational gradients. Results are promising that with adjustment of loaded Q, incident phase, and fixed detuning during the pulse a spread of up to 5% can be accepted. Higher spreads can be reduced to about 5%. However with freely programmable time varying detuning during the rf pulse, the gradient spread can be completely recovered and each cavity can be operated at its maximum operable gradient. The limitations in power and limited range of tuners for loaded Q, incident phase and cavity detuning suggest a possible range of +/- 20% in gradient spread. A few percent of the average gradient may be lost by limitations in fast detuning control due to the mechanical resonances of the cavities. This requires further investigations.

Progress: In line with schedule.

Milestones and deliverables: None for the reporting period.

Deviations from schedule: None

Task 9.2 LLRF cost and reliability

Sub-task 9.2.1 Cost and reliability study

Cost reduction by integration of down-converters with analog to digital converters and pre-processing of data locally in FPGA (partial vector-sum) have been discussed. The down-converters could be placed close to the cryomodules (rf patch panel) and partial vector-sums could be sent with optical Gigalink interface to the main processing unit. This would result in significant saving in temperature stabilized RF cables.

The reliability of one RF station has been estimated. Assuming that the LLRF system consists of 9 crates from which 3 are critical for operation and that these crates have a MTBF of 100,000 hours, one would expect one RF station failure (out of 30 stations) every 4 months. With the redundant feed-forward the overall failure rate would be then only one failure every 3 years. This assumes that feedback and redundant feed-forward would fail in the same month.

Progress: In line with schedule.

Milestones and deliverables: None for the reporting period.

Deviations from schedule: None

Sub-task 9.2.2 Radiation damage study

A dedicated system for neutron fluence and gamma radiation monitoring in real-time was installed on the VUV-FEL. The system was equipped with a SRAM-based neutron detector, for which the operation is based on counting parasitic Single Event UpSet (SEU) generated in SRAM device by neutrons. The detector is connected to radiation tolerant read-out system; therefore the whole system can be installed in a radioactive environment.

A series of experiments were carried out to select memory the most sensitive to neutrons. The 512 kB Samsung memory, which has the highest sensitivity factor S, was finally chosen as a neutron detector. The detector consists of four K6T4008C1B-GB70 chips mounted on the small PCB board. The memories are 11 times more sensitive then 1 MB SRAM used before.

A supplementary cylindrical neutron moderator, made of polyethylene, was applied to assure a flat response of the SRAM-based detector to neutrons with energies up to tens of MeV. The dimension of the moderator was calculated using the MCNP 4A code. The neutrons passing through the moderator are thermalized. The construction of the moderator assures that enough thermal neutrons are produced to generate a flat response of the detector (taking into consideration neutrons with energies up to tens of MeV). Application of 9 cm moderator allows one to increase sensitivity more or less 4 times.

Finally the sensitivity to neutrons of the RadMon system was improved 45 times. A comparison of sensitivities for two different memories: 1 MB and 4x512~kB-stacked detector with and without moderator is presented in Figure 9.4.

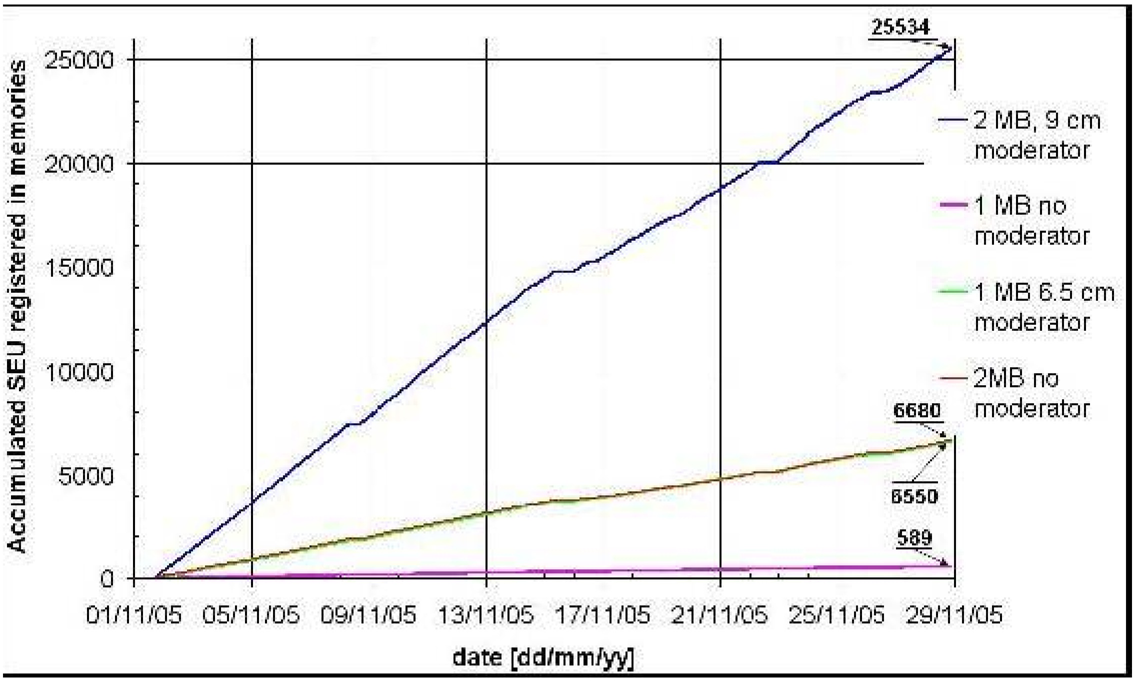

Figure 9.4. A comparison of SRAM devices

The accumulated dose was collected within one month. The memories were calibrated using a ^{241}AmBe (n, a) source. Moreover, a preliminary, in-situ, calibration was carried out in VUV-FEL tunnel. One SEU generated in memory corresponds to 256000 n*cm^{-2}.

The dose of gamma radiation produced in the accelerator is substantial therefore it is important to measure the radiation in real-time as well. RadFET-radiation sensitive Field Effect Transistor was used to measure gamma radiation. Figure 9.5 presents the accumulated dose of the gamma radiation and neutron fluence measured in VUV-FEL tunnel during November 2005. It is worth to mention that the characteristic is flat for a few hours every Tuesday - this is the VUV-FEL maintenance day and the accelerator is switch off. Therefore no radiation is produced.

According to the presented graph and carried out calibration the raw radiation dose produced during operation of the accelerator: gamma dose produced during one day is estimated to 13.35 Gy and neutron fluence is 2.38*10^{8} n*cm^{-2}.

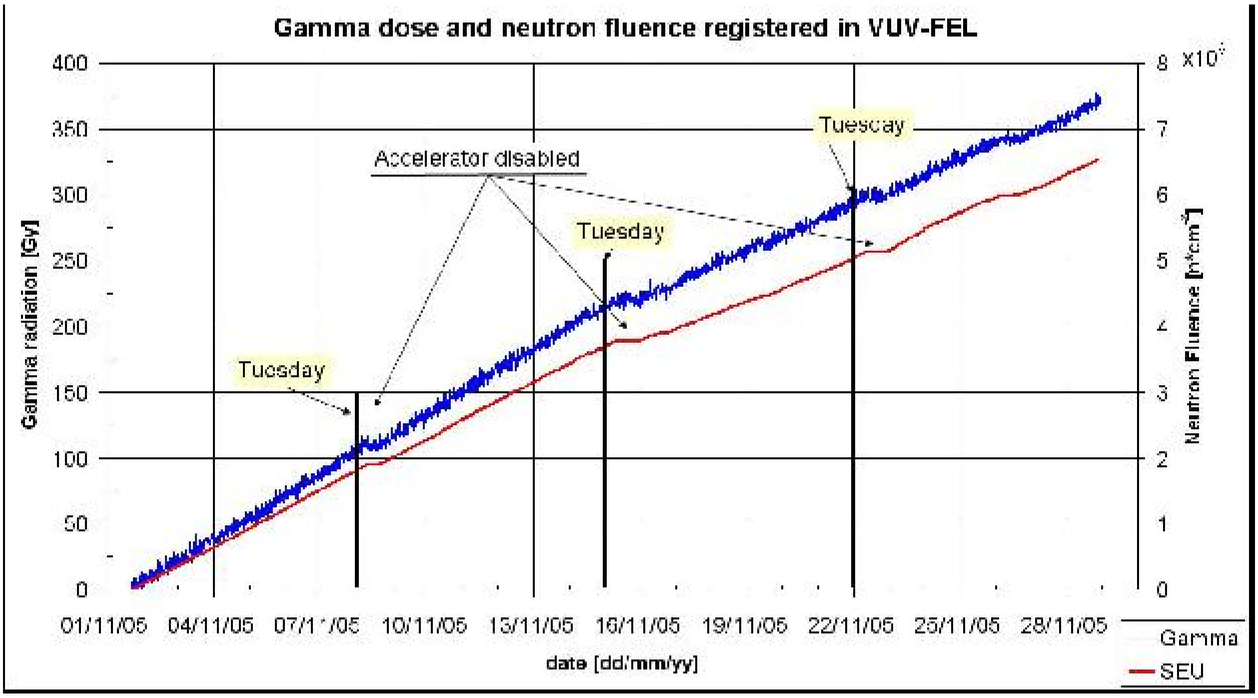

Figure 9.5 Neutron fluence and gamma radiation measured in VUV-FEL

The measurement were carried out near the output of the first cavity module ACC1. Four RadMon systems are currently mounted on the concrete wall opposite module ACC1, see Figure 3 The data are accessible through the web-based interface (http://neo.dmcs.p.lodz.pl:9999/).

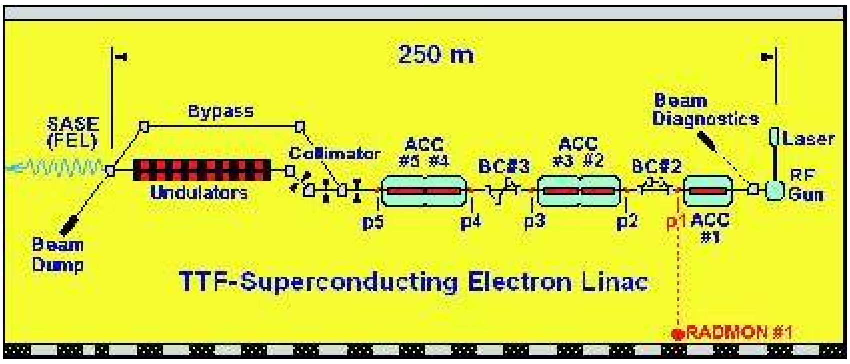

Figure 9.6. A view of the VUV-FEL cross-section with pointed out installed

There were also performed some experiments with radiation tolerant software algorithms. The main aim was to design the fault tolerant operating system which should be able to work on standard computers architectures subjected to the radiation impact.

The modified sCore operating system is used for research. It provides only a indispensable functionality such as preemptive multitasking environment. The sCore kernel was changed to provide the software redundancy. The special process, called EDAC task, was build in sCore (fig. 9.7). The system memory is divided by EDAC task for three parts: program memory and two copies. The EDAC task is run periodically by the sCore scheduler (Round Robin algorithm). System memory is checked by the EDAC task and compared with one of copy. If occurs any difference the EDAC task chooses a validity data and copy it to system memory region.

Two experiments were conducted at DESY. They showed the impact of radiation on the software part of the computer system. Checking the effectives of EDAC Task algorithm was the main aim of both experiments. A software redundancy (EDAC Task) can be very efficient and reliable when microprocessor system is subjected to weak radiation and small number of SEU events what was confirmed by the results of experiment with 241AmBe neutron source. The experiment conducted inside Linac II tunnel opposite to electron-positron converter proved that strong radiation source generates SEUs not only in main memory but also in registers inside CPU. The EDAC Task can not prevent SEU inside registers and its application is not sufficient for intensive neutrons radiation. Further development will utilise two or more microprocessors (e.g. PowerPC microprocessors embedded in Virtex2Pro FPGAs) working in parallel.

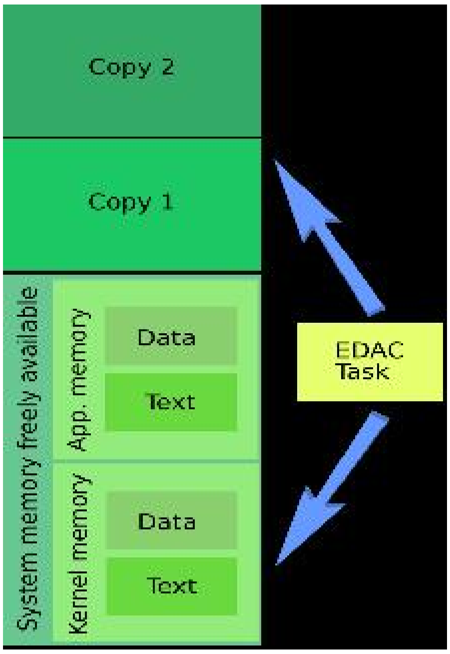

Fig 9.7: Memory protection using EDAC Task

Milestones and deliverables: None defined in contract for this period
Significant achievements and impact:

- The most sensitive memory to neutrons was chosen,
- An additional moderator was designed to assure flat characteristics and increase sensitivity,
- Four RadMon systems were installed in VUV-FEL, which represent a distributed system for on-line radiation monitoring,
- The data are collected in database and accessible through www-based interface (next step is the handler for DOOCS system),
- Patent application describing the system was registered.

Deviations from schedule: None

Task 9.3 Hardware

9.3.1 Multi-channel down-converter

Based on the current state of design and realization of the RF Feedback System in order to perform new frequency conversion down-converter unit project, a series of analysis were made, which were verified by calculations as well as practical realization of considered circuit solutions.

In first stage of the conducted research a characterized frequency conversion process influence on parameters measurement of mapping signal of fluctuations gradient and phase of field in cavity was defined, with taking into consideration current realization of the control loop parameters as well as algorithms which assure the stabilization of period of beam generation. At the next stage a maximum acceptable measuring errors of change of gradient and phase values for single measurement receiver for incoherent averaging in 32 cavity system was specified, the values of which are calculated by:

$$\Delta A_{\max} \le 1{,}1892 \cdot (\sigma_E/\mathrm{E})_{RMS}\ ,\ \Delta\varphi_{\max} \le 0{,}5946 \cdot \pi^{-1} \cdot (\sigma\varphi)_{RMS}$$

On the basis of above-mentioned dependences of frequency conversion system parameters was defined using behavioral model. The primary factor that has an influence on stabilization gradient and phase value is dynamic range, however taking into consideration the distortion that results from nonlinear measurement receiver is Spurious-Free Dynamic Range (SFDR)[1]:

$$SFDR_{kaskady,dB} = \frac{2}{3}\left[3 - 10\log\left(kTB \cdot \log\left(\sum_{i=1}^{N} \frac{10^{\frac{NF_i}{10}} - 1}{10^{\frac{\sum_{j=0}^{i-1} G_j}{10}}}\right) \sum_{i=1}^{N}\left(IP3_i \prod_{j=i+1}^{N} G_j\right)^{-1}\right)\right]$$

Primary effect on possible acceptable phase fluctuation coefficient of field has complete additive total phase noise, which consists of internal phase noise for the each frequency conversion stage, as well as master oscillator phase noise. The general form of phase noise level is given by [1]:

$$PN_{rms\_total} = \frac{180}{\pi}\left[{}^{ADC}PN_{rms}^2 + {}^{div}PN_{rms}^2 + \left[\left(2 - R_{\xi\eta}\left(t_{LO1}, t_{CLK1}\right)\right)10^{\frac{k_{fo}}{20}} \cdot \right.\right.$$
$$\left.\left. \cdot\left(f_c\left(1 + 10^{\frac{p}{10}}\right) + 2 \cdot 10^{\frac{p}{10}}\right) \cdot \left(10^{\frac{k_{fo}}{20} + \log N} + 10^{\frac{k_{fo}}{20} - \log M}\right)\right]^2\right]^{\frac{1}{2}}$$

thus the distortion level of phase mapping in frequency conversion processing depends on architecture of conversion unit, fluctuation mapping techniques in digital form. The indirect coefficient that has an influence on fluctuation mapping accuracy on digital form of mapped signal of field in cavity is intermediate frequency value [1][2]. Along with the increase of intermediate frequency, the phase of mapping error also increases; as well as indirect influence on representation of instantaneous amplitude value, that results from SNR decrease.

On the basis of obtained results from a system analysis, a frequency conversion project was made for two different intermediate frequencies. An individual stages of conversion unit was designed (band-pass filter on 1,3GHz, bad-pass filter on intermediate frequencies, couplers, intermediate frequency amplifiers, matching circuit for proposed double balance mixers, as well as matching circuits for ADC's).

On the basis of defined parameters in the analysis process, a required ADC's parameters was estimated, as well as selected one of the available commercial model, using evaluation board for the measurement. For confirmation of conducted analysis a number of measurements of practical realization were made. As a result of conducted theoretical and practical research there was specified a design and build solution of optimal conversion unit on the basis of commercial components. The conducted number of research present direction, in which further conduct works need to be done for obtaining the target stabilization parameters in retaliated TTF2 project, as well as for the next research in other control system for EM field stabilization in cavity projects.

Progress: In line with schedule.

Milestones and deliverables: None for the reporting period.

Deviations from schedule: None.

Sub-task 9.3.2 Third generation RF control

New 3rd generation LLRF system called SIMCON3.1 is based on Xilinx FPGA chip XC2VP30 Virtex-IIPro with 2 built-in processors and DSP blocks as a main control element. The board under development consists of 10 input analog broadband channels of 270 MHz and the voltage range ±1 V (matched to the wave impedance of 50 Ω) as well as 4 DACs channels with corresponding to ADCs parameters. Several digital inputs and outputs are supplied for timing and triggering signals. The board is also equipped with precision timing distribution system with planned jitter performance about 0.3 ps (RMS) and memory blocks – static, of capacity 512K of 36-bit words and dynamic, of capacity 128Mb and the word width of 32-bit for data storage.
The board is developing as VME 6U card which can work also as stand-alone board using for communication additional interfaces like fast opto-giga-link with maximum throughput 2.125 Gbps as well as standard Ethernet 100Mbps link. Block diagram of this device is presented in figure 9.8.

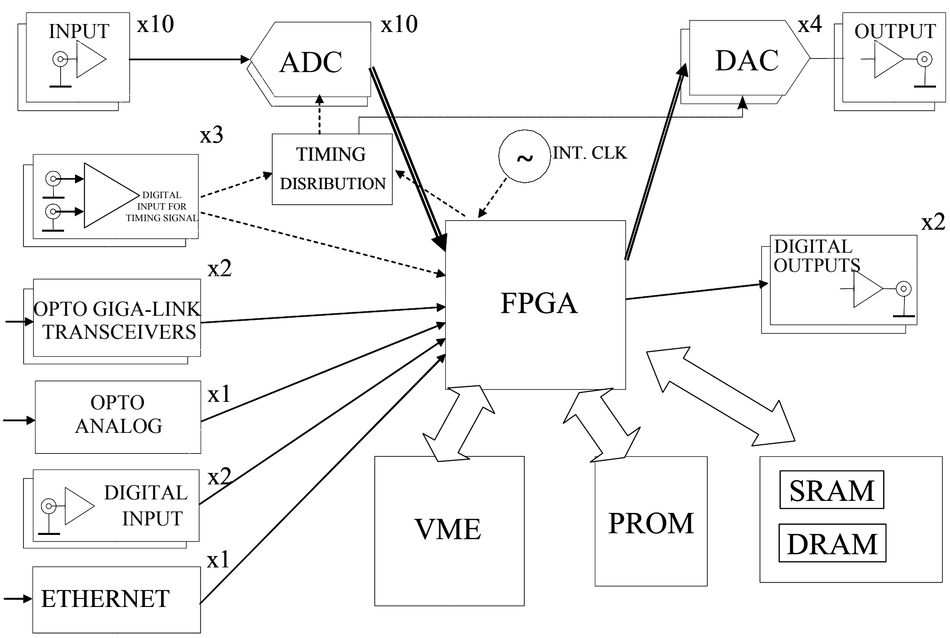

Figure 9.8 SIMCON3.1 block diagram

PCB board for SIMCON3.1 device has two realisations one of which is finished, debugged and currently under test. Eleven pieces of those boards have already been produced (figure 9.9).

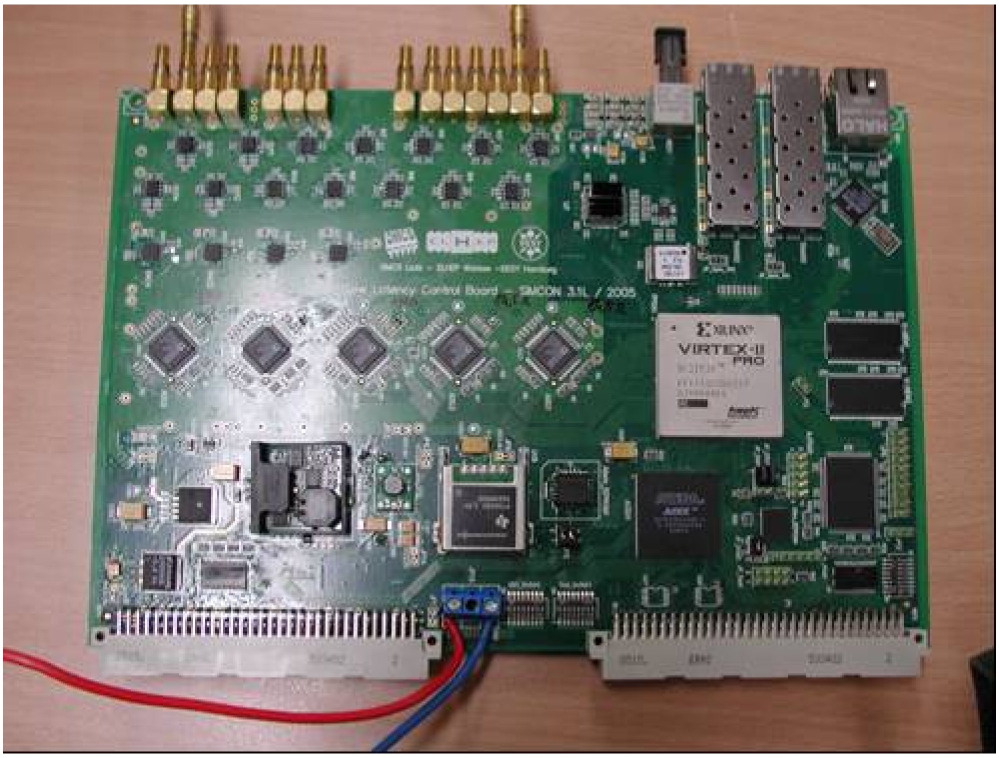

Figure 9.9 One realisation of the SIMCON3.1 board

The second realisation of SIMCON3.1 is still in the fabrication process.

FPGA board SIMCON 2.1 was tested in CHECHIA with success in January 2005. The firmware, software and Matlab algorithm for control one superconductive cavity were tested with this board. DOOCS server for SIMCON 2.1 board was made.

New firmware for FPGA board called SIMCON 3.0 was tested. This firmware was written in VHDL and the idea was presented in quarter report 1-2005. Additional functionality is the detection of vector sum deviation and handler to it, which cut the controller driving signals. Hardware and software of SIMCON 3.0 was tested in TTF2 on accelerating module ACC1. The tests were performed in May and September during LLRF studies. Module ACC1 of VUV-FEL accelerator in DESY was controlled by the SIMCON 3.0. The vector sum of field in eight cavities was stabilized. Proportional controller was used for fast feedback loop. Figure 9.10 presents plots of working system. A DOOCS server for SIMCON 3.0 board was made.

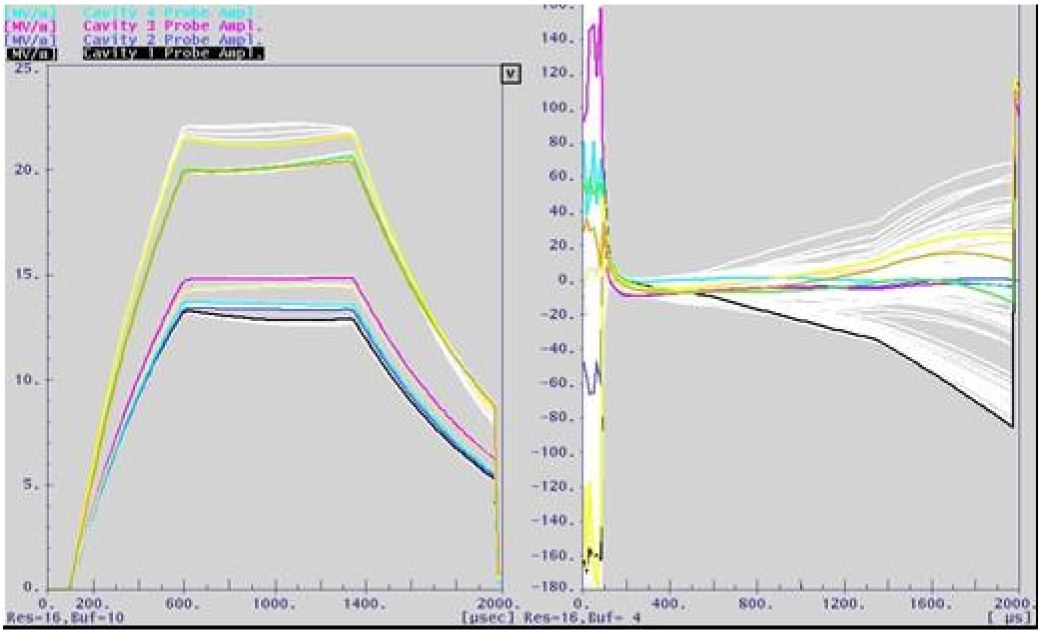

Figure 9.10. Amplitude and phase of eight cavities from ACC1 in VUV-FEL

Figure 9.11 SIMCON3.0 ready for tests

The firmware which was developed for SIMCON 3.0 was compiled and loaded to new control board SIMCON 3.1. The firmware works properly on SIMCON 3.1.

Sub-task 9.3.3 - Stable frequency distribution.

Progress:
New Master Oscillator:
Low power part: a lot of modules were redesigned in order to meet our spec; e.g. new design for the 81 MHz and 108 MHz VCXO´s including a power gain stage (1 W output) and four way power splitter at the output to eliminate phase drifts between outputs; low phase noise

dividers in separate modules to minimize heating of individual modules due to their power dissipation , 9 MHz 1 W power amplifier and four way power splitter. Frequencies lower than 81 MHz (i.e. 27 MHz, 13,5 MHz, 9 MHz 1 MHz) are now derived from the 81 MHz master. A new block diagramme for the low power part was developed, the modules are wired according to this scheme, mounted onto a chassis and cabled. RF cabling was done using semi rigid cables.

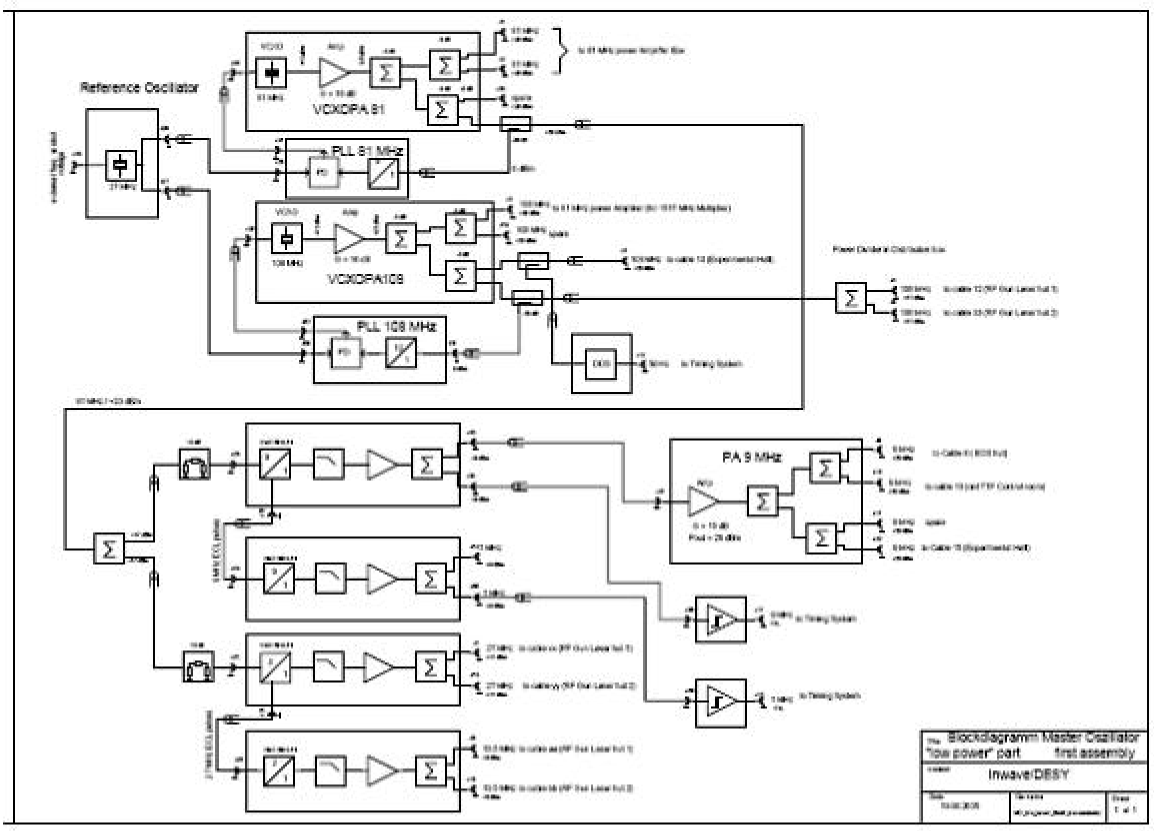

As the 9 MHz OCXO from MTI does not meet the spec given in their data sheet (but was the baseline for our spec), a 9 MHz OCXO from Wenzel Associated was ordered. The three delivered OCXO´s had strong spurs at about 50 Hz offset from the carrier and therefore ware sent back for repair. They arrived in August this year.

A new scheme for generating 1.3 GHz and 2.856 GHz signals was developed using commercial, off the shelf, 2,488 GHz SAW based VCXO´s mixing this frequency with a 112 MHz crystal oscillator, filtering and dividing the resultant 2.6 GHz signal by a factor of 2 and phase locking this 1.3 GHz signal to the 81 MHz reference frequency of the low power part. A similar scheme is used for generating 2.856 GHz.
The 1.3 GHz oscillator and PLL are housed in a sperate crate and powered by a low noise power supply.
The required phase noise spec is not fulfilled. A DRO type oscillator is being developed at Warzaw university and Posidon Scientific Instruments.

High power part: amplifiers for 1.3 GHz and 81 MHz and associated monitoring circuitry were assembled into their 19´´ crates. The 1.3 GHz amplifiers do not meet the gain spec, therefore testing of different amplifiers with respect to gain, output power and phase drift are under test. New “customers” for the 81 MHz reference signal requested extra outputs, therefore the design of a new 81 MHz power part is taking place. For 81 MHz a new amplifier is under development.

Frequency Distribution

Temperature control circuitry for stabilizing the temperature of the coaxial cables in the TTF II tunnel is installed, the controller is installed

Phase stable fiber-optic frequency distribution link was installed and successfully tested in the TTF II environment. Stability requirements have been fulfilled but several problems and room for improvements were found. See figures 9.12 and 9.13 for example measurement results from 11 days long measurement. Phase change of three signals have been shown (system controller output, stable signal at the end of the link (after passing ~400 meters in the accelerator tunnel) and signal with no feedback applied, which passed the same way as controlled signal).

In figures 9.12 and 9.13 one can observe that long term drifts have been significantly suppressed (order of 10) in the stable signal comparing to the signal with no feedback applied. Long term drift plots (1 hour range) in figure 2 show this effect more precisely. Obtained phase stability 2 ps RMS stays within the required 5 ps range but it still can be improved by solving a problem of asymmetric phase drifts observed in the system.

Unfortunately there was a problem with short term drifts (1 minute range). Due to problems with the phase shifter control, the short term stability of controlled signal was a little bit worse than the signal with no feedback. In both cases phase drifts do not exceed 0.6 ps RMS, which is less than requires 1 ps but here also is a room for improvements. Fortunately, reasons for short term drift problems were found. Improvements are in progress.

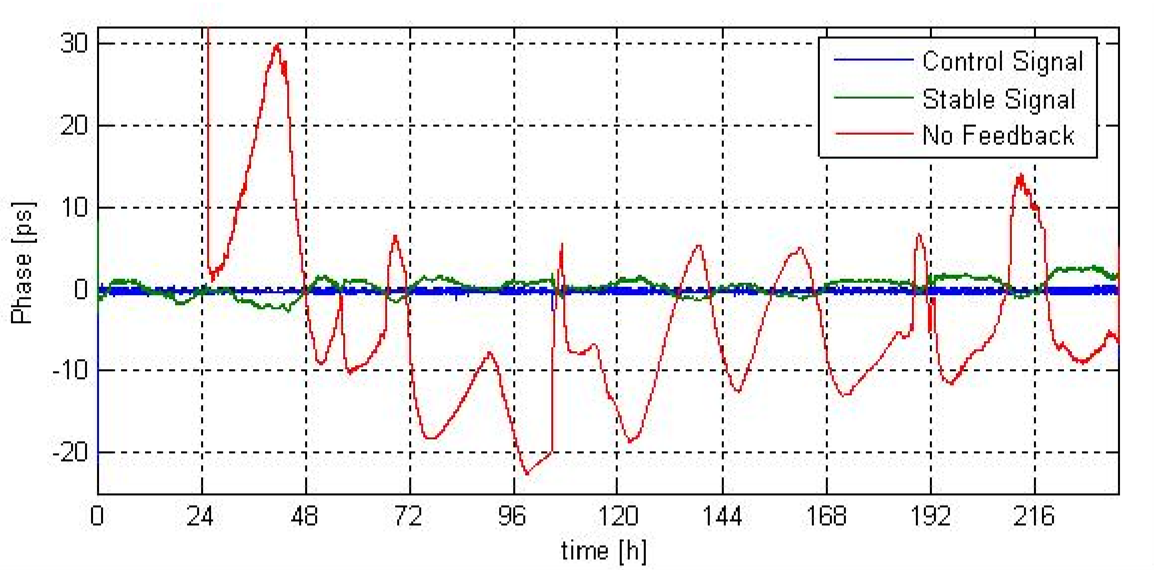

Figure 9.12: Phase drift measurement.

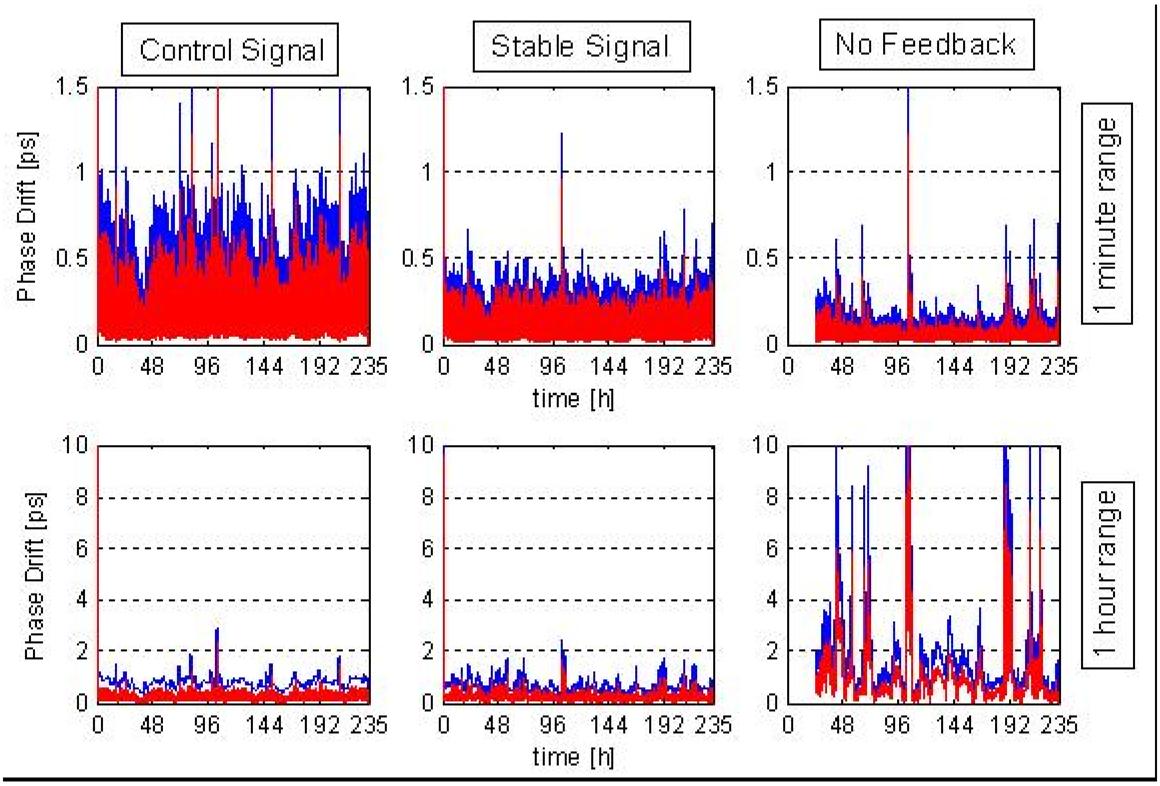

Figure 9.13: Phase stability results (Red: RMS, Blue: Peak-Peak)

In the near future a study on phase detector accuracy improvements will be performed. Proper calibration of existing phase detectors will be applied in order to remove errors from the measurement data gathered during last measurements.

Milestones and deliverables: None defined in contract for this period
Significant achievements and impact:
Still need to use the old and existing Master Oscillator.

Task 9.4 Software

Sub-task 9.4.1 - Data management development

Progress: In line with schedule.

The database structure has been modified (ex. new fields like type of stored value has been added) to allow adding new types later. The user interface to the database was redesigned and improved. The C++ interface has been extended; few bugs (possible leading to the database inconsistency) were removed. Interfaces for Java and Matlab have been prepared. Batch application (**t_db_doocs** – Figure 9.16**)** to compare/transfer data between database and DOOCS servers has been developed for external programs and scripts. The GUI front-end (**gtk_db_doocs** – Figure 9.15**)** to this application has been developed as well. Example data from DOOCS servers (calibration parameters) was transferred to database using GUI application (Figure 9.15).

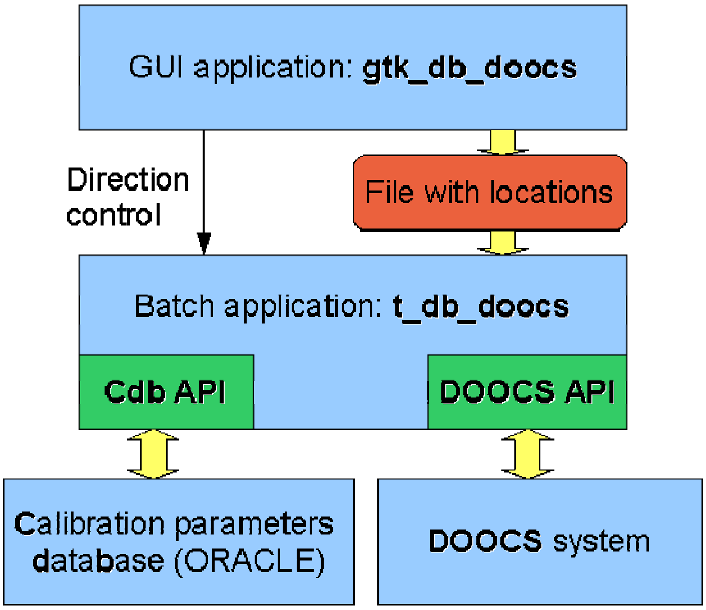

Figure 9.14. Diagram of data flow between CDB and DOOCS

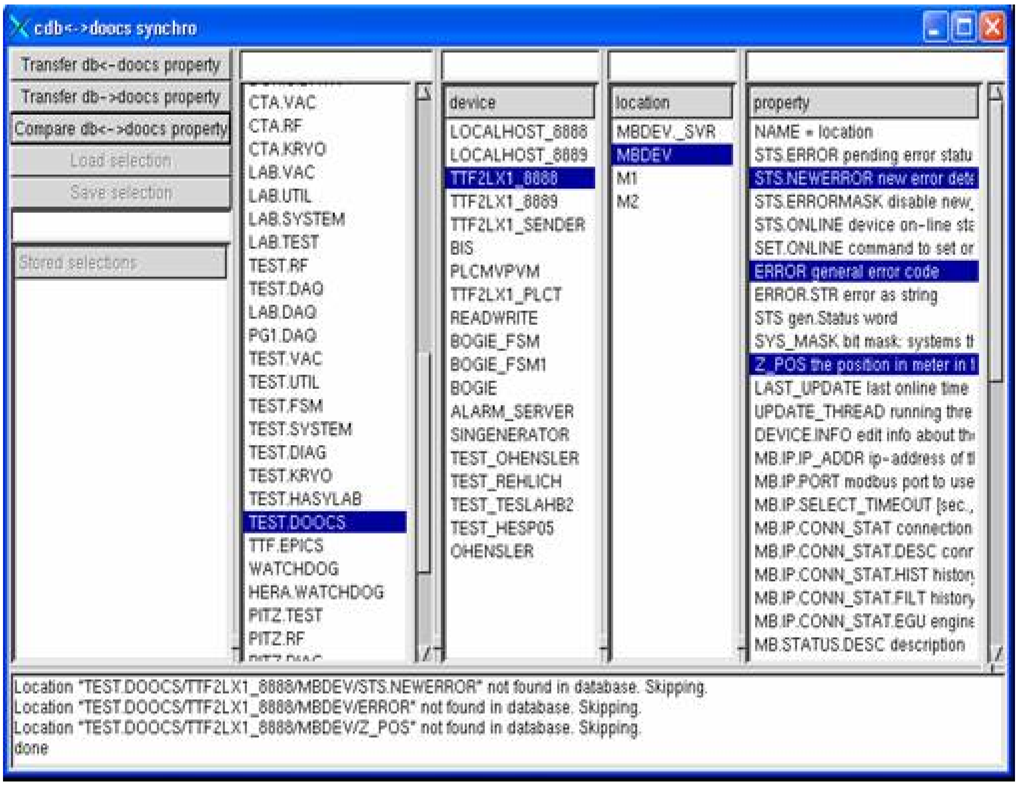

Figure 9.15. Screenshot from gtk_db_doocs application.

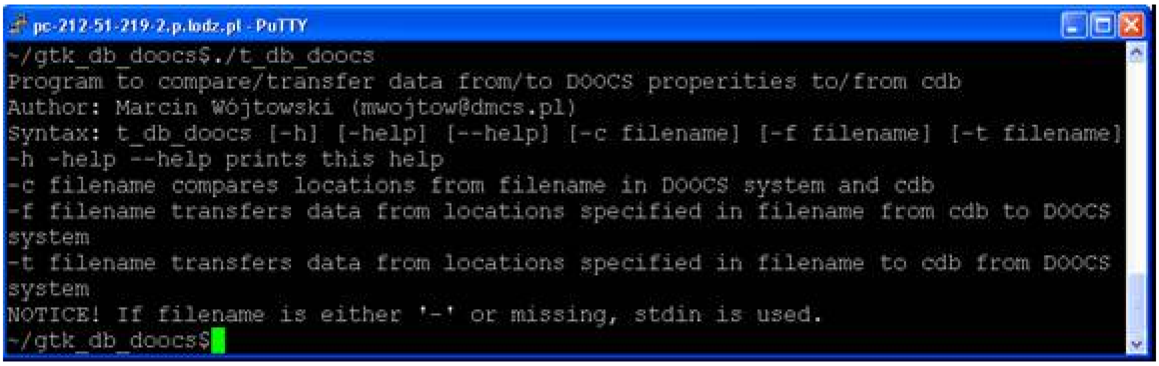

Figure 9.16. Screenshot from batch application.

Milestones and deliverables: Final Report
Significant achievements and impact: the database is ready for tests.
Deviations from plan: small delay (1 month) in the preparation of Final report.

Sub-task 9.4.2 - RF Gun control

Progress:
During LLRF studies in September 2005 the RF Gun was controlled by SIMCON 3.0 board. New software was written for controlling of the RF Gun. The RF Gun controller was written in VHDL and implemented in FPGA on SIMCON 3.0. Matlab scripts and DOOCS server were written for communication with the SIMCON 3.0 board. Figure 9.17 presents the block diagram of VHDL code, inputs and outputs used for RF Gun controller.

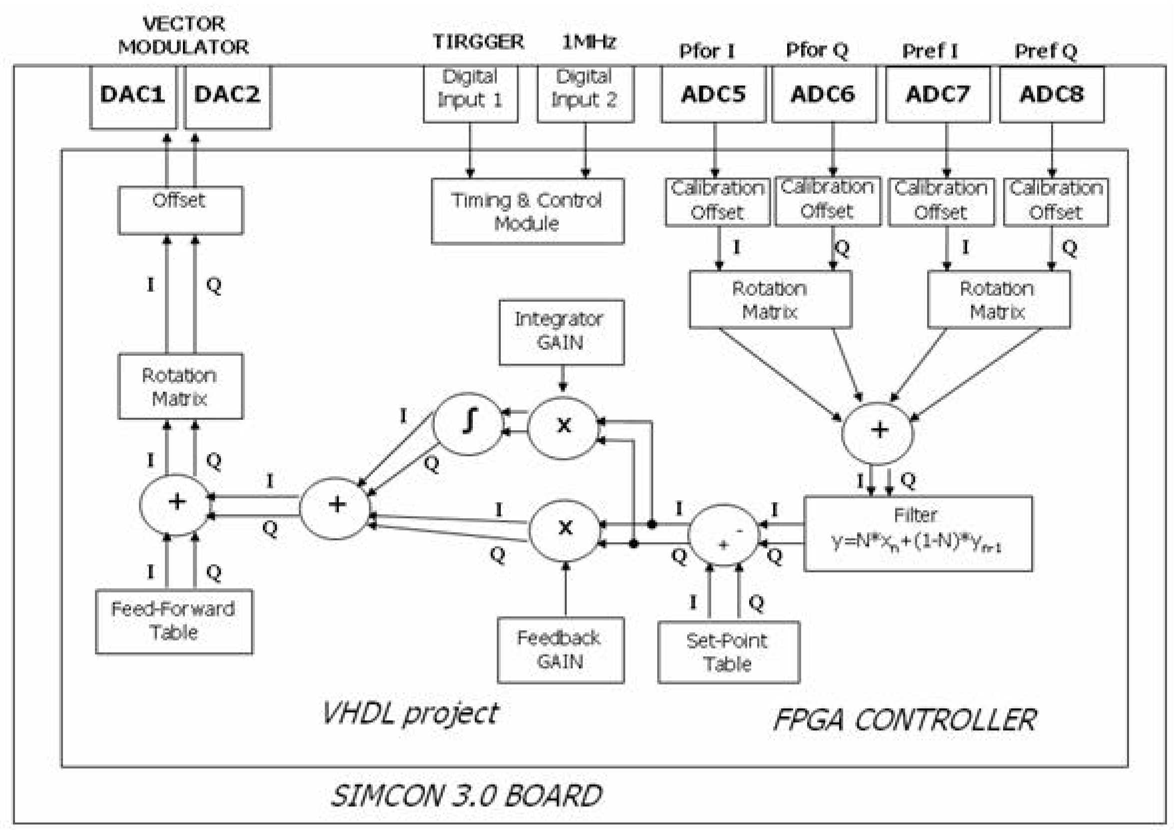

Figure 9.17. Block diagram of VHDL firmware for RF Gun controller

This version of the firmware and software was tested with RF Gun in VUV-FEL in DESY. All functions of the controller were tested. The controller stabilized the field in cavity calculated from forward power minus reflected power. For the fast feedback loop PI controller was applied in SIMCON 3.0. After initial tests the stability of the amplitude and phase of the field was as good as with current control system. The stability of the amplitude during flattop was about 1% and phase – 1 deg. The beam was accelerated by the RF Gun. The stability of phase and energy of the beam was measured. The results are presented in Figure 9.18.

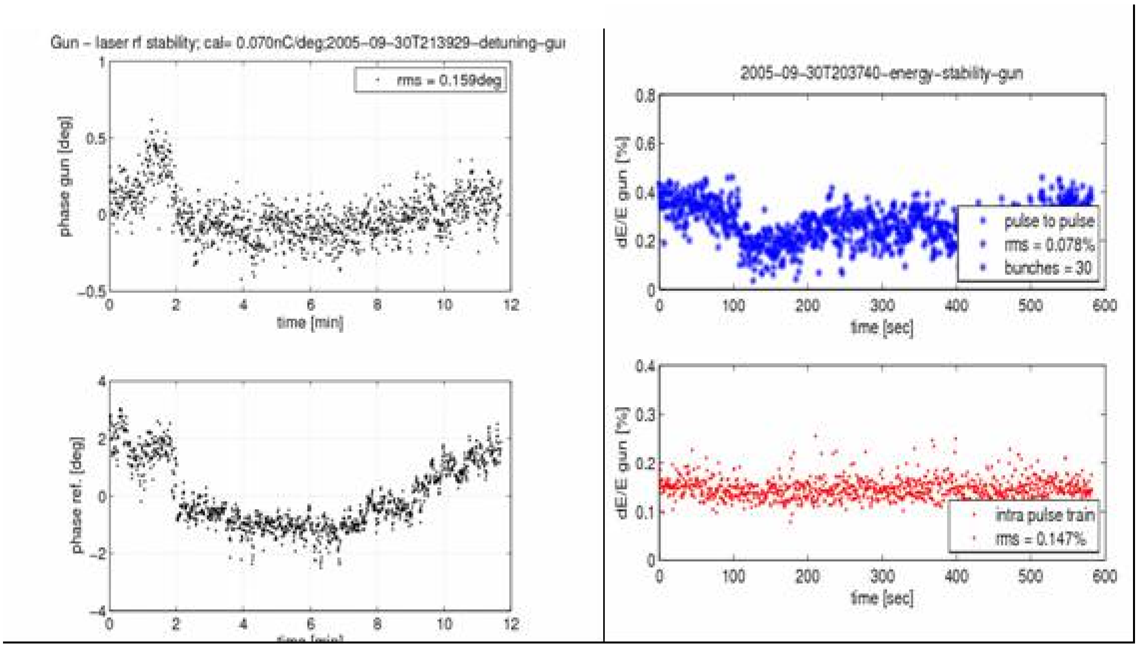

Figure 9.18. Phase and energy stability of the beam after RF Gun

Milestones and deliverables: None defined in contract for this period.

Significant achievements and impact: None

Deviation from schedule: None

Work-Package 10 - Integrated RF tests in a horizontal cryostat

Activity status

Before starting the different tests planed in the CARE proposal (cold tuning system, piezo and magnetostrictive fast tuners, new couplers) it was necessary to first qualify a standard “nine cell cavity” equipped with a high power TTF-III coupler in CryHoLab.

The first part of this qualifying test was to check possible cryogenic problems (helium tank filling, coupler cool down, temperature measurements and helium bath pumping…). During the cool down @ 1.8K, in January 2005, no specific problem appeared, except the very long time of the whole structure thermalisation: as a consequence, we improved the thermal connections between cavity support and He gas pipe.

The second part of this test was to check the possible problems linked to the cavity working at high RF power. Some problems appeared on the water cooling system and klystron modulator (which was being used beyond its rated values) involving the complete changing of the insulating-oil (4500 liters). As a consequence, the “high power pulsed test” was performed with delay in July.

Fig.10.1 The klystron-modulator components are transferred, after cleaning, in the oil-tank refilled with 4300 liters of new oil.

After the RF coupler conditioning (300 K, 1 MW, 1 ms, 3.8 Hz), the pulsed RF power was injected in the 9-cell cavity after cool down at 4K. We can see on figure 10.2 the reflected power and the transmitted power signals from pick-up probes. In RF pulsed mode (4 K, 900 kW, 250 µs, 0.8 Hz), the maximum accelerating field reach 18 MV/m with a power limitation due to a strong field emission with X-rays detected (7 µSv/h around the cryostat).

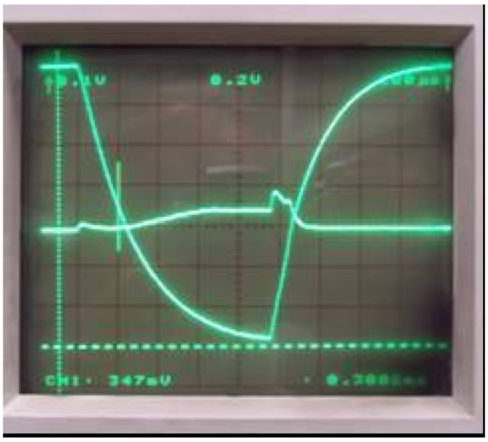

Fig.10.2 Oscilloscope traces of transmitted (upper) and reflected power (lower).

After these qualifying tests, "CEA Cold Tuning System" has been assembled on nine cell cavity at the beginning of September 2005.

Preliminary measurements of "microphonics" resonances have been performed at the room temperature in the RF laboratory (see WP8) and in CryHoLab (November 2005). At the present time, RF tests are under way at 4 K.

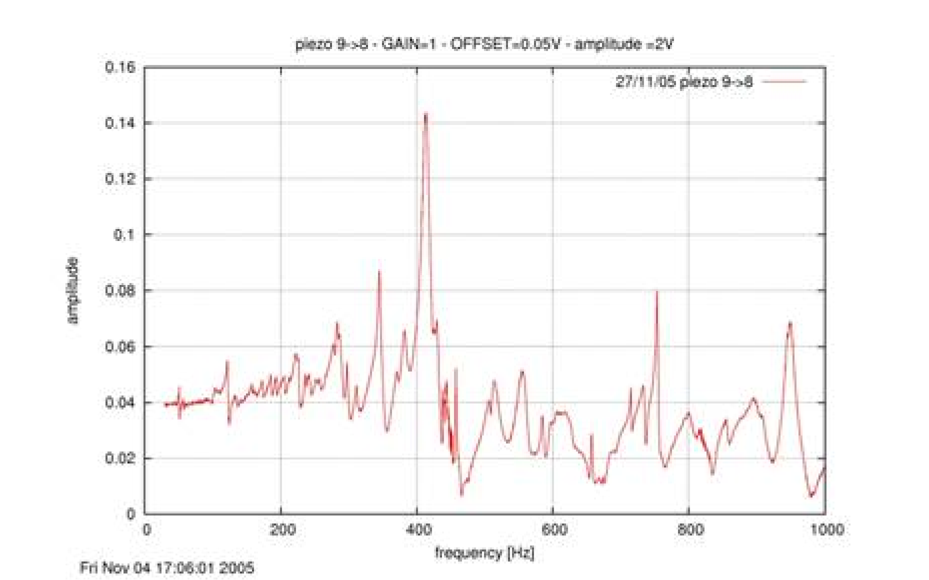

Fig. 10.3 Cold Tuning System (CTS) with Noliac Piezo Tuner mounted on 9-cell cavity for cold test in CryHoLab.

The removal of CryHoLab from "l'Orme des Merisiers" area to the main Saclay Center is delayed once again. The transfer should take place in April 2006, after the CTS tests with piezo and magnetostrictive tuners.

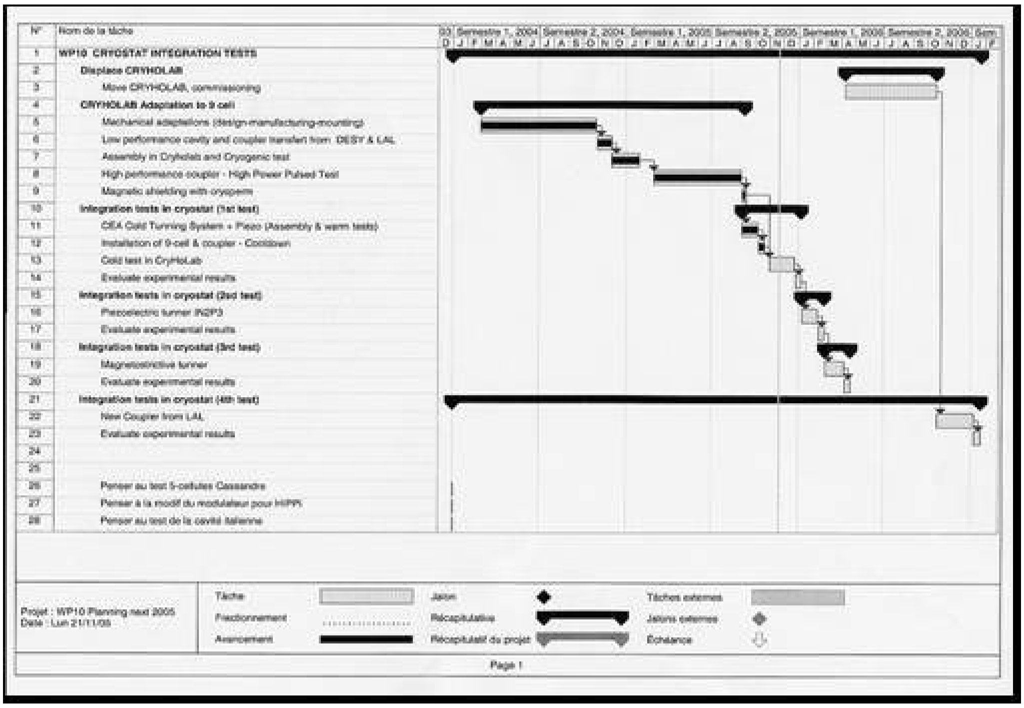

Work Package 11: Beam diagnostics

Task 11.1 – Beam Position Monitor

Activity status

The activity of this year has been to design a new version of the monitor (new mechanical and RF characteristics) to have a good resolution (around 1 µm) and a high time resolution (around 10 ns). Another part of the activity has been to start testing the monitor (BPM) inside the ACC1 cryostat with the beam to observe its performance. As of September 2005, in agreement with the CARE Steering Committee, the research activity on the possible use of the dipolar Higher Order Modes (HOM) of the accelerating superconducting cavities to monitor the beam position along the TTF2 linac has been included in the Work Package 11.

Sub-task 1 : Development of the re-entrant RF BPM.

New design of the BPM cavity

The mechanical structure (Fig. 11.1) has an overall length of 170 mm and is quite similar to the BPM in ACC1 on TTF2. The gasket is a conflat gasket.
The position and the design of feed-throughs changed (Fig. 11.2). Indeed, a critical point was the feed-through fragility, 50% of the feed-throughs had to be rejected. With the new design, the feed-throughs are simpler and more robust. Moreover, this new design has no resonant mode. To have a higher Q and therefore a longer signal in time, the feed-throughs moved from 31.5 mm in the re-entrant part. With this moving, the distinguishing of the monopole and dipole signals is clearer and the rejection of the monopole signal is better.

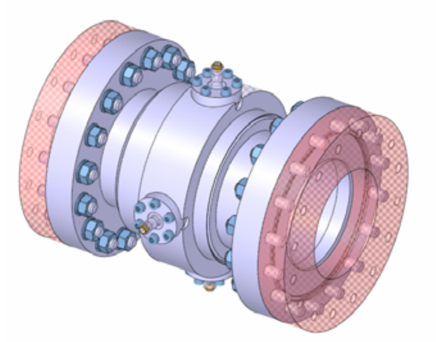

Fig. 11.1: Design of the new cavity BPM

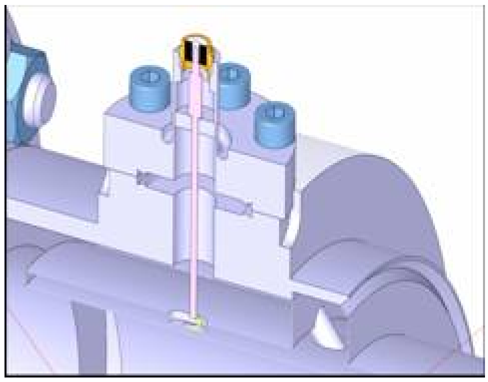

Fig. 11.2: Design of the new feedthrough

One of the biggest problems on the cavity in ACC1 was the cleaning. As the BPM is designed to be used in a clean environment and at cryogenic temperatures, twelve holes of 5 mm diameter were drilled at the end of the re-entrant part. A simulation was carried out to check that the RF characteristics of the re-entrant cavity do not change. Cleaning tests were successfully preformed at DESY and validated the system for the cleaning.

The simulation of the new design gives the RF characteristics (Table 11.1).

	New BPM			
	F (GHz)	Q	R/Q at 5mm of the center of cavity	R/Q at 10mm of the center of cavity
Monopole Mode	1.25	24	13 Ω	13 Ω
Dipole Mode	1.72	51.4	0.25 Ω	1.11 Ω

Tab. 11.1: RF characteristics of new BPM calculated with HFSS

The choice of resonant mode frequencies was determined according to the 180° junction hybrid available on the market. The resolution around 1 µm but also the mechanical feasibility of the structure determined the quality factors, Q, of the monopole and dipole modes. They are not able either to be too high to keep a time resolution around 10 ns or too low to have a centering accuracy better than 1 µm.

Development of new hybrid coupler

The new hybrid coupler is the Anaren model 3A0055. It's a 180° hybrid coupler and its isolation is more than 25 dB in the band 1-2 GHz. It can be optimized at the frequency of the dipole mode with attenuators and phase shifters to have an isolation around 50 dB.

Signal processing of the new BPM

The signal processing of the new re-entrant BPM is composed of a 180° hybrid junction, which is connected to each pair of opposite antennae with 33 m of semi-rigid cables. The rejection of the monopole mode proceeds in three steps. One is made by the new hybrid coupler, the second with the pass band filter, which rejects the monopole mode on the delta channel and the third with the synchronous detection. The noise is limited by the bandpass filters. The one on the Δ channel has to have the centre frequency of the dipole mode and the one on the Σ channel the centre frequency of the monopole mode. To perform the synchronous detection, the signals must be amplified. The 9 MHz reference signal, from the control system on TTF2, combined with some PLLs generates signals at the monopole and dipole modes frequencies. These are used as local oscillators for the mixers. Some phase shifters, controlled by the digital electronics, adjust the PLL signals, which have to be in phase with the signals coming from the hybrid. The digital electronics, also, makes the sampling, the calibration of the system and the control-command interface. The signal on the Σ channel is used in order to normalize the Δ signal, which determines the position of the beam. This normalization is, also, made by a digital electronics. The schematic of the new electronics is shown figure 11.3.

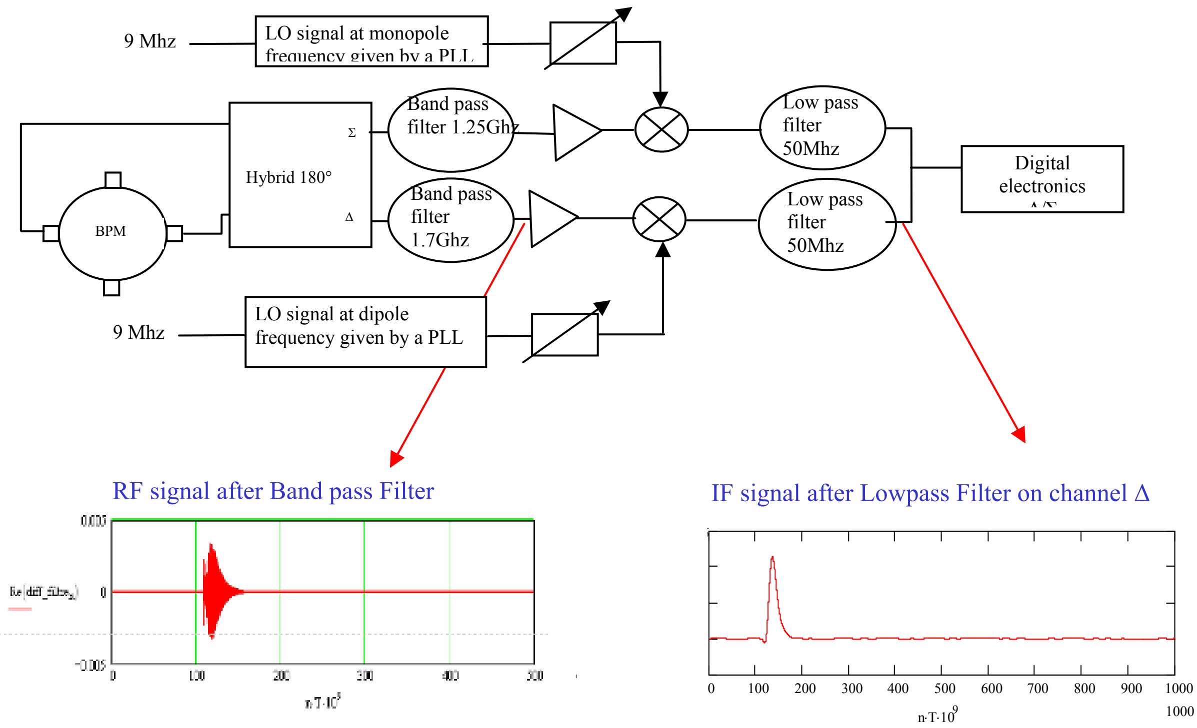

Fig. 11.3: Electronics of the new system

Beam tests of BPM in ACC1

The RF calibration is done:

- A high isolation between sum and delta is achieved: x channel 46 dB, y channel 57 dB.
- The synchronous detection works and the phase tuning is done to give a 'good' sensitivity. The LO signals was adjusted with some phase shifters to have the max of the dipole signal.
- The simultaneous sampling has to be done at the peak of the sum signal, which does not correspond to the maximum peak of the delta signals.

The calibration with the beam is also done (We thank N. Baboi from DESY who made all these measurements):

- The BPM charge (BPM9ACC1) is calibrated by correlating with the signal from a toroid (3GUN) (cf: Fig. 11.4 & Fig.11.5).

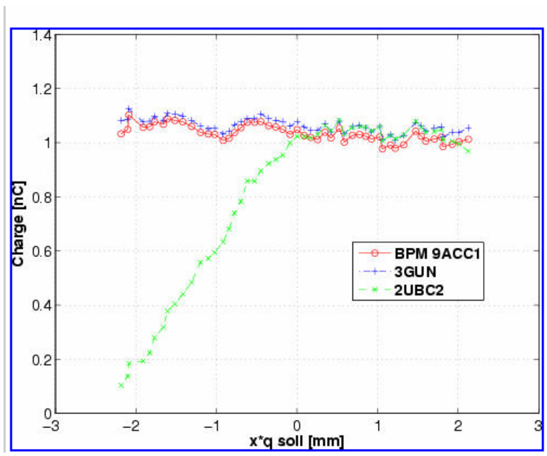

Fig. 11.4: Charge vs beam position

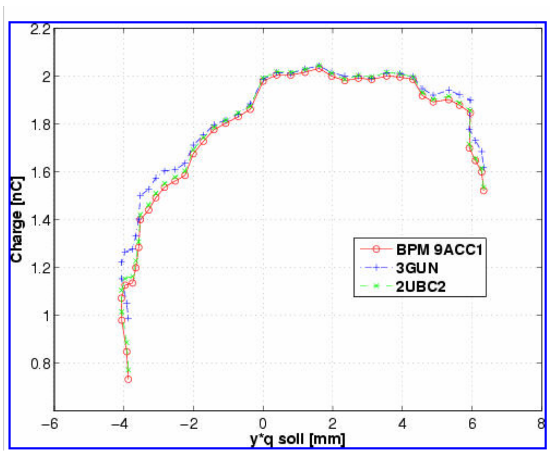

Fig. 11.5: Charge vs beam position

The plots (Fig. 11.6 and Fig. 11.7) show the beam position read by the BPM vs the beam position that we should have. The range of the BPM linearity is 4 mm then there is saturation. It may be caused by electronics and in particular saturation of some amplifiers.

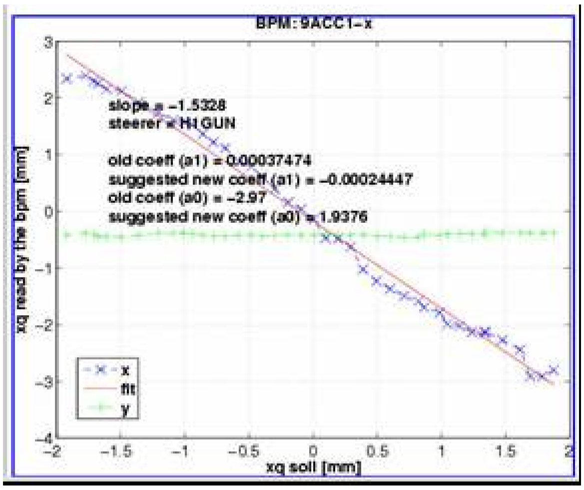

Fig. 11.6: Beam position read by the BPM vs expected beam position (horizontal).

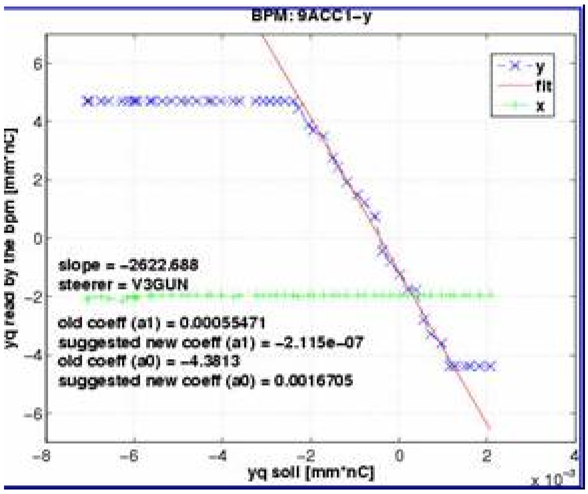

Fig. 11.7: Beam position read by the BPM vs expected beam position (vertical).

More beam tests have to be done on this BPM, which is in ACC1, to understand its saturation and to know its resolution.

Schedule the re-entrant BPM

The status and planning for the re-entrant BPM are as follows:

- Design and mechanical drawings of the BPM cavity are ready.
- Design of the RF electronics and signal processing are made.
- Signal processing board will be fabricated for March 2006.
- A BPM cavity will be fabricated for the beginning of 2006.
- Tests on the electronics will be made at the beginning of 2006.
- Preliminary tests on this new BPM to verify RF characteristics of the cavity and validate the fabrication process: brazing, heat treatment, cleaning and dust free mounting, will be done during the spring of 2006.

Sub-task 2: the HOM-BPM program

Activity historical background

The possibility to use the lowest frequency dipole modes of the accelerating SC cavities in order to measure the beam transverse position has been studied at TTF since 2002 by a CEA-DESY collaboration. In October 2003, the PhD thesis of R. Paparella on the subject has been co-funded by these two institutes. The first evidence for 50 μm beam centering accuracy and position resolution (10 times smaller than the cavity alignment in the cryomodules) was obtained in June 2004 with four dipole modes on the first two ACC1 cavities (see Fig 11.8). This result was published at the LINAC'04 conference. In the fall 2004, the SLAC instrumentation group joined the collaboration with the aim of building dedicated acquisition electronics and to equip all the HOM couplers of the 40 TTF linac cavities. In June 2005, such prototype electronics was used to show that a 5 µm BPM resolution was at reach. This result was published at the PAC'05 conference.

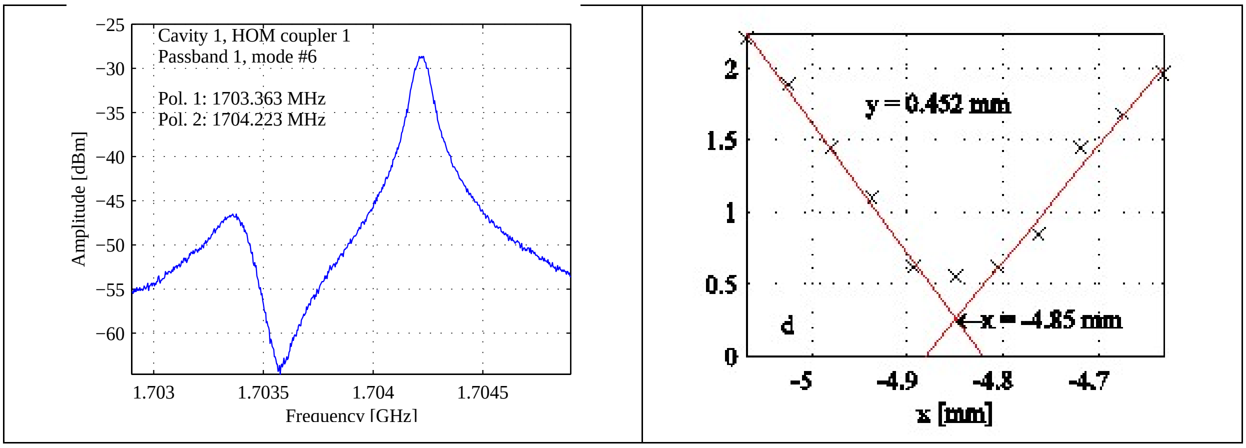

Fig.11.8 : Beam excitation of a pair of dipole HOM polarisations in ACC1 first cavity (left), and beam steering through the electric centre of this mode (right).

In September 2005 the CARE steering committee approved the CEA proposal to include the HOM-BPM activity within the BPM task of the beam instrumentation work package. Since the material cost and the manpower dedicated to this activity is entirely provided by CEA, DESY and SLAC internal resources, the CARE/SRF support aims at helping and reinforcing the collaborative work with travel funds used by CEA personnel.

Objectives, deliverable and milestone within CARE-JRA1

The main objectives of the HOM-BPM collaboration are:

1. prove (or disprove) the potential of the HOM-BPM instrumentation to monitor the beam orbit through the TTF2 linac cryomodules in order to minimize the bunch emittance growth;
2. measure the cavity centres and relative misalignments within the five TTF cryomodules.

Given the relatively modest support requested from JRA1, it is suggested that the corresponding deliverable is a report evaluating of the HOM-BPM experimental operation with respect to these two objectives. This deliverable should add up to the CARE-JRA1-WP11 deliverables, with a delivery date at the end of 2006 (month 36).

On the way to these objectives, the most important milestone of the activity is the commissioning the complete SLAC-built 80-channel HOM electronics (see Fig. 11.9). This commissioning is planned during the TTF2 beam time period dedicated to the linear collider developments in the spring 2006. This milestone should thus occur by mid-2006 (month 30).

Activity in 2005

By October 2005, Claire Simon, from CEA, visited SLAC for one month to collaborate in the test program of the complete set of 40 HOM electronics boards. Once the test program successfully finished, the complete HOM electronics have been shipped to DESY and installed on the TTF linac in November 2005.

Beam induced HOM signals have been recorded and will be analyzed in the beginning of 2006.

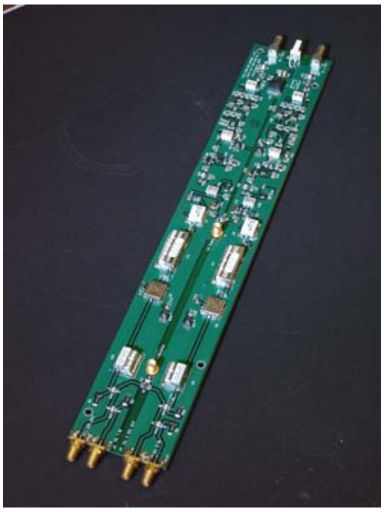

Fig. 11.9: HOM electronics board for one cavity (left) and HOM electronics drawer for one TTF module of eight cavities (right), designed, built and tested at SLAC.

Task 11-1: The Emittance Monitor

In this year all the hardware of the experiment has been contructed and installed on the accelerator, and the integration of the dedicated software for image acquisition and analysis in the general control system of TTF is completed, fulfilling the milestone of being ready for data taking.
The target was realized with lithography technique starting from a silicon nitride wafer and opening the slits by means of chemical etching
The surface roughness, the planarity of the target mounted in the holder, and the sharpness of the apertures borders were carefully measured.

Fig. 11.10 – The DR screen with two slits of 0.5 and 1 mm respectively

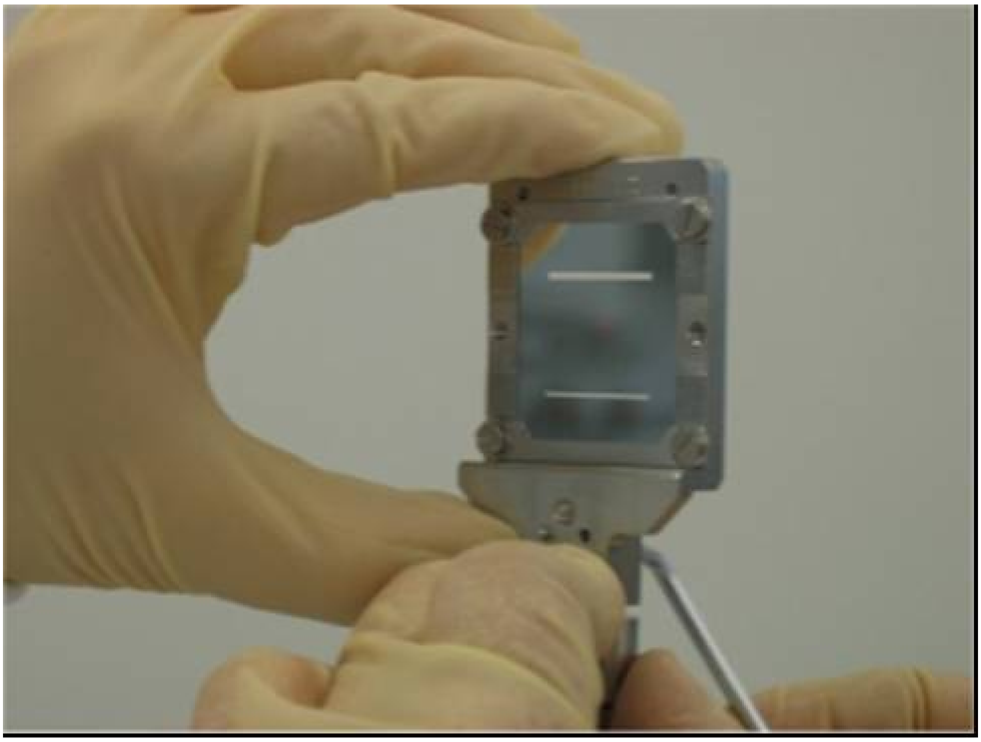

Fig. 11.11 – The DR screen mounted on the vacuum linear actuator

A modified version of the optical system has been installed, allowing both the standard beam imaging and the radiation angular distribution. Two interferential filters and a polarizer are also present and can be remotely inserted on the radiation path.

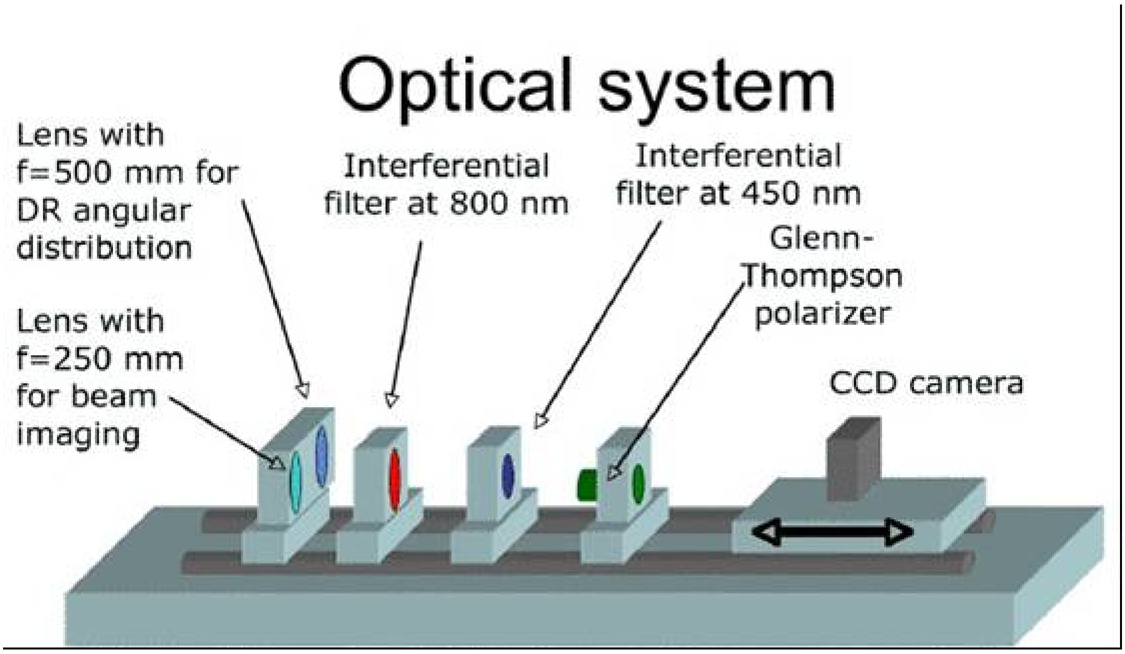

Fig. 11.12 – Sketch of the optical system

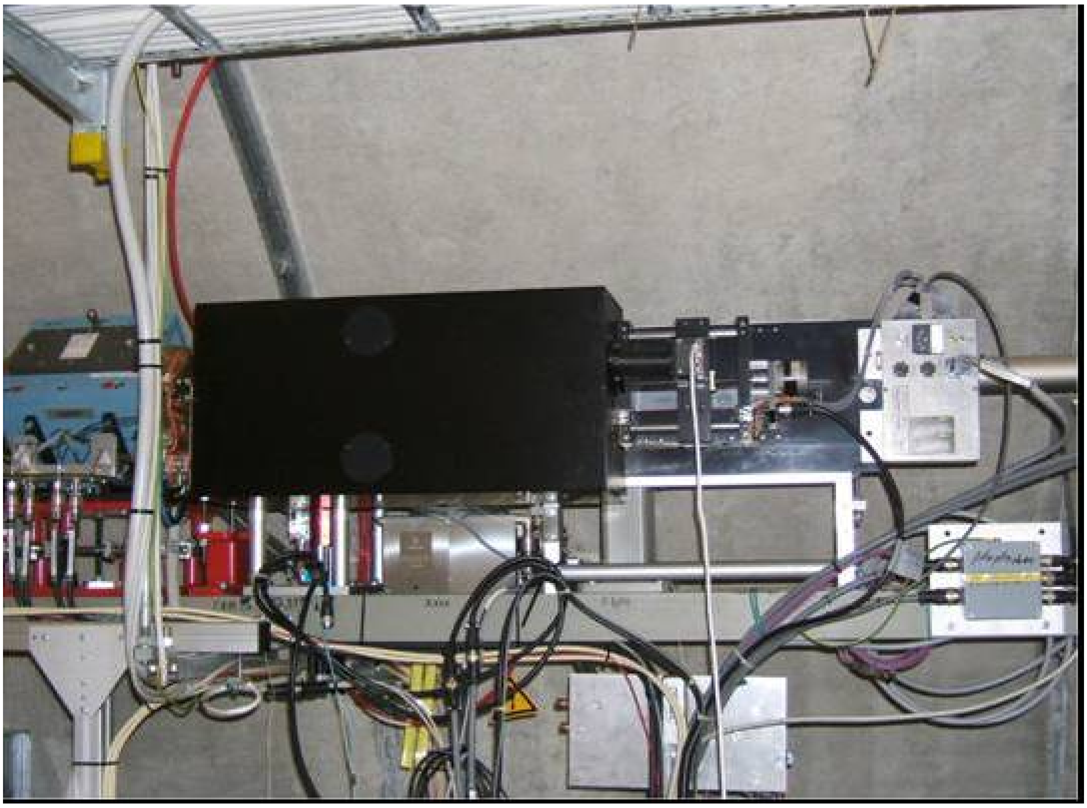

Fig. 11.13 – The complete optical system installed on the vacuum pipe of the by-pass line.

The transport optics in the by-pass has been verified for the possibility of having a waist of suitable dimension at the DR screen position.

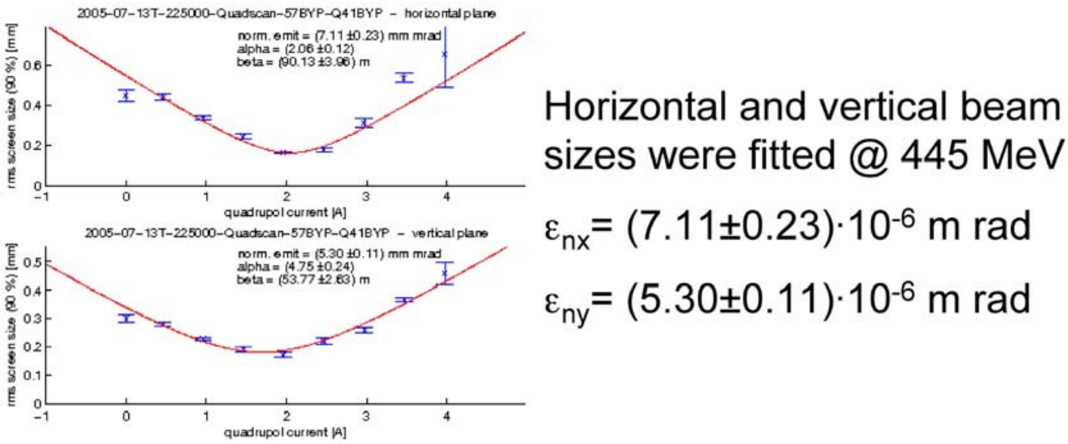

Fig. 11.14 – Quadrupole scan at the DR screen location

We are now ready for data taking, satisfying the milestone fixed for December 31st 2005. Adequate beam time has been requested to the TTF Facility.